SYNTHESIS TECHNIQUES FOR ACTIVE RC FILTERS USING OPERATIONAL AMPLIFIERS

by

Hernani Mationg Jover

United States
Naval Postgraduate School

THESIS

SYNTHESIS TECHNIQUES FOR ACTIVE RC FILTERS

USING OPERATIONAL AMPLIFIERS

by

Hernani Mationg Jover

June 1970

Synthesis Techniques for Active RC Filters

Using Operational Amplifiers

by

Hernani Mationg Jover
Lieutenant, Philippine Navy
B.S., Philippine Military Academy, 1962

Submitted in partial fulfillment of the
requirements for the degree of

MASTER OF SCIENCE IN ELECTRICAL ENGINEERING

from the

NAVAL POSTGRADUATE SCHOOL
June 1970

ABSTRACT

The stimulus provided by the trend towards microminiaturization has generated considerable interest in active RC filters utilizing operational amplifiers. A comprehensive and unified presentation of the many different techniques to synthesize such filters is made along the lines of modern filter theory in this thesis.

TABLE OF CONTENTS

LIST OF TABLES

LIST OF ILLUSTRATIONS

ACKNOWLEDGEMENT

The author would like to express his most sincere appreciation and thanks to Professor Shu-Gar Chan, who provided professional guidance and personal encouragement in his capacity as Thesis Advisor to the author; to LTJG Arthur L. Partarrieu, who assisted the author in the preparation of Computer Program 1 which was used to great advantage in this thesis; and finally to Mrs. Cecelia Reese, who prepared the final manuscript of this thesis.

I. INTRODUCTION

Technological progress in the last two decades has brought about the microminiaturization of many electrical components and systems. The natural consequence of the transistor was the monolithic integrated circuit (IC). The future promises not only medium-scale circuit integration (MSI) but even large-scale integration (LSI). To make electrical filter networks compatible to this trend, the development of inductorless filters, better known as active RC filters, came about.

A. DISADVANTAGES OF INDUCTORS

Inductance-capacitance (LC) filters were found reliable and easy to design at high frequencies but at frequencies below 1000 Hertz, they were found limited to a maximum quality factor, Q, of about 100. Higher Q's were possible only with large and bulky inductors, Attempts to reduce inductor size with high-permeability materials and ferrite cores met with failure. Inductor quality deteriorated rapidly at lower frequencies.

There were other disadvantages that came with the use of inductors. Because of their associated magnetic fields resulting in mutual coupling effects and because of their nonlinear behavior, they created complications in practical circuit applications. They gave the circuit designer additional problems because of incidental dissipation resulting from their core loss and winding resistance. Furthermore,

inductors were found to be prone to noise pickup. Because of all these reasons, the concept of inductorless filters became very attractive for many applications.

B. DEFECTS OF PASSIVE RC FILTERS

Using resistors and capacitors to meet certain filter specifications was found possible but such passive RC filters suffered from two defects:

1. They introduced considerable loss in the passband.

2. For a given filter specification, they were more complex than an equivalent RLC filter.

C. EVOLUTION OF THE ACTIVE RC FILTER

It seemed, then, that the answer to those difficulties mentioned in the last section was not simply eliminating inductors but replacing them with active elements. The basic ideas of associating active elements like high-gain and phase-inverting amplifiers with passive networks were developed from feedback-amplifier theory [Ref. 1] in 1945. Guillemin [Ref. 2] in 1949 suggested the use of vacuum tubes in conjunction with passive RC elements in a circuit employing the principles of feedback. Dietzold [Ref. 3] came up with a patent for his RC filter employing a stabilized amplifier in 1951. In 1954 it was Linvill [Ref. 4] who finally gave this type of circuit a name - RC Active Filters.

Since the publication of Linvill's article, many other synthesis methods have appeared and the study of active RC filters has expanded considerably. Four active elements have received the most attention:

1. Controlled sources
2. The negative-immitance converter
3. The gyrator
4. The operational amplifier

D. ADVANTAGES OF THE OPERATIONAL AMPLIFIER

There are many reasons for the considerable attention given to the operational amplifier. Its biggest advantage, perhaps, over the other three active elements is its easy off-the-shelf availability at prices that have gone down with the price of the transistor. Because of its solid-state construction (transistor and FET differential-input configurations) [Ref. 5], it lends itself perfectly to the current trend toward microminiaturization. Because of its very high gain (ideally infinite), the circuit using it as the active element has very low sensitivity to changes in gain. Because of its very low (ideally zero) output impedance, cascading low-order functions without the necessity of isolating amplifiers is easily accomplished. And, finally, because of its very high (ideally infinite) input impedance, resulting in virtual ground at its input terminals, circuit analysis and synthesis are both simplified.

E. PREVIEW AND PURPOSE

Chapter III will show the type of analysis involved when operational amplifiers are used. The subsequent chapters will show the different synthesis techniques that have evolved over the years. These techniques have been classified into distinct categories for the purpose of unified development and easy comparison. A common starting point for all these techniques, namely, the generation of an appropriate transfer function to be synthesized, will be developed along the lines of modern filter theory in the next chapter.

It is the purpose of this paper to present a unified and comprehensive study of active RC filters using operational amplifiers.

II. MODERN FILTER THEORY

This chapter will present the development of Modern Filter Theory and provide a common starting point for the different synthesis methods - the determination of the desired transfer function, H(s).

A. HISTORY AND EVOLUTION

Since the discovery of the electric-wave filter by Campbell and Wagner in 1915, filter theory has evolved along two different lines. One is known by the name Classical Filter Theory and the other Modern Filter Theory.

The classical theory is more commonly known as the Image-Parameter Theory of Filter Design. Originated in the 1920's by Zobel, this theory assumes that, in the design of a filter, its load impedance is matched to its image impedance. In practice, however, this assumption proves to be inaccurate because most loads are constant-value resistances while the image impedance is frequency dependent. Consequently, design methods based on this theory involve trial and error and often, final adjustments are required to meet design specifications.

Modern filter theory, on the other hand, consists of techniques which are more ideal in terms of meeting exact specifications. Developed in the 1930's through the efforts of several individuals, prominently Norton, Foster, Cauer, Bode, Brune, Guillemin and Darlington, this theory has gained considerable acceptance. Essentially,

it involves the approximation of given specifications with a rational transfer function and the realization of this function through the use of synthesis techniques. Since such synthesis procedures are analytical and exact, no trial and error is involved in designing a filter from its transfer function.

It is along the lines of modern filter theory that the synthesis techniques in this paper follow.

B. TYPES OF FILTERS

Filters have numerous and varied applications but they all boil down to the basic operation of passing through a desired signal and rejecting other unwanted signals.

Every filter is characterized by a range of frequencies over which the attenuation of a signal is negligible and a range of frequencies over which the attenuation is severe. Such regions of frequency passage are termed passbands and the regions of attenuation are called stopbands. In physically realizable filters, there is also a range of frequencies between passband and stopband over which the attenuation builds up from negligible to severe. Such bands are called transition regions. Filters are classified commonly according to their passband location in the frequency spectrum.

The four basic filter types based on this classification are:

1. Low-Pass Filter: A low-pass filter is a two-port which passes all frequencies less than a certain cutoff frequency ω_c and attenuates all frequencies greater than ω_c .

2. High-Pass Filter: A high-pass filter is a two-port which passes all frequencies greater than a certain cutoff frequency ω_c and attenuates all frequencies less than ω_c.

3. Bandpass Filter: A bandpass filter is a two-port which passes all frequencies between certain lower and upper frequency limits, ω_l and ω_u, and attenuates all frequencies outside these limits.

4. Band-Reject Filter: A band-reject filter is a two-port which attenuates all frequencies between certain lower and upper frequency limits, ω_l and ω_u, and passes all frequencies outside these limits.

The effect of a filter on the passage of frequencies is presented graphically in terms of gain or magnitude and phase characteristics. In their ideal form, the magnitude and phase characteristics of the four basic types are shown in Figure 2-1. H(s) is the filter transfer function representing the ratio of filter output to input transforms, where s is the complex frequency variable. In their more practical form, the attenuation characteristic of the four basic types are shown in Figure 2-2.

C. THE FILTER DESIGN PROBLEM

The ideal filter is one which passes all frequencies without attenuation within its passband, completely attenuates all frequencies within its stopband and has a linear phase response in its passband.

Such ideal filter characteristics, however, are physically unrealizable. No quotient of rational, finite-degree polynomials can

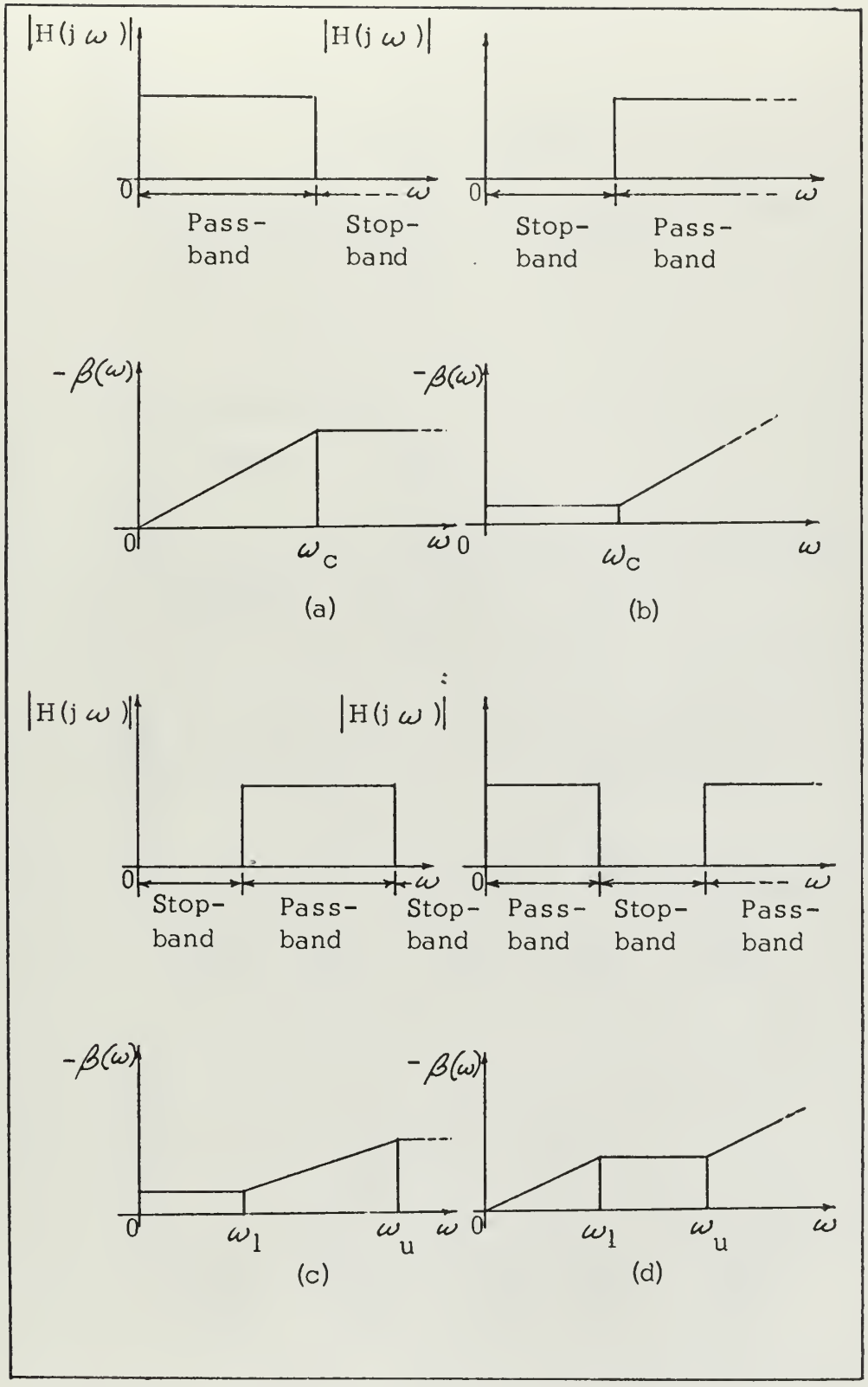

Figure 2-1. Ideal magnitude and phase characteristics of
(a) a low-pass filter (b) a high-pass filter
(c) a bandpass filter (d) a band-reject filter

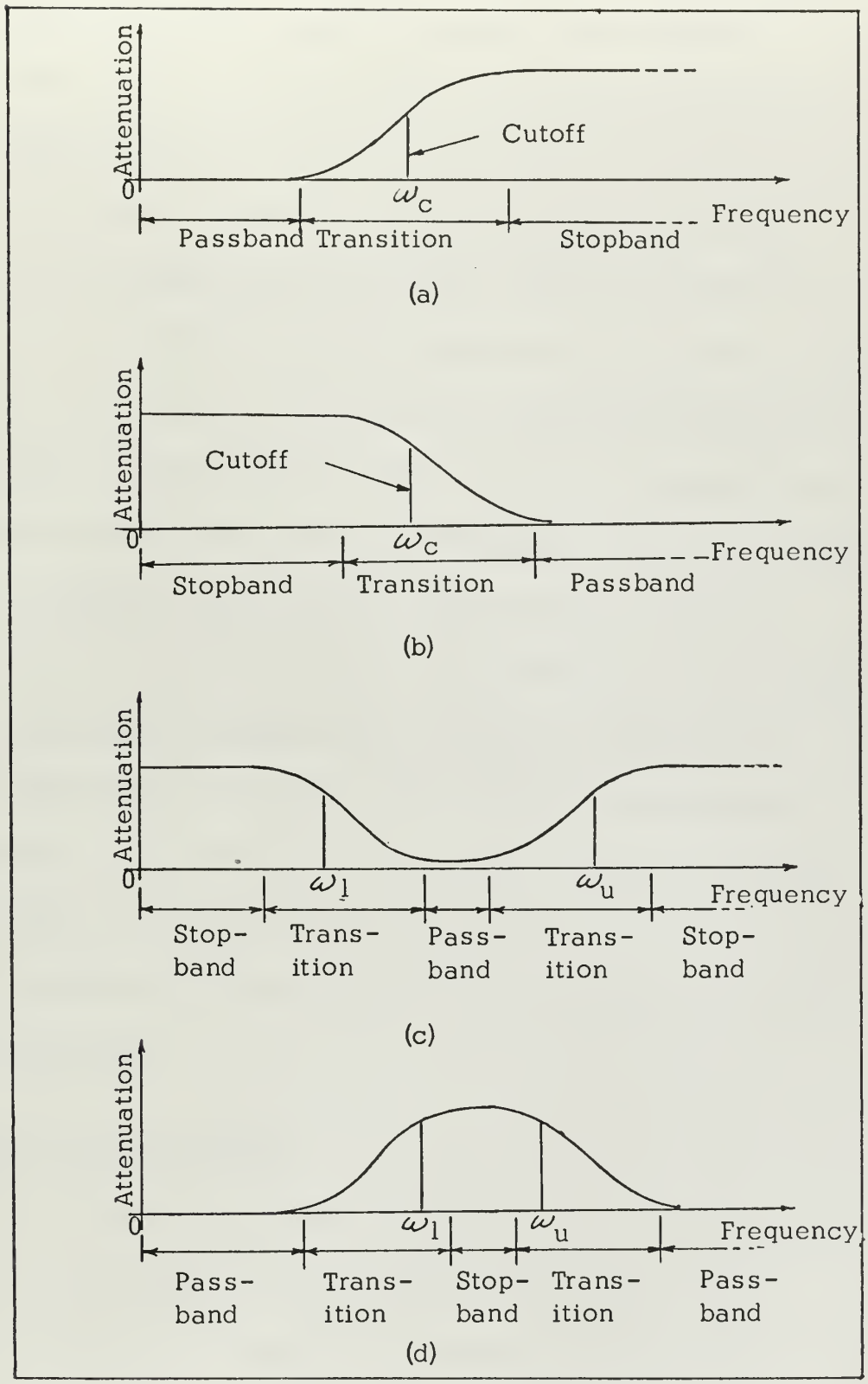

Figure 2-2. Attenuation characteristics of (a) a low-pass filter (b) a high-pass filter (c) a bandpass filter (d) a band-reject filter

represent exactly the ideal magnitude and phase characteristics. In fact, the desirable abrupt transition from zero to infinite attenuation with negligible change in frequency in the gain characteristic would wreck havoc to a filter's transient response because of the infinite phase shifts and infinite lags in frequencies within the passband, or in effect, a drastic departure from the desired linear phase characteristic. On the other hand, a more gradual fall off of magnitude with frequency change results in a more acceptable phase response. In general, then, the fundamental problem in modern filter design is in finding the transfer function H(s) that best approaches the ideal magnitude and phase characteristics. For other particular filter applications, it can happen that one characteristic's requirements are relaxed in favor of more stringent requirements in the other. This process of finding the best H(s) depending on the desired filter application is known as the approximation problem. Once this H(s) is known, the other half of the modern filter theory problem is the exact realization of the filter network using synthesis techniques.

D. FILTER CHARACTERISTICS

In this section, three approximations to the ideal low-pass filter will be discussed briefly to give the reader an idea of the kind of compromise involved in meeting both frequency- and time-response specifications. These are the Butterworth, Chebyshev, and Bessel or Thompson filters. Each approximates the characteristics of the ideal filter in a different way and each has its area of application.

There are other types of filters such as the Cauer or elliptic-function filters, the monotonic Legendre filters and the filters with parabolic pole distribution, more commonly known as the P filters. Detailed information about their frequency and time responses as compared with those of the types to be discussed in the following paragraphs may be found in Refs. 6, 7, and 8.

Only the normalized low-pass version of each type will be shown since the high-pass, bandpass and band-reject transfer functions exhibiting the same characteristics of the low-pass prototype can be easily derived using the appropriate frequency transformations. Such transformations will be discussed in the next section.

1. Butterworth Class

Butterworth filters are characterized by the normalized magnitude-squared function:

$$\left|H(j\omega)\right|^2 = \frac{1}{1+\left(\frac{\omega}{\omega_c}\right)^{2n}} \qquad (2\text{-}1)$$

where n is the number of poles in the network, ω is the frequency of interest and ω_c is the cutoff frequency. $\omega_c = 1$ for the normalized case. From equation (2-1), it can be observed that regardless of the number of poles, the output at the cutoff frequency is always 3 dB below that at $\omega = 0$. The derivative of this function shows that the slope of the response curve is zero at $\omega = 0$. For this reason the Butterworth filter is called a maximally flat amplitude filter. At cutoff ($\omega = \omega_c$), the slope of the response curve is (-n/2), showing

an increasing rate of attenuation with increasing number of poles. Beyond cutoff the filter response falls at an approximately constant 20n dB / decade.

By using the stable poles of the magnitude-squared function, it can be shown that the Butterworth low-pass transfer function is of the form:

$$H(s) = K/Bn(s) \qquad (2\text{-}2)$$

where K is a constant multiplier and the polynomials Bn(s) are called the Butterworth polynomials. They are given in Table 2-1 up to order 5. Their roots, all of which lie on the unit circle, are listed in Table 2-2. The low-pass amplitude response for different values of n is shown in Figure 2-3. It can be noted that the amplitude response flatness over the entire passband increases with the number of poles.

The phase characteristic, however, is not very linear. Consequently, the time delay changes with change in frequency. The effect of this is an overshoot and some ringing in the filter's response to a step function. The amount of overshoot increases with the number of poles. The rise time of the output is satisfactory but increases rather slowly with increasing n.

2. Chebyshev Class

The Chebyshev filter is characterized by the magnitude-squared function:

$$\left|H(j\omega)\right|^2 = \frac{1}{1 + \left[\epsilon \; Tn\left(\frac{\omega}{\omega_c}\right)\right]^2} \qquad (2\text{-}3)$$

Table 2-1. The Butterworth Polynomials

n	
1	$s + 1$
2	$s^2 + \sqrt{2}\,s + 1$
3	$s^3 + 2s^2 + 2s + 1 = (s + 1)(s^2 + s + 1)$
4	$s^4 + 2.613s^3 + 3.414s^2 + 2.613s + 1 = (s^2 + 0.765s + 1)(s^2 + 1.848s + 1)$
5	$s^5 + 3.236s^4 + 5.236s^3 + 5.236s^2 + 3.236s + 1$ $= (s+1)(s^2 + 0.618s + 1)(s^2 + 1.618s + 1)$

Table 2-2. Roots of the Butterworth Polynomials

n = 1	n = 2	n = 3	n = 4	n = 5
-1.0000000	-0.7071068 $\pm$ j0.7071068	-1.0000000	-0.3826834 $\pm$ j0.9238795	-1.0000000
		-0.5000000 $\pm$ j0.8660254	-0.9238795 $\pm$ j0.3826834	-0.3090170 $\pm$ j0.9510565
				-0.8090170 $\pm$ j0.5877852

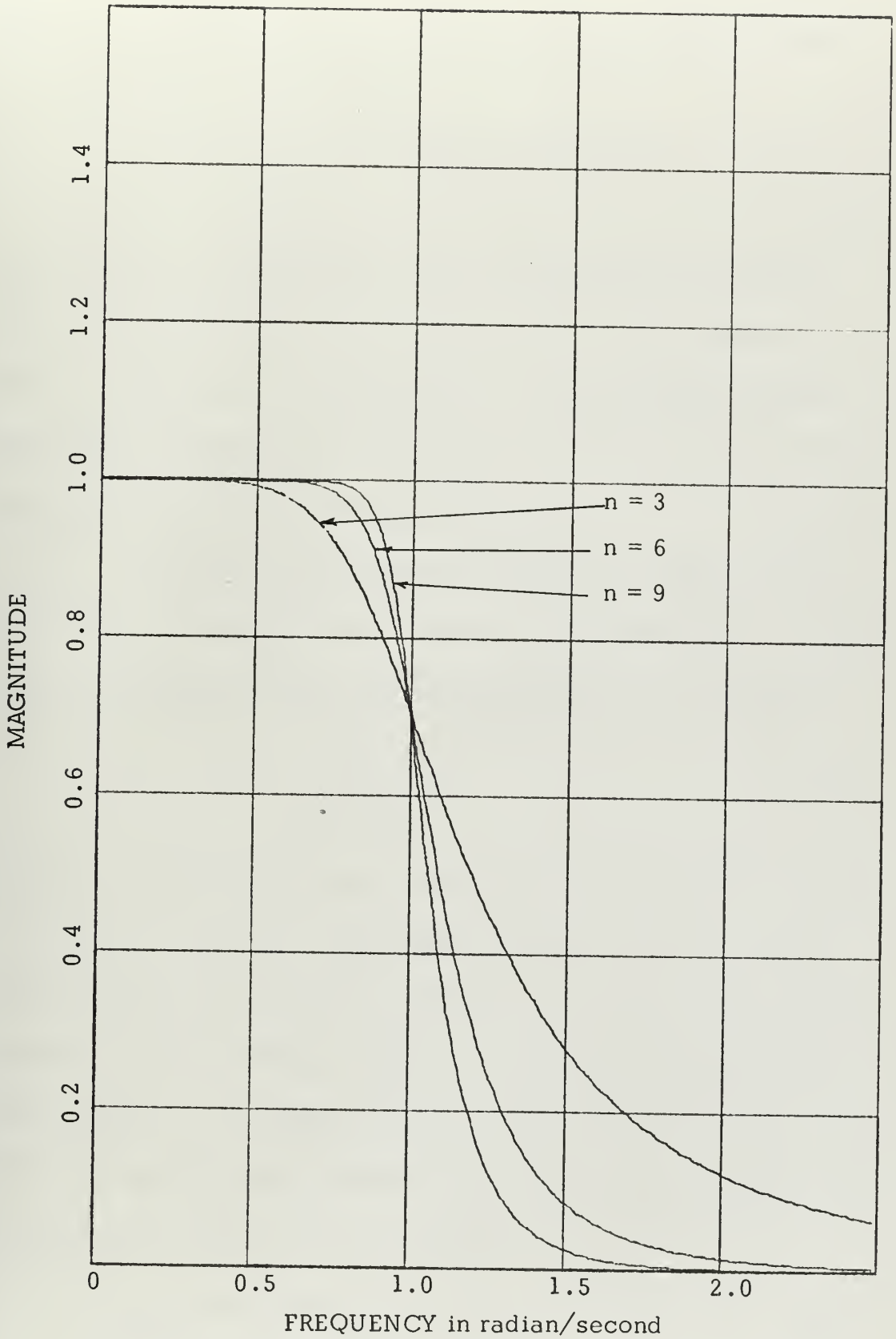

Figure 2-3. Butterworth low-pass amplitude responses for various values of n.

where ϵ is the ripple parameter and $Tn(\omega / \omega_c)$ is the Chebyshev Polynomial of order (and degree) n.

The transfer function can be shown to be:

$$H(s) = K/Vn(s) \qquad (2-4)$$

where K again is a constant and Vn(s) is formed from the left half plane zeros of the denominator of equation (2-3). Each value of ϵ yields a different set of Vn polynomials. The coefficients of these polynomials corresponding to two values of ϵ up to n = 5 are given in Table 2-3; their roots are given in Table 2-4.

The magnitude response of this class of filters is distinguished by an equal-magnitude ripple in the passband and a maximum rate of fall off beyond cutoff. The ripple height, δ, is given by:

$$\delta = 1 - \frac{1}{\sqrt{1 + \epsilon^2}} \qquad (2-5)$$

The sum of the number of maxima and minima in the passband is equal to the order of the filter. A fifth-order Chebyshev low-pass filter response is shown in Figure 2-4. The response at the cutoff frequency is always that of a minimum. Thus, a Chebyshev filter with $\pm$ 1-dB ripples will be - 1 dB down at cutoff. For the $\pm$ 3-dB ripple case, both Butterworth and Chebyshev filters will have the same cutoff frequency. In general, the 3-dB-down point will be at:

$$\omega_{3dB} \approx \cosh\left[\frac{\cosh^{-1} 1/\epsilon}{n}\right] \omega_c \qquad (2-6)$$

Table 2-3. Polynomials for Chebyshev Filters

(a) 1/2 dB Ripple

n	
1	$s + 2.863$
2	$s^2 + 1.425s + 1.516$
3	$s^3 + 1.253s^2 + 1.535s + 0.716 = (s+0.626)(s^2+0.626s+1.142)$
4	$s^4 + 1.197s^3+1.717s^2+1.025s+0.379 = (s^2+0.351s+1.064)(s^2+0.845s+0.356)$
5	$s^5 + 1.172s^4+1.937s^3+1.309s^2+0.753s+0.179 = (s+0.362)(s^2+0.224s+1.036)(s^2+0.586s+0.477)$

(b) 1 dB Ripple

n	
1	$s + 1.965$
2	$s^2 + 1.098s + 1.103$
3	$s^3 + 0.988s^2 + 1.238s + 0.491 = (s+0.494)(s^2+0.494s+0.994)$
4	$s^4 + 0.953s^3+1.454s^2+0.743s+0.276 = (s^2+0.279s+0.987)(s^2+0.674s+0.279)$
5	$s^5 + 0.937s^4+1.689s^3+0.974s^2+0.581s+0.123 = (s+0.289)(s^2+0.179s+0.988)(s^2+0.468s+0.429)$

Table 2-4. Roots of Chebyshev-derived Polynomials

(a) 1/2 dB Ripple ($\epsilon = 0.3493114$)

-2.8627752	-0.7128122 $\pm$ j1.0040425	-0.6264565	-0.1753531 $\pm$ j1.0162529	-0.3623196
		-0.3132282 $\pm$ j1.0219275	-0.4233398 $\pm$ j0.4209457	-0.1119629 $\pm$ j1.0115574
				-0.2931227 $\pm$ j0.6251768

(b) 1 dB Ripple ($\epsilon = 0.5088471$)

-1.9652267	-0.5488672 $\pm$ j0.8951286	-0.4941706	-0.1395360 $\pm$ j0.9833792	-0.2894933
		-0.2470853 $\pm$ j0.9659987	-0.3368697 $\pm$ j0.4073290	-0.0894584 $\pm$ j0.9901071
				-0.2342050 $\pm$ j0.6119198

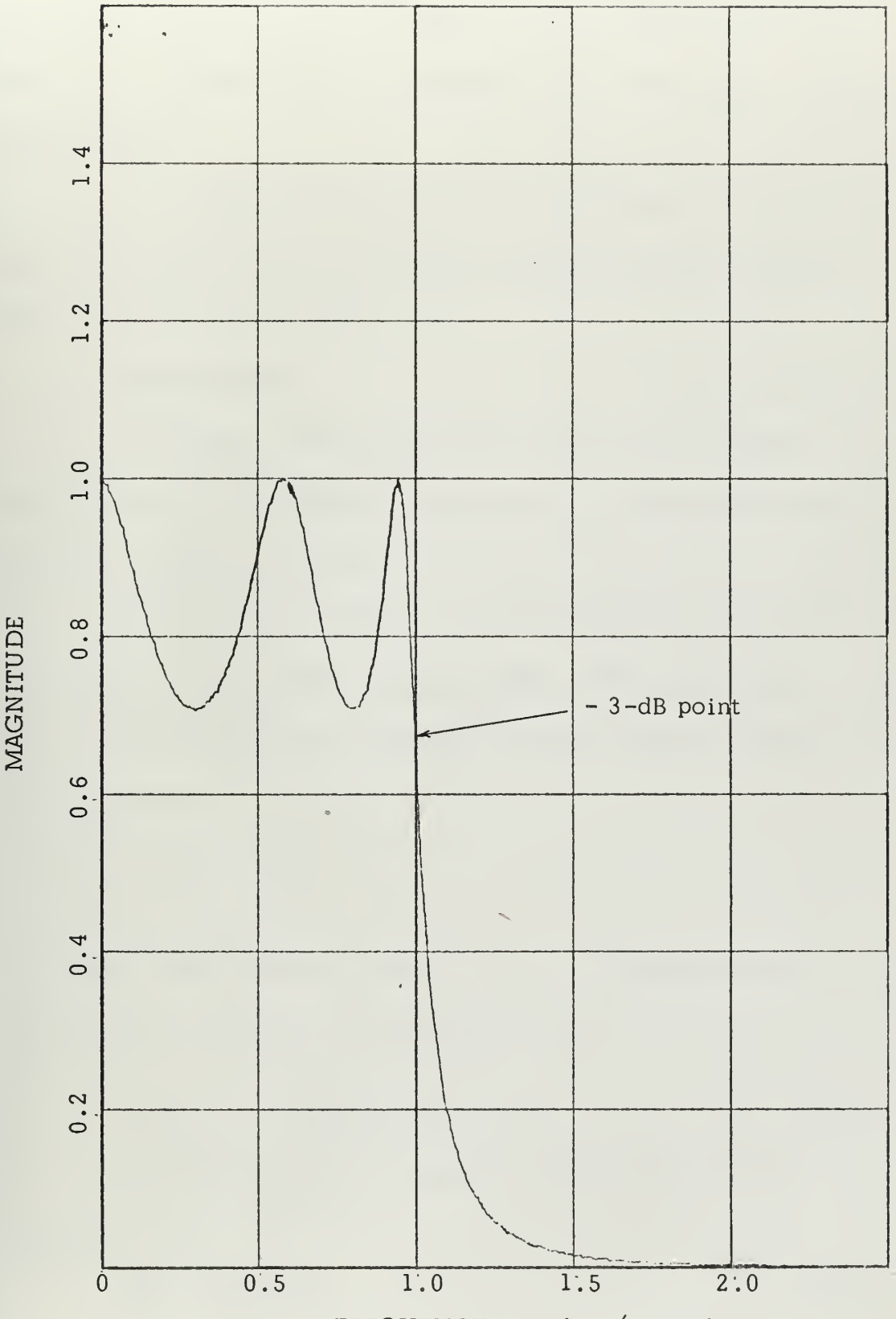

Figure 2-4. A fifth-order Chebyshev approximation to a low-pass filter.

The rate of attenuation beyond cutoff is initially greater than 20n dB/ decade and increases with the magnitude of the allowed ripple and the number of poles.

The phase response is even more nonlinear than that of the Butterworth class and this nonlinearity increases with the allowed ripple and the number of poles.

3. Bessel Class

The Bessel filter exhibits maximally flat time delay (linear phase) and subsequently its response to a step function shows less than one percent overshoot.

The amplitude response, on the other hand, is not flat but decreases monotonically in the passband. The cutoff frequency, ω_c , is not the 3-dB-down point but is defined in terms of the zero-frequency time delay, t_o, as:

$$\omega_c = \frac{1}{t_o} \tag{2-7}$$

The location of the half-power point, ω_{3dB}, is a function of the order and for $n > 3$ is given approximately by:

$$\omega_{3dB} \approx \sqrt{0.69315(2n-1)}\ \omega_c \tag{2-8}$$

The Bessel class of filters is represented by the low-pass transfer function:

$$H(s) = K/Hn(s) \tag{2-9}$$

where K is a constant and Hn(s) are the Bessel Polynomials. Their coefficients up to n = 5 are given in Table 2-5; their roots are given in Table 2-6.

4. Comparison of Classes

Figure 2-5 contrasts the magnitude characteristics of the three filter classes. For a given pole order, magnitude flatness changes drastically as one goes from Butterworth to Bessel to Chebyshev. Sharpness of cutoff improves from Bessel to Butterworth to Chebyshev. Linearity of phase deteriorates rapidly in the same order. Consequently, percentage of overshoot of step input response increases while rise time improves in this same order. A comparison of these last two figures of merit is given in Table 2-7. From this comparison of approximations, it can be seen dramatically how the choice of filter type must depend on the relative importance of amplitude and phase responses to the particular application desired.

E. FREQUENCY TRANSFORMATIONS

High-pass, bandpass and band-reject filters exhibiting the same characteristics as their low-pass prototype may all be obtained by making the following frequency transformations:

Low-pass to high-pass:

$$Sn = \frac{\omega_c}{s} \qquad (2\text{-}10a)$$

Table 2-5. The Bessel Polynomials

$p_o(s) = 1$

$p_1(s) = s + 1$

$p_2(s) = s^2 + 3s + 3$

$p_3(s) = s^3+6s^2+15s+15 = (s+2.322)(s^2+3.678s+6.460)$

$p_4(s) = s^4+10s^3+45s^2+105s+105 = (s^2+5.792s+9.140)(s^2+4.208s+11.488)$

$p_5(s) = s^5+15s^4+105s^3+420s^2+945s+945$

$= (s+3.647)(s^2+6.704s+14.272)(s^2+4.649s+18.156)$

.....

$p_n(s) = (2n - 1)\, p_{n-1}(s) + s^2 p_{n-2}(s)$

Table 2-6. Roots of the Bessel Polynomials

n	
1	- 1.0000000
2	- 1.5000000 $\pm$ j0.8660254
3	- 2.3221854; - 1.8389073 $\pm$ j1.7543810
4	- 2.8962106 $\pm$ j0.8672341; - 2.1037894 $\pm$ j2.6574180
5	- 3.6467386; - 3.3519564 $\pm$ j1.7426614; - 2.3246743 $\pm$ j3.5710229

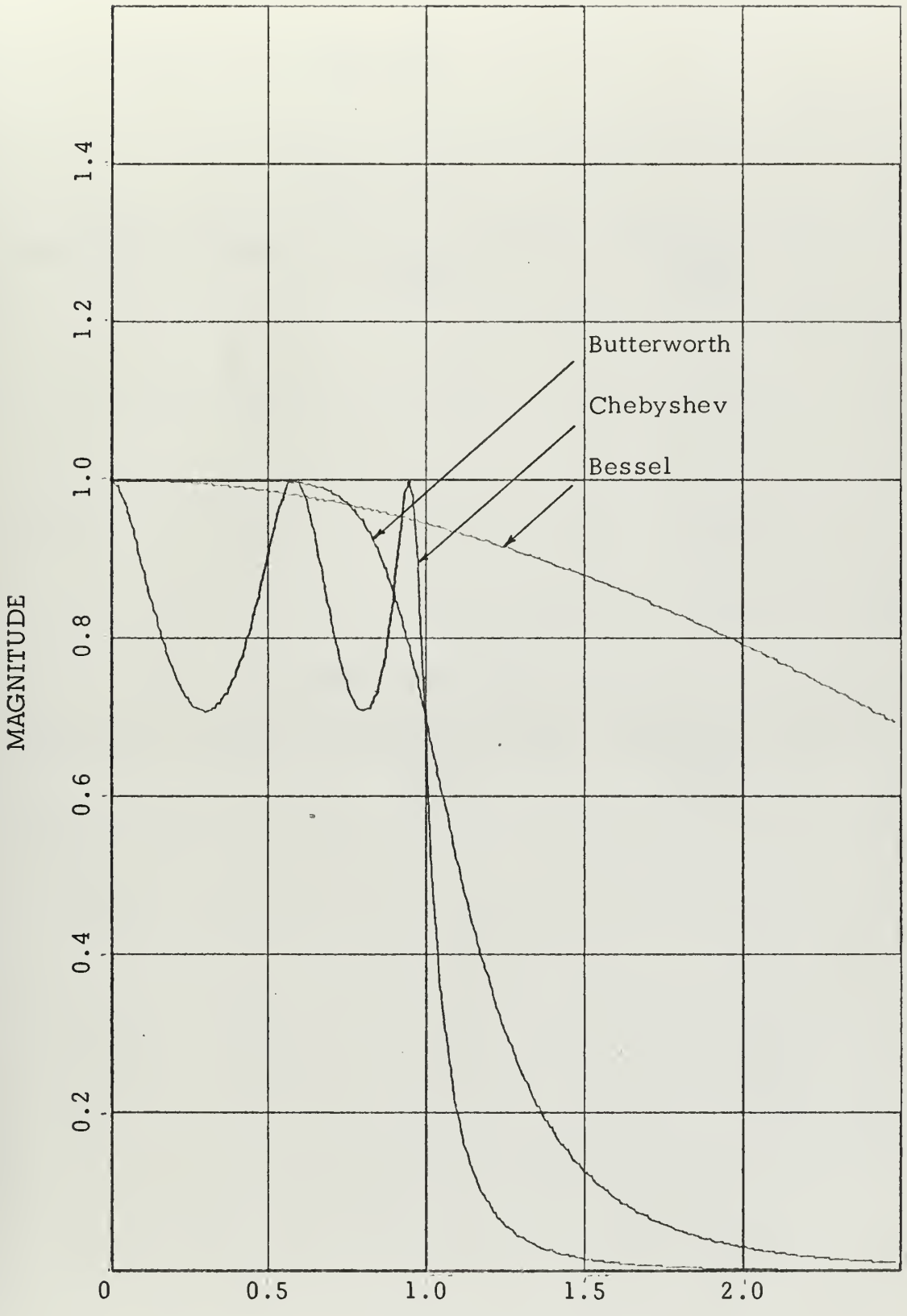

Figure 2-5. Normalized magnitude responses of various fifth-order filters.

Table 2-7

% Overshoot				
n	Butterworth	Bessel	Chebyshev 1/2 dB Ripple	Chebyshev 1 dB Ripple
1	0.	0.	0.	0.
2	4.3	0.43	10.5	14.6
3	8.15	0.75	9.2	6.6
4	10.9	0.83	17.8	22.2
5	12.8	0.77	13.1	10.2

Rise Time (10 to 90%)

n	Butterworth	Bessel	Chebyshev 1/2 dB Ripple	Chebyshev 1 dB Ripple
1	2.2	2.2	2.2	2.2
2	2.15	2.73	1.85	2.0
3	2.29	3.07	1.81	1.97
4	2.43	3.36	2.0	2.03
5	2.56	3.58	1.98	1.97

Low-pass to bandpass:

$$Sn = \frac{\omega_o}{BW}\left(\frac{s}{\omega_o} + \frac{\omega_o}{s}\right) \tag{2-10b}$$

Low-pass to band-reject:

$$Sn = \frac{BW}{\omega_o\left(\frac{s}{\omega_o} + \frac{\omega_o}{s}\right)} \tag{2-10c}$$

where S_n represents the normalized low-pass complex frequency variable, ω_o the center frequency and BW the bandwidth of the bandpass and band-reject filters. Center frequency is defined as:

$$\omega_o = \sqrt{\omega_l \ \omega_u} \tag{2-11}$$

while bandwidth is

$$BW = \omega_u - \omega_l \tag{2-12}$$

where ω_l is the lower frequency limit and ω_u the upper frequency limit of a bandpass or band-reject filter.

Strictly, bandwidth is defined for only the low-pass and bandpass filters. For the low-pass one, the bandwidth is equal to ω_c. For the bandpass case, it is represented by equation (2-12). Normally, the half-power points in the amplitude response are used to indicate these lower and upper frequency limits. In this case, the bandwidth is called the half-power bandwidth.

These transformations are performed on the normalized low-pass transfer function H(s). It can be noted that the center frequency is the geometric mean of the upper and lower frequency limits and will

not be necessarily in the center of the bandwidth, BW. Consequently, final designs may be expected to be slightly asymmetric with respect to the intended center frequency.

F. FREQUENCY SCALING

It can be noted that the low-pass transfer function, H(s), of the different filter classes has been presented on a normalized frequency basis (i.e., $\omega_c = 1$ rad / sec). One reason for this is the ease of working with simple normalized coefficients. If it is desired to shift the response of the filter up to a desired cutoff frequency, ω_c, frequency scaling is easily accomplished using the relation:

$$Sn = \frac{s}{\omega_c} \qquad (2\text{-}13)$$

Another reason is flexibility. In frequency transformations, the equations have already been conveniently scaled to operate on the normalized low-pass transfer function. For these reasons, filter design handbooks and tables [Refs. 9, 10] publish only the poles and zeros of the normalized low-pass transfer function of the different classes of filters for different orders. A frequency transformation procedure operating directly on poles and zeros given in Ref. 9 was shown by J. Tow [Ref. 11] and is contained in Appendix A.

G. THE FILTER DESIGN PROCEDURE

At this point, a filter design procedure may now be outlined. It will consist of two phases:

1. Determining the transfer function, H(s), from the given specifications.

2. Realizing the transfer function by means of available synthesis procedures.

Given a set of specifications consisting of a desired amplitude response and a desired phase response or a desired time response to a step input, the best approximation from the different filter classes is selected. If the filter desired is low-pass, then all that is involved is frequency scaling to the desired cutoff frequency, ω_c. If the filter desired is high-pass, bandpass, or band-reject, then the appropriate frequency transformation is done to come up with the required transfer function, H(s).

Once this transfer function has been decided upon and determined, the active filter network may be synthesized using any of the different synthesis procedures that will be discussed in the following chapters.

It is useful, at this point, to observe that if the general second-order transfer function

$$H(s) = \frac{a_2 s^2 + a_1 s + a_o}{s^2 + b_1 s + b_o} \qquad (2\text{-}14)$$

can be written as

$$H(s) = K \cdot \frac{s^2 + (\omega_n/Q_n)\, s + \omega_n^2}{s^2 + (\omega_o/Q)\, s + \omega_o^2}, \qquad (2\text{-}15)$$

where K is an arbitrary gain factor, ω_o is the resonant frequency, Q the selectivity factor, ω_n the "notch frequency," and Q_n the "notch attenuation factor," then the four different filter types may be conveniently written as follows:

Low-pass:

$$H(s) = \frac{K \omega_o^2}{s^2 + (\omega_o/Q)\, s + \omega_o^2} \tag{2-16}$$

High-pass:

$$H(s) = \frac{K s^2}{s^2 + (\omega_o/Q)\, s + \omega_o^2} \tag{2-17}$$

Bandpass:

$$H(s) = \frac{K \omega_o s}{s^2 + (\omega_o/Q)\, s + \omega_o^2} \tag{2-18}$$

Band-reject:

$$H(s) = K \cdot \frac{s^2 + \omega_n^2}{s^2 + (\omega_o/Q) s + \omega_o^2} \tag{2-19}$$

where, in each case, the numerator polynomial of equation (2-15) has been modified to conform with the transfer function characteristics of each filter type.

The second-order transfer function is emphasized because not only does it serve as a simple model to realize using the different

synthesis techniques but, more important, the current trend in realizing filter transfer functions of any desired order is to break them up into first- and second-order product terms, realize each of these terms individually using first- and second-order building-block networks and cascade these to produce the desired transfer function. This concept will be treated in greater detail in Chapter VII of this paper.

H. EXAMPLES

Several examples to illustrate the first phase of the design procedure outlined in the preceding section follow.

Example 2-1. A second-order Butterworth filter operating at a low-pass cutoff frequency of 10 Hz is to be realized. Specify its transfer function.

The desired transfer function can be specified directly by using equation (2-16):

$$H(s) = \frac{3947.84}{s^2 + 88.84s + 3947.84} \qquad (2\text{-}20)$$

where $K = 1$, $\omega_o = 2\pi(10)$ and $1/Q = 1.414$.

Computer Program 1 contained in Appendix B was used to give a magnitude-frequency plot of this low-pass filter. The plot is shown in Figure 2-6.

Example 2-2. Specify a transfer function for a low-pass filter with a cutoff frequency of 10 Hz. Its magnitude response is to be essentially flat in the passband. A fall-off rate of 100 dB / decade beyond cutoff is desired. Linearity of phase is desirable but not necessary.

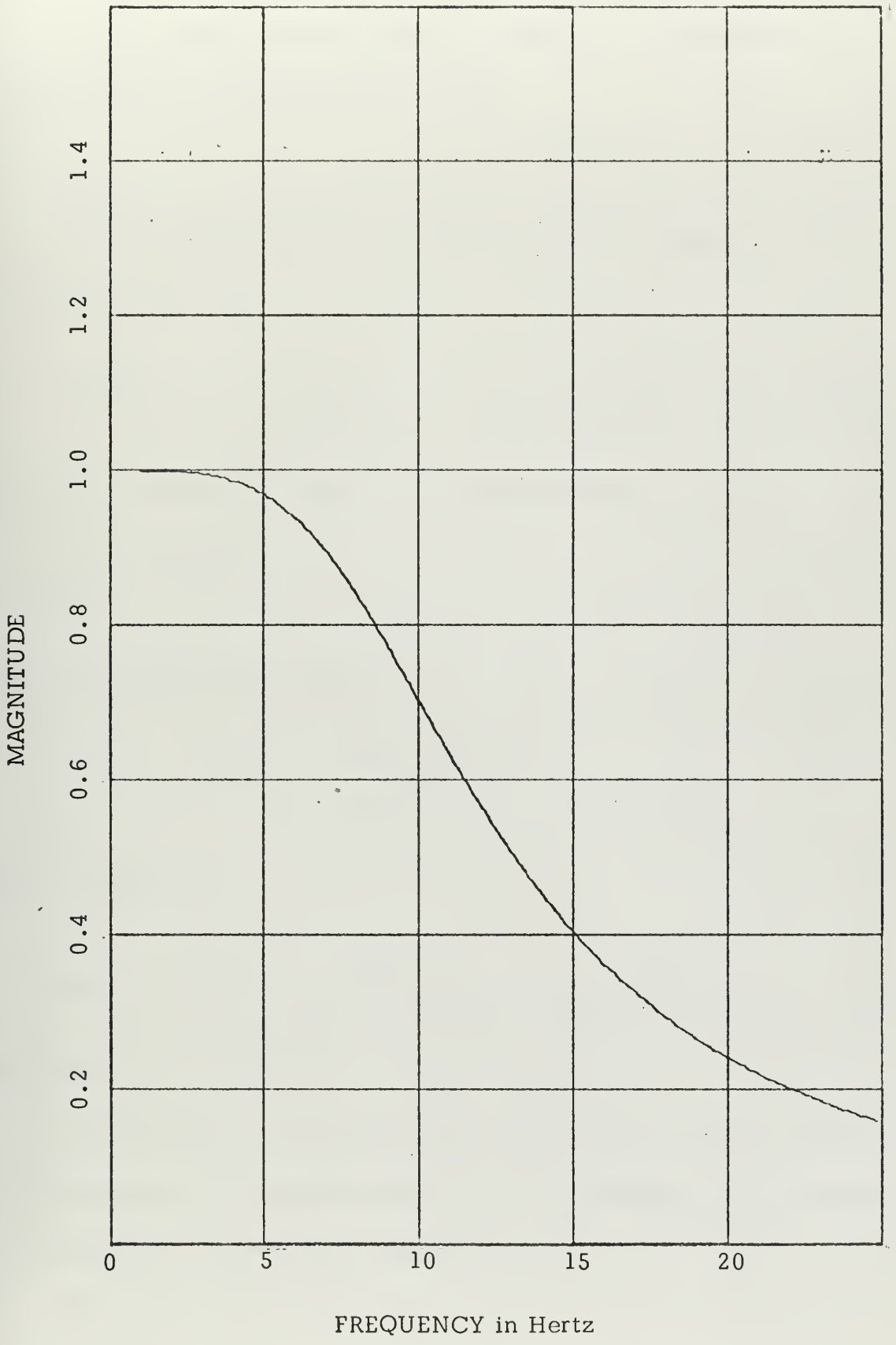

Figure 2-6. Magnitude vs Frequency Plot of Filter Transfer Function of Example 2-1.

A fifth-order Butterworth filter is chosen. Its normalized low-pass transfer function from Table 2-1 is

$$H(s) = \frac{1}{s^5 + 3.236s^4 + 5.236s^3 + 5.236s^2 + 3.236s + 1} \qquad (2\text{-}21)$$

or, in factored form,

$$H(s) = \frac{1}{s+1} \cdot \frac{1}{s^2 + 0.618s + 1} \cdot \frac{1}{s^2 + 1.618s + 1} \qquad (2\text{-}22)$$

Frequency scaling is called for and the substitution

$$Sn = s/2\ \pi\ (10) \qquad (2\text{-}23)$$

is applied to equations (2-21) and (2-22) resulting in the desired low-pass filter transfer function

$$H(s) = \frac{979261972.65}{s^5 + 203.32s^4 + 20670.89s^3 + 1298790.11s^2 + 50434489.00s + 979261972.65} \qquad (2\text{-}24)$$

or, in factored form,

$$H(s) = \frac{62.83}{s+62.83} \cdot \frac{3947.84}{s^2+38.83s+3947.84} \cdot \frac{3947.84}{s^2+101.66s+3947.84} \qquad (2\text{-}25)$$

Its magnitude response plot is shown in Figure 2-7.

Example 2-3. A high-pass filter with a 3-dB ripple in the pass-band operating at a cutoff frequency of 10 Hz is desired. Phase response is not critical. Specify its transfer function.

A 3-dB ripple Chebyshev filter would satisfy the requirements. Its normalized low-pass transfer function [Ref. 10] is

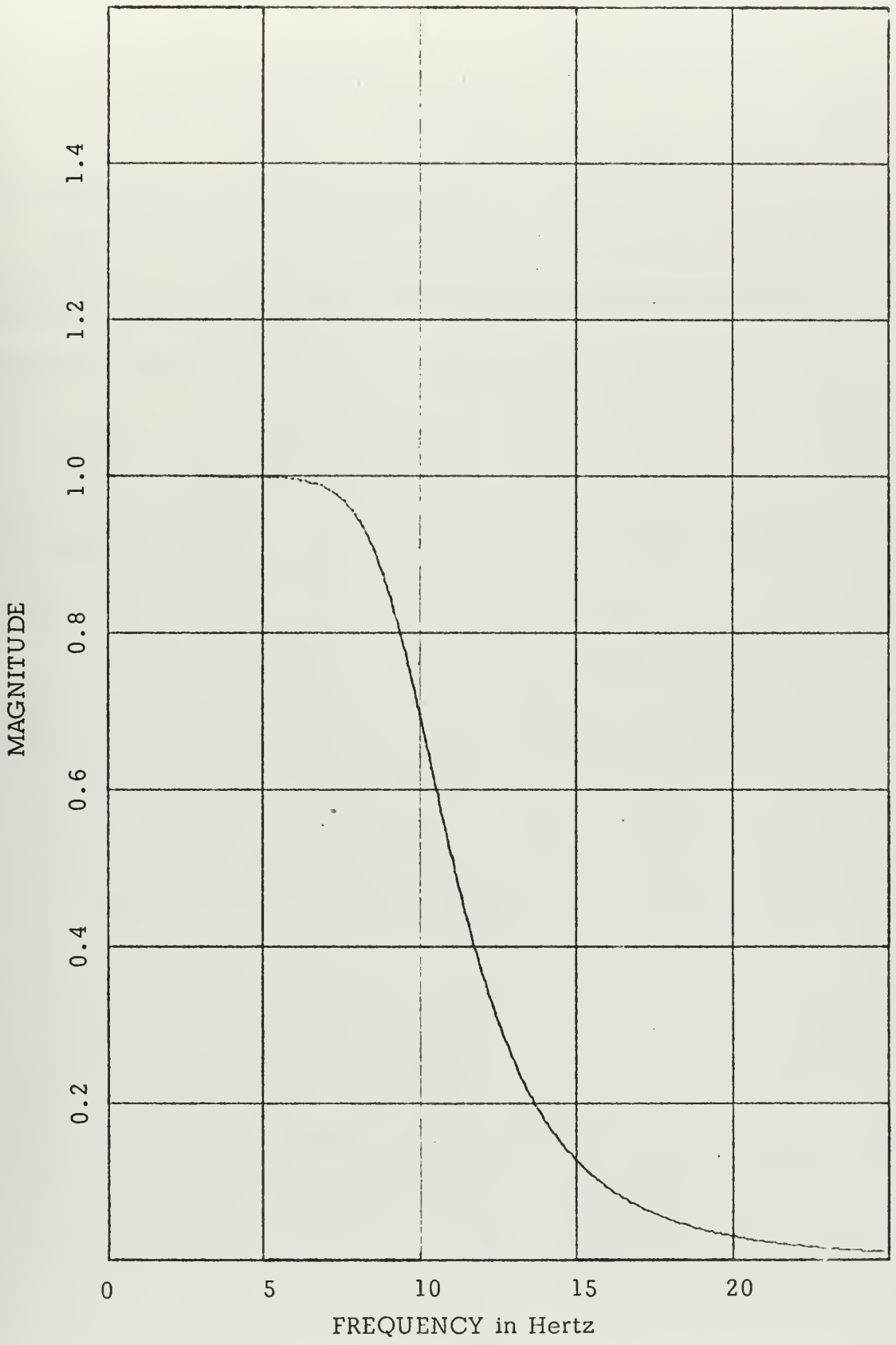

Figure 2-7. Magnitude vs Frequency Plot of Filter Transfer Function of Example 2-2.

$$H(s) = \frac{0.7079478}{s^2 + 0.6448996s + 0.7079478} \quad . \qquad (2\text{-}26)$$

The frequency transformation relation

$$Sn = 2\ \pi\ (10)/s \qquad (2\text{-}27)$$

is applied to equation (2-26). The resulting frequency-transformed transfer function is

$$H(s) = \frac{s^2}{s^2 + 57.24s + 5576.46} \quad . \qquad (2\text{-}28)$$

The magnitude-frequency plot using Computer Program 1 is shown in Figure 2-8.

Example 2-4. Specify a second-order bandpass transfer function with center frequency at 10 Hz and a Q of 50.

Application of equation (2-18) gives

i. this is $\frac{\omega_0}{Q} = \frac{2\pi \times 10}{50} = 1.257$

$$H(s) = \frac{62.83s}{s^2 + (62.83/50)s + (62.83)^2} \quad ,$$

or

$$H(s) = \frac{62.83s}{s^2 + 1.257s + 3947.84} \quad . \qquad (2\text{-}29)$$

The magnitude response plot is shown in Figure 2-9.

Example 2-5. A bandpass filter is desired with center frequency at 10 Hz and Q of 100. Essentially linear phase is desired within the passband. Specify its transfer function.

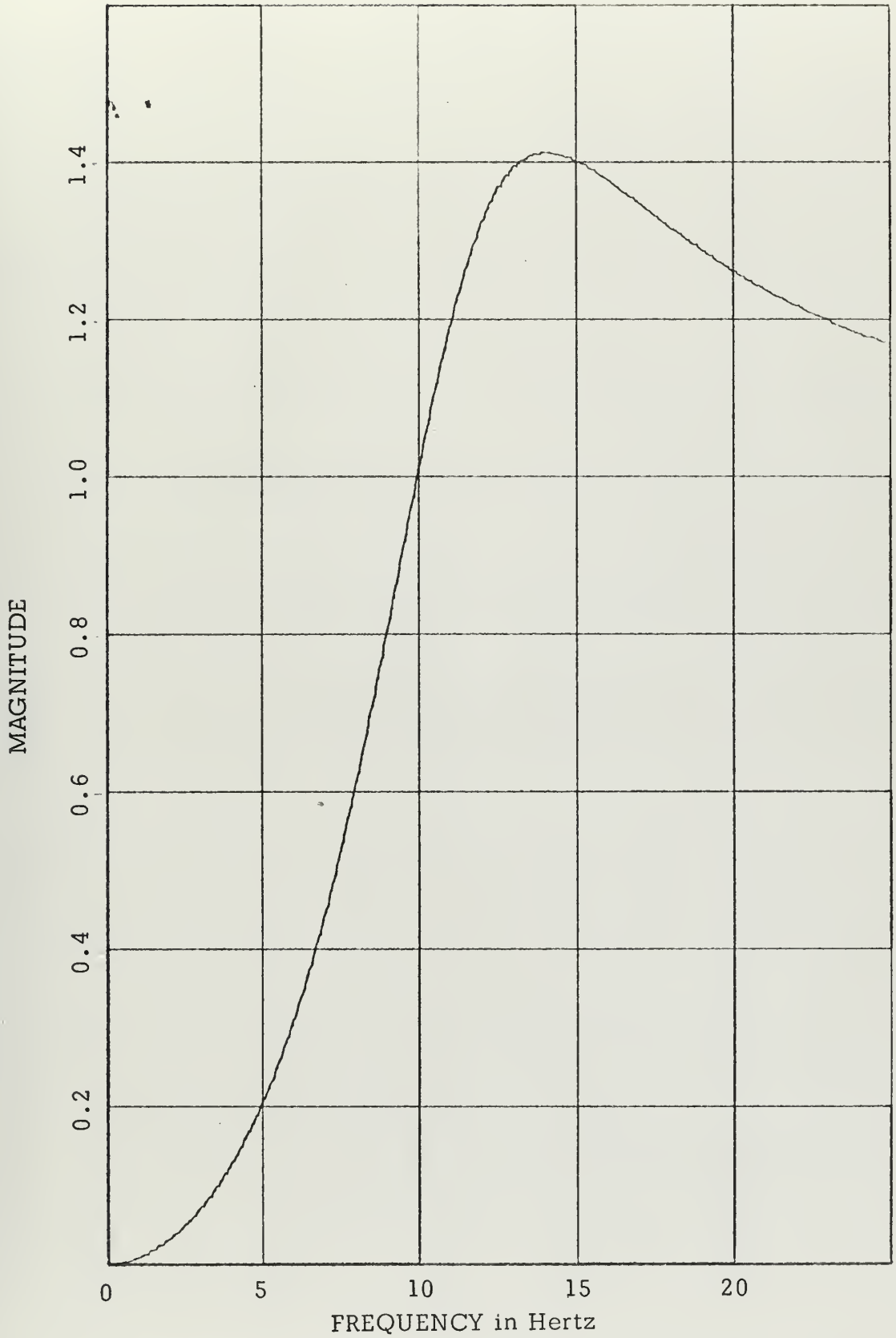

Figure 2-8. Magnitude vs Frequency Plot of Filter Transfer Function of Example 2-3.

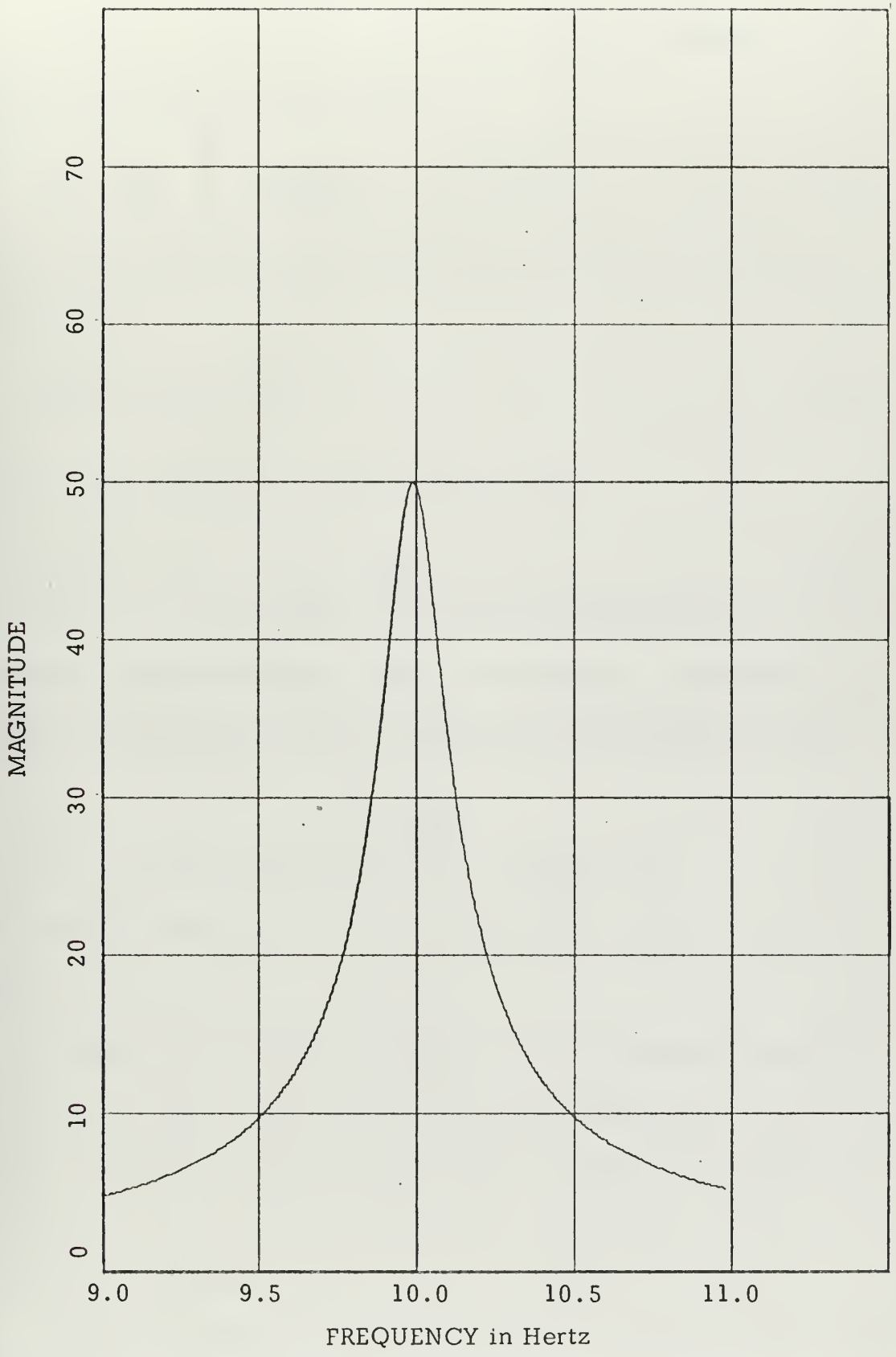

Figure 2-9. Magnitude vs Frequency Plot of Filter Transfer Function of Example 2-4.

The linear phase requirement calls for a Bessel response, so the appropriate frequency transformation

$$Sn = \frac{1}{100}\left[\frac{s}{2\pi(10)} + \frac{2\pi(10)}{s}\right] \qquad (2\text{-}30)$$

is applied to the normalized low-pass Bessel transfer function from Table 2-5,

$$H(s) = \frac{3}{s^2 + 3s + 3} \cdot \qquad (2\text{-}31)$$

A fourth-order bandpass transfer function results:

$$H(s) = \frac{1.18s^2}{s^4+1.88s^3+7896.86s^2+744.50s+15585441.60} \cdot \qquad (2\text{-}32)$$

The fourth-order denominator of the transfer function in equation (2-32) may be factored [1] into two second-order polynomials to give

$$H(s) = \frac{1.18s^2}{(s^2+0.94s+3913.80)\,(s^2+0.95s+3982.18)} \cdot \qquad (2\text{-}33)$$

The magnitude-frequency plot of equation (2-32) is shown in Figure 2-10.

Example 2-6. A filter to reject signals at frequencies between 9 to 11 Hz is desired. Second-order Chebyshev characteristics with 1/2-dB ripples are specified. Generate the transfer function to be synthesized.

---

[1] Subroutine POLRT was used to determine the roots of the fourth-order denominator polynomial.

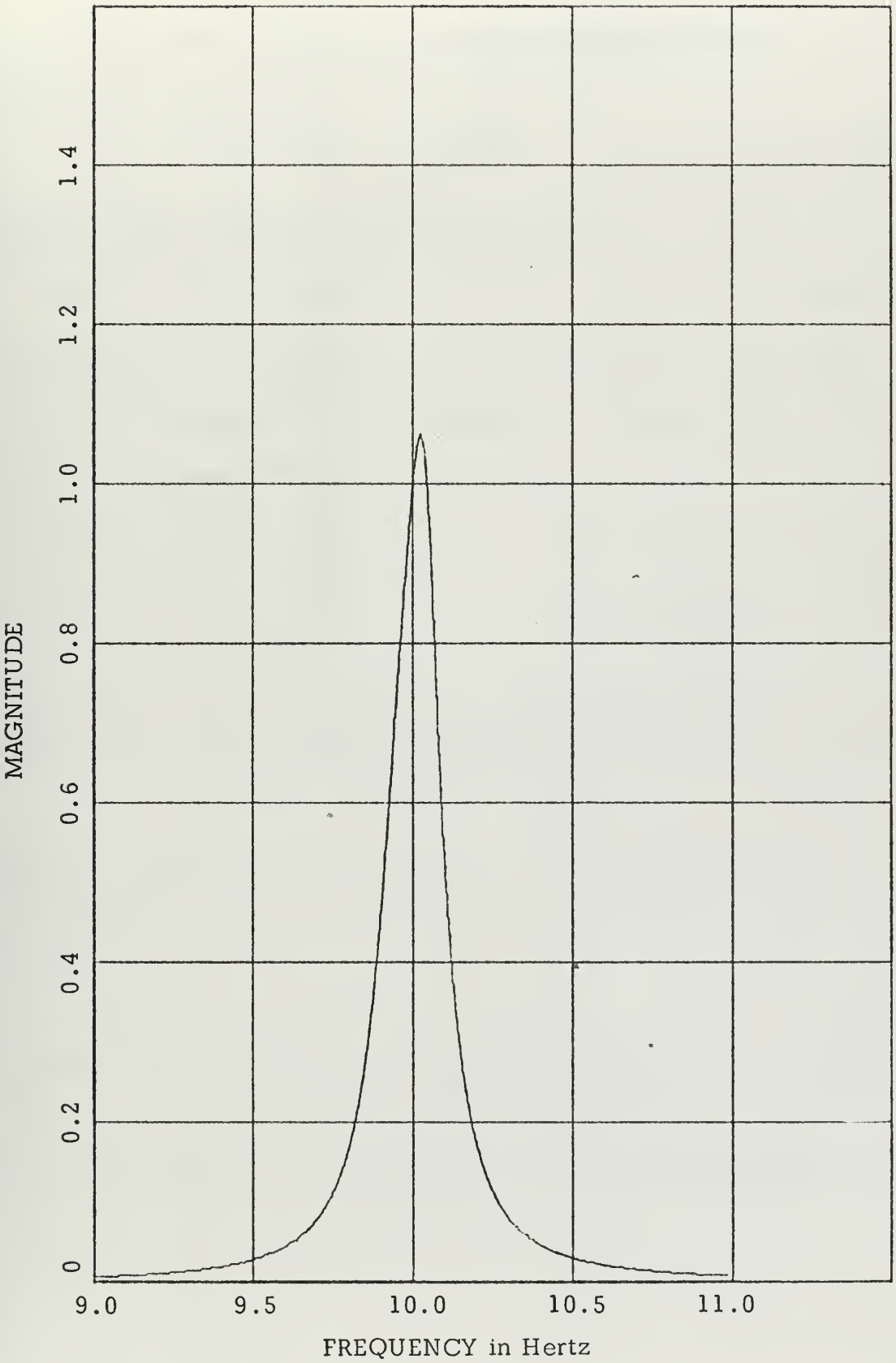

Figure 2-10. Magnitude vs Frequency Plot of Filter Transfer Function of Example 2-5.

Using equation (2-11), the appropriate center frequency, ω_o, is calculated: $\omega_o = \sqrt{\omega_l \omega_u} = \sqrt{27\pi \times 9 \times 27\pi} =$

$$\omega_o = \sqrt{2\pi(9.11)} = \sqrt{198\pi}\,. \tag{2-34}$$

Bandwidth, BW, is determined by equation (2-12):

$$BW = 2\pi(11-9) = 4\pi\,. \tag{2-35}$$

Low-pass-to-band-reject frequency transformation given by equation (2-10c) is then applied to the normalized second-order low-pass Chebyshev transfer function from Table 2-3a:

$$H(s) = \frac{1.516}{s^2 + 1.425s + 1.516}\,. \tag{2-36}$$

The resulting transfer function is

$$H(s) = \frac{s^4 + 7816s^2 + 15275291.31}{s^4 + 11.81s^3 + 7920.89s^2 + 46165.78s + 15275291.31}\,. \tag{2-37}$$

Factored for easy second-order realization, the transfer function becomes:

$$H(s) = \frac{s^2+3908.36}{s^2+5.51s+3420.98} \cdot \frac{s^2+3908.36}{s^2+6.30s+4465.19}\,. \tag{2-38}$$

The magnitude response plot of equation (2-37) is shown in Figure 2-11.

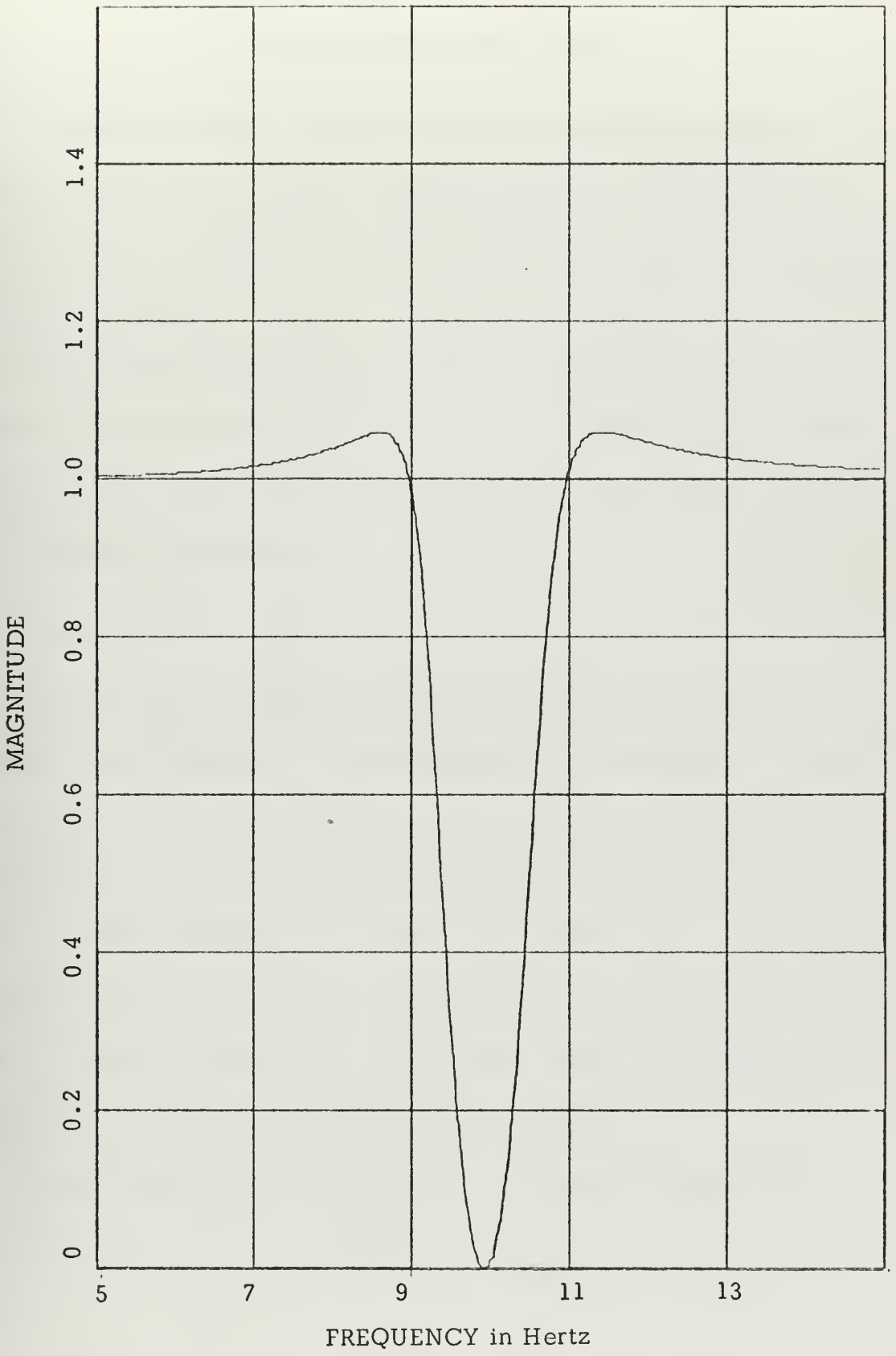

Figure 2-11. Magnitude vs Frequency Plot of Filter Transfer Function of Example 2-6.

III. THE OPERATIONAL AMPLIFIER

Having established a common starting point for the different synthesis techniques, it is now important to take a closer look at the common active element that is used in all of these methods and the type of analysis involved.

This chapter defines [1] the operational amplifier and shows how its distinctive characteristics simplify analysis of circuits using it. These same characteristics will be used to justify some fundamental assumptions in the synthesis techniques.

A. DEFINITION

The operational amplifier is a high-gain, DC-coupled amplifier having either a differential or single-ended input. The output is usually single-ended with respect to ground. For the differential-input type, a circuit model is shown in Figure 3-1. Signals applied to the terminal marked + In are amplified by a positive non-inverting gain, + A. Signals applied to the terminal marked - In are amplified by a negative - A. The output is given by $E_o = A(E_2 - E_1)$. The single-ended amplifier may be treated as the special case where + In is grounded.

The idealized characteristics of the operational amplifier are:

1. Gain = ∞ $(A \longrightarrow \infty)$

---

[1] Courtesy of the Burr-Brown Research Corporation from the "Burr-Brown Handbook and Catalog of Operational Amplifiers," 1969.

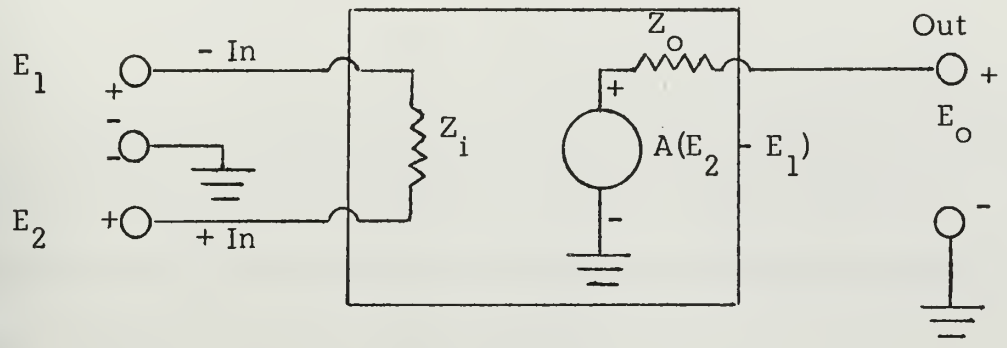

Figure 3-1. Circuit model for the differential-input type of operational amplifier

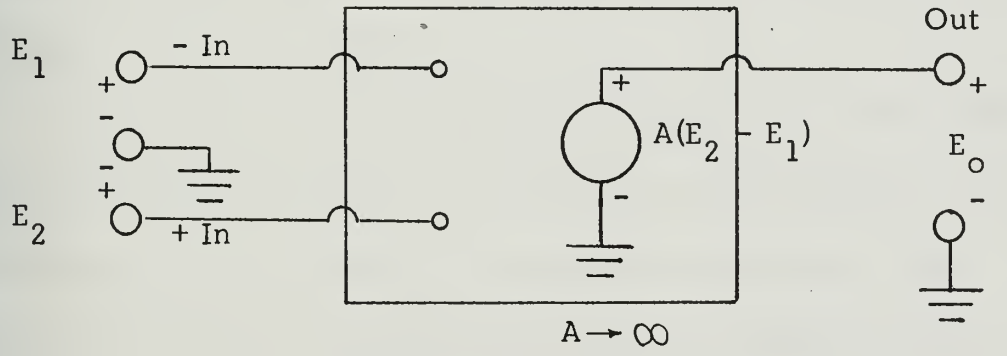

Figure 3-2. Idealized model of the differential-input type of operational amplifier

2. $E_o = O$ when $E_1 = E_2$

3. Input Impedance = ∞ ($Z_i \longrightarrow \infty$)

4. Output Impedance = O ($Z_o \longrightarrow$ O)

5. Bandwidth = ∞ (response time = O)

When these idealized characteristics are incorporated, the circuit model of the operational amplifier reduces to that of Figure 3-2. This idealized model will be used in developing equations for many of the basic feedback circuits in later chapters.

The most common circuit symbols for the operational amplifier are shown in Figure 3-3.

B. ANALYSIS

To illustrate the kind of circuit analysis that follows from the idealized model, a fundamental inverting circuit such as Figure 3-4 will be used as an example.

The common feature of these circuits is that the non-inverting input is connected to ground. Feedback and input networks are attached to the inverting input terminal. In analyzing the circuit, a gain A is assumed. This gain is subsequently allowed to approach infinity. Since amplifier input impedance is infinite, zero current flows into the amplifier; consequently R_1 and R_2 carry equal currents. This may be stated as $I_1 = I_2$ or

$$I_1 = \frac{E_1 - E_s}{R_1} = \frac{E_s - E_o}{R_2} = I_2. \qquad (3\text{-}1)$$

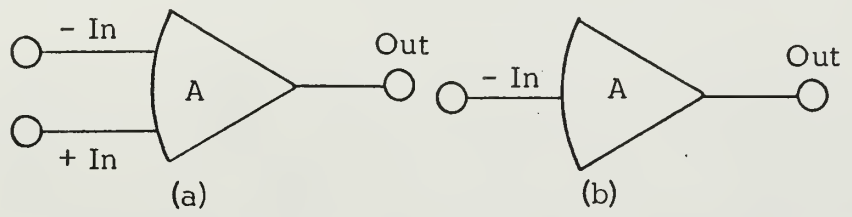

Figure 3-3. Common circuit symbols for the operational amplifier (a) Differential-input (b) Single-ended

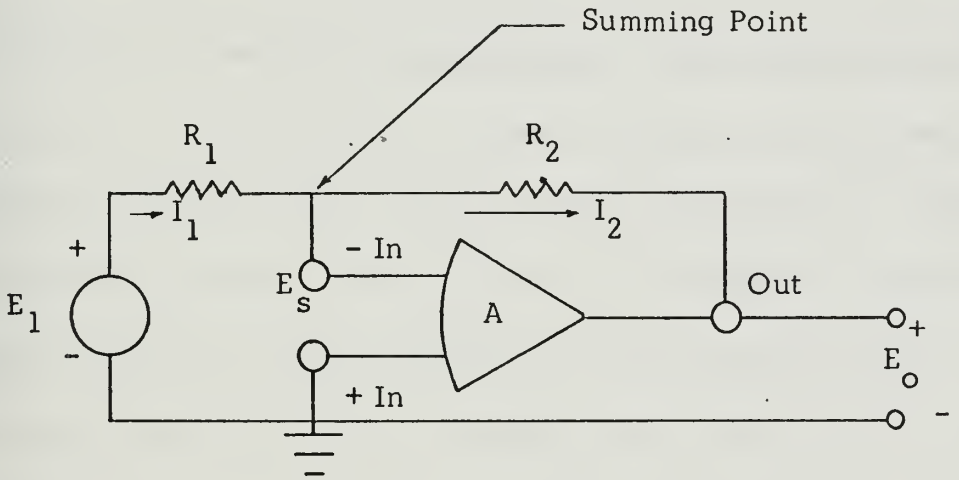

Figure 3-4. Fundamental inverting amplifier circuit

The amplifier gain enforces the condition

$$E_o = -AE_s \tag{3-2}$$

Solving equation (3-2) for E_s and substituting into equation (3-1) yields

$$\frac{E_1 + \frac{E_o}{A}}{R_1} = \frac{-\frac{E_o}{A} - E_o}{R_2} . \tag{3-3}$$

If the assumption $A \longrightarrow \infty$ is now applied, equation (3-3) becomes

$$\frac{E_1}{R_1} = -\frac{E_o}{R_2} . \tag{3-4}$$

The overall (closed loop) gain, or transfer function, is

$$\frac{E_o}{E_1} = -\frac{R_2}{R_1} . \tag{3-5}$$

Note that the gain includes a sign inversion. This sign inversion will be appropriately indicated in the different transfer functions that were generated in Chapter II when these are used as examples for realization in the following chapters. Note also that its magnitude is determined solely by the ratio of external resistors. Another important point is that the summing point voltage, E_s, approaches zero as the gain, A, approaches infinity.

$$E_s = -\frac{E_o}{A} \longrightarrow 0 \; ; \; A \longrightarrow \infty . \tag{3-6}$$

This condition is described by referring to the summing point as a "virtual ground" (since it is held at virtually zero or ground potential).

With the summing point at ground potential, the current through R_1 is $I_1 = E_1 / R_1$ and therefore entirely independent of R_2. Since no current flows into the amplifier, the input circuit may be thought of as a source of current which must flow through the feedback impedance, in this case R_2. Since one end of R_2 is at ground potential (the summing point), the other end must be at a voltage of $- I_1 R_2 = E_o$.

The feedback element need not be a resistor but can be any impedance Z_2. This will be seen in the next chapter. In fact, it need not be a linear element but can be any element, or set of elements, for which there is a linear relation between short-circuit current and terminal voltage. Similarly the input circuit is subject to equal freedom. Figure 3-5 illustrates a complex network of this type.

If neither input to the operational amplifier is grounded, the same analysis still holds. Consider the network in Figure 3-6. The output voltage, E_o, is

$$E_o = A(E_{g2} - E_{g1}). \tag{3-7}$$

As A approaches infinity,

$$E_{g2} - E_{g1} = O. \tag{3-8}$$

Observe that the operational amplifier's infinite gain forces its two inputs to be equal. It will also be noted that since no current flows into the operational amplifier

$$E_2 = E_{g2} = E_{g1}, \tag{3-9}$$

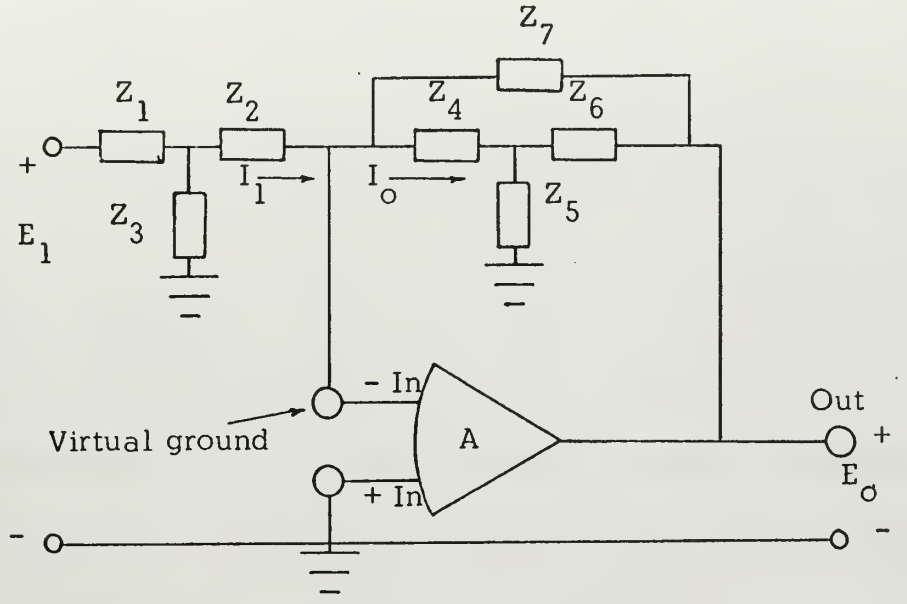

Figure 3-5. Complex linear feedback circuit

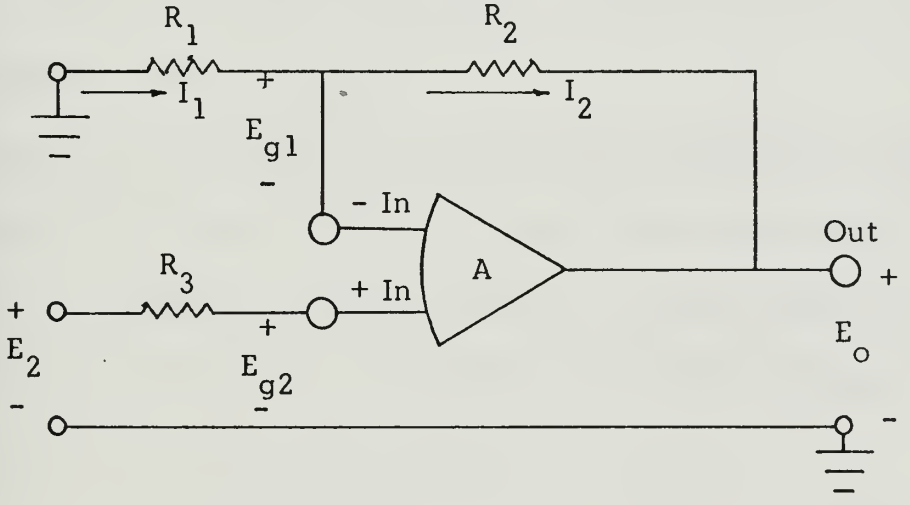

Figure 3-6. Feedback circuit with neither input to the operational amplifier grounded

and

$$I_1 = \frac{-E_2}{R_1} = I_2 = \frac{E_2 - E_o}{R_2} \quad . \tag{3-10}$$

Simplifying equation (3-10), the voltage transfer function of the network is

$$\frac{E_o}{E_2} = \frac{R_1 + R_2}{R_1} \tag{3-11}$$

Regardless of the complexity allowed in the input and feedback networks, the same summing point restraints will always be found to hold:

1. The summing point is a virtual ground.

2. No current flows into the amplifier; current flowing into the input circuit must flow into the feedback circuit.

C. NATHAN'S MATRIX ANALYSIS

Since matrix analysis lends itself to more complicated circuits, it would also be convenient to know a matrix analysis of circuits constrained by an operational amplifier proposed by Nathan [Ref. 12]. Such analysis will be illustrated in later chapters and a brief discussion of it is contained in Appendix C of this paper.

IV. INFINITE-GAIN SINGLE-FEEDBACK REALIZATIONS

This chapter presents the first of five categories into which synthesis techniques for active RC filters using operational amplifiers have been classified. The synthesis procedures involve one infinite-gain operational amplifier with a single feedback loop and consequently, the significant contributions falling under this general category are presented and are collectively known as Infinite-Gain Single-Feedback Realizations.

A. THEORETICAL DEVELOPMENT

The basic active filter configuration using one operational amplifier is shown in Figure 4-1. It employs one RC feedback network, N_B, across the operational amplifier, an RC network, N_A, in series with the inverting input source and another RC network, N_C, in series with the non-inverting input source.

The following two-port equations may be written for this active configuration:

$$I_1 = y_{11A}E_1 + y_{12A}E_3 \qquad (4\text{-}1a)$$

$$I_3 = y_{21A}E_1 + y_{22A}E_3 \qquad (4\text{-}1b)$$

$$I_2 = y_{11C}E_2 + y_{12C}E_4 \qquad (4\text{-}2a)$$

$$I_4 = y_{21C}E_2 + y_{22C}E_4 \qquad (4\text{-}2b)$$

$$I_5 = y_{11B}E_5 + y_{12B}E_6 \qquad (4\text{-}3a)$$

$$I_6 = y_{21B}E_5 + y_{22B}E_6 \; . \qquad (4\text{-}3b)$$

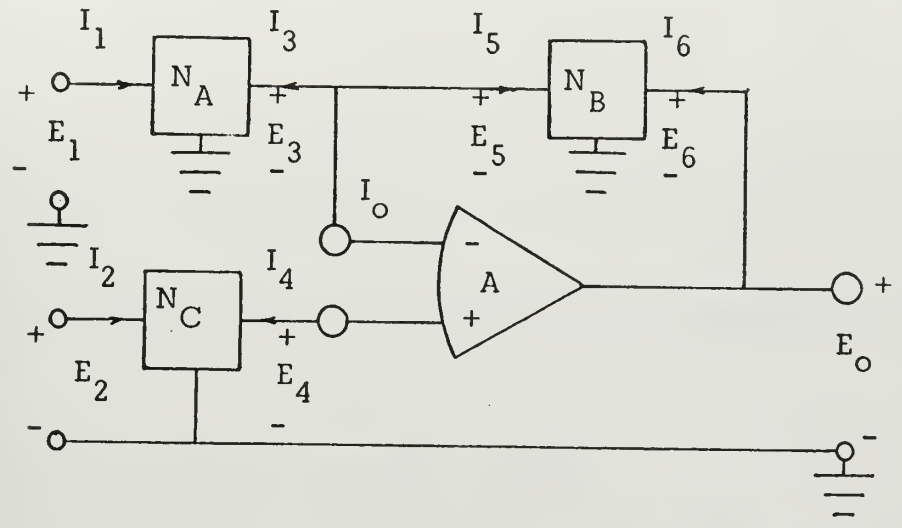

Figure 4-1. Basic single-feedback active filter configuration

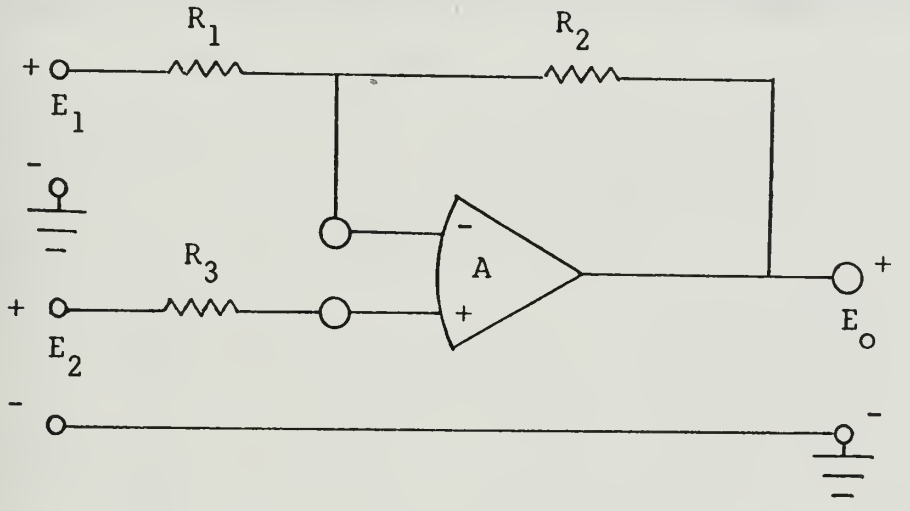

Figure 4-2. Differential-input operational amplifier using resistors for input and feedback elements

Application of one of the summing point restraints developed in Chapter III, namely, that no current flows into the operational amplifier because of its infinite input impedance, results in:

$$I_o = 0 \ , \tag{4-4}$$

$$I_4 = 0 \ . \tag{4-5}$$

Because of equation (4-4), $I_3 = - I_5$, so that from equations (4-1b) and (4-3a):

$$y_{21A}E_1 + y_{22A}E_3 = - y_{11B}E_5 - y_{12B}E_6 . \tag{4-6}$$

As a consequence of equation (4-5), equation (4-2b) becomes:

$$E_4 = \frac{-y_{21C}}{y_{22C}} E_2 \ . \tag{4-7}$$

Use of the other summing point restraint, namely, that the summing point is a "virtual ground" yields:

$$E_3 = E_4 = E_5 . \tag{4-8}$$

Applying equation (4-8) to equation (4-7) gives:

$$E_5 = \frac{- y_{21C}}{y_{22C}} E_3 \ , \tag{4-9}$$

$$E_3 = \frac{- y_{21C}}{y_{22C}} E_3 \ . \tag{4-10}$$

Substituting equations (4-9) and (4-10) into equation (4-6) gives an expression for E_6:

$$E_6 = E_o = \frac{-y_{21A}}{y_{12B}} E_1 + \left(\frac{y_{21C}}{y_{22C}}\right)\left(\frac{y_{11B} + y_{22A}}{y_{12B}}\right) E_2 \qquad (4\text{-}11)$$

Note that E_o is expressed as a function of the two input voltages and the admittance parameters of the three passive networks, N_A, N_B and N_C. To verify this result, note that if the three passive networks were each single resistors as shown in Figure 4-2, such that

$$\begin{aligned} y_{21A} &= -1/R_1 & y_{22A} &= 1/R_1 \\ y_{12B} &= -1/R_2 & y_{11B} &= 1/R_2 \\ y_{21C} &= -1/R_3 & y_{22C} &= 1/R_3 \,, \end{aligned} \qquad (4\text{-}12)$$

application of equation (4-11) gives:

$$E_o = \frac{-R_2}{R_1} E_1 + \left(\frac{R_1 + R_2}{R_1}\right) E_2 \,, \qquad (4\text{-}13)$$

Note that if the non-inverting input, $E_2 = 0$, equation (4-13) corresponds to equation (3-5) and if $E_1 = 0$, equation (4-13) corresponds to equation (3-11).

The general expression given by equation (4-11) can now be applied to a more restricted case where the non-inverting input voltage, $E_2 = 0$, giving:

$$\frac{E_o}{E_1} = -\frac{y_{21A}}{y_{12B}} \,, \qquad (4\text{-}14)$$

which is the open-circuit voltage transfer function of the more common network configuration shown in Figure 4-3. This is the basic network

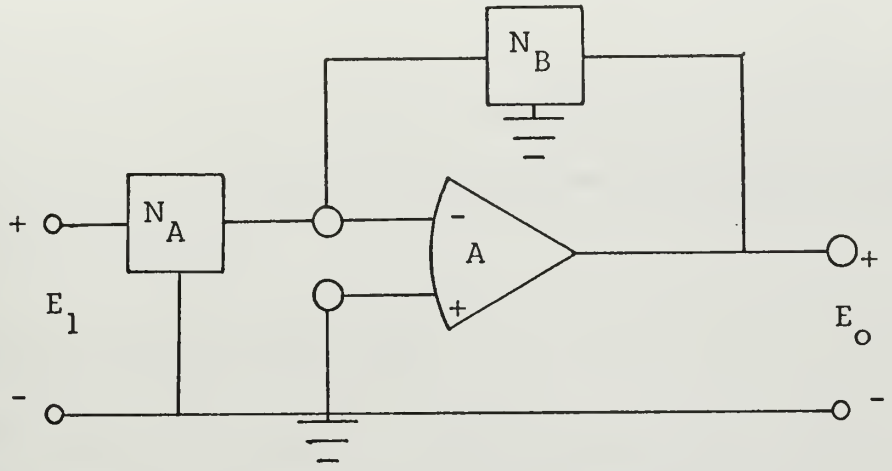

Figure 4-3. Single-ended operational amplifier in basic single-feedback configuration

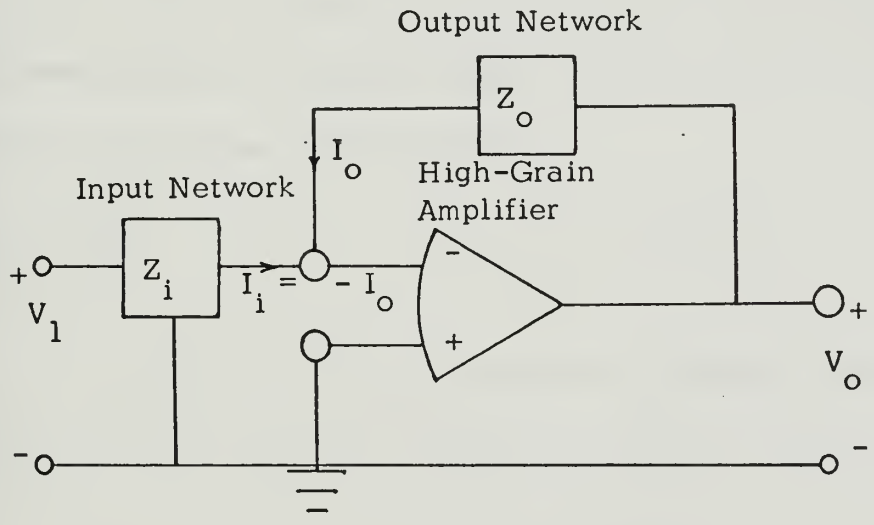

Figure 4-4. Active Network configuration of Bradley and McCoy

configuration to produce second-order transfer functions. Its importance lies in the fact that higher orders are achieved by simply cascading such configurations.

Equation (4-14) is the starting point for all the synthesis methods that fall under this category. A more rigorous derivation of this equation is contained in Ref. 22.

B. BRADLEY AND McCOY [1952]

Writing about driftless DC amplifiers for a Reeves model A-105 computer, Bradley and McCoy [Ref. 13] proposed the use of DC amplifiers in combination with passive networks to generate complex transfer functions as a generalization of summation or integration. Calling Z_i and Z_o the short-circuit transfer impedances of the input and feedback networks respectively, as shown in Figure 4-4, they used as a basis for their work the voltage transfer function,

$$\frac{V_o}{V_1} = \frac{Z_o}{Z_i} \quad , \tag{4-15}$$

where $Z_o = 1/y_{12B}$ and $Z_i = 1/y_{21A}$ in relation to equation (4-14).

They generated an extensive table of transfer impedance functions with their corresponding RC networks and accompanying relations to determine element values for the networks.

Synthesis of a desired transfer function involves choosing appropriate input and output networks such that their transfer impedances, when applied to equation (4-15), produce the desired transfer function.

Element values of each network may then be chosen by coefficient-matching.

An example of this procedure follows.

Example 4-1. Realize the low-pass Butterworth filter transfer function of Example 2-1, where the negative sign is introduced because of operational amplifier inverting action:

$$H(s) = \frac{V_o(s)}{V_1(s)} = - \frac{3947.84}{s^2 + 88.84\, s + 3947.84} , \qquad (4\text{-}16)$$

or, in a more convenient form for this procedure,

$$H(s) = - \frac{1}{1 + \frac{88.84}{3947.84}\, s + \frac{1}{3947.84}\, s^2} . \qquad (4\text{-}17)$$

Two transfer impedance functions are now taken off the transfer impedance table in Ref. 13:

$$A_1 (1 + sT) , \qquad (4\text{-}18a)$$

where

$$A_1 = R_1$$

$$T = R_1 C , \qquad (4\text{-}18b)$$

and

$$A_2 \left(\frac{1 + sT_2}{1 + sT_1 + s^2 T_1 T_2} \right) , \qquad (4\text{-}19a)$$

where

$$A_2 = 2R_2$$

$$T_1 = 2R_2C_2$$

$$T_2 = R_2C_1/2 \quad . \tag{4-19b}$$

The RC configuration corresponding to equation (4-18) is shown in Figure 4-5a; that for equation (4-19) is shown in Figure 4-5b.

It can be observed that if $Z_i = A_1 (1 + sT)$ and $Z_o = A_2 (1 + sT_2)/(1 + sT_1 + s^2T_1T_2)$,

$$H(s) = \frac{A_2 (1 + sT_2)/(1 + sT_1 + s^2T_1T_2)}{A_1 (1 + sT)} \quad . \tag{4-20}$$

Setting $T = T_2$ gives

$$H(s) = \frac{A_2/A_1}{1 + sT_1 + s^2T_1T_2} \quad . \tag{4-21}$$

Equating coefficients of equations (4-21) and (4-16) yields

$$\frac{A_2}{A_1} = 1$$

$$T_1 = \frac{88.84}{3947.84} \tag{4-22}$$

$$T_1T_2 = \frac{1}{3947.84} \quad .$$

Simplified, the relations in equation (4-22) become

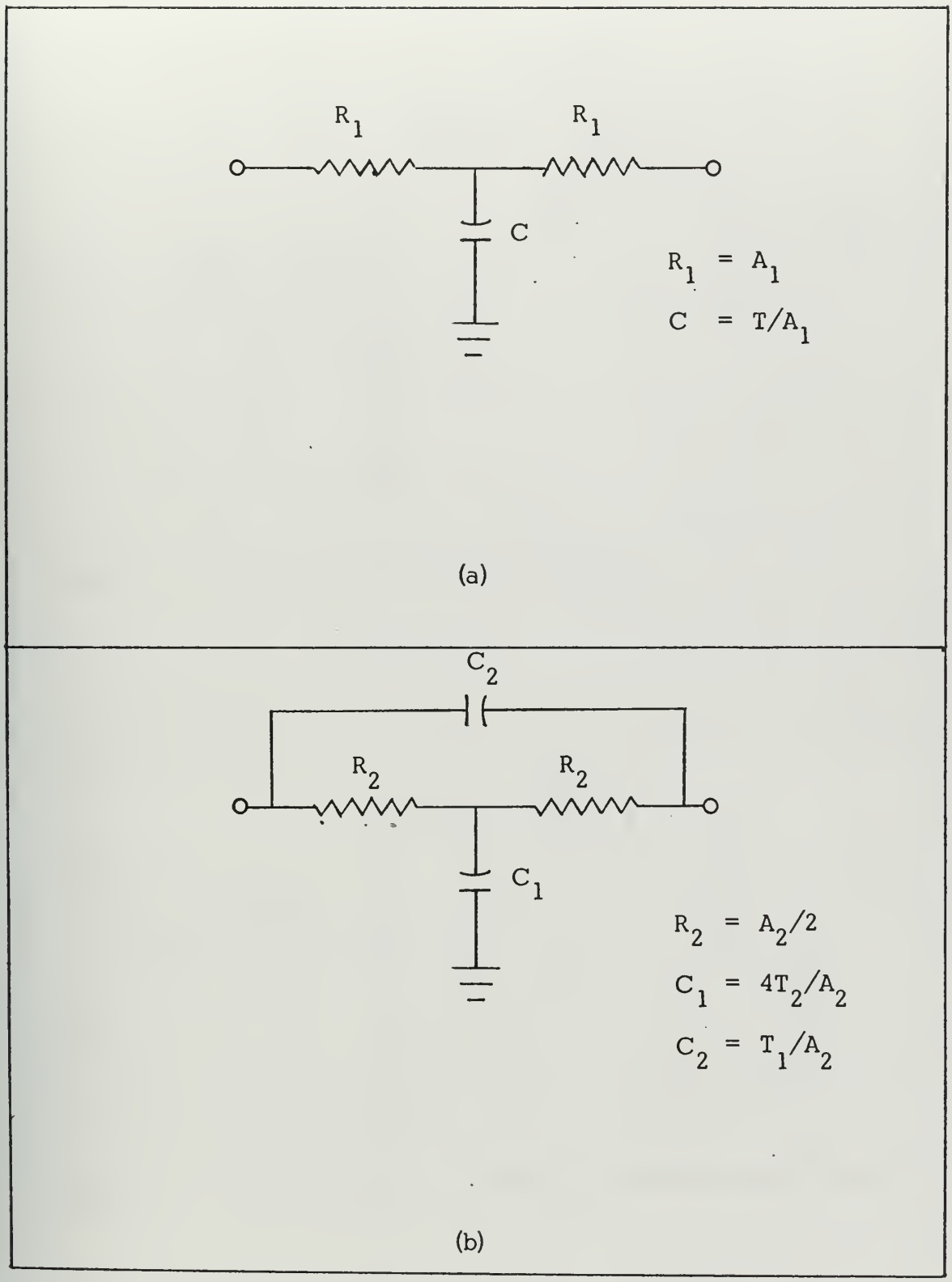

Figure 4-5. Transfer impedance networks from the table of Bradley and McCoy

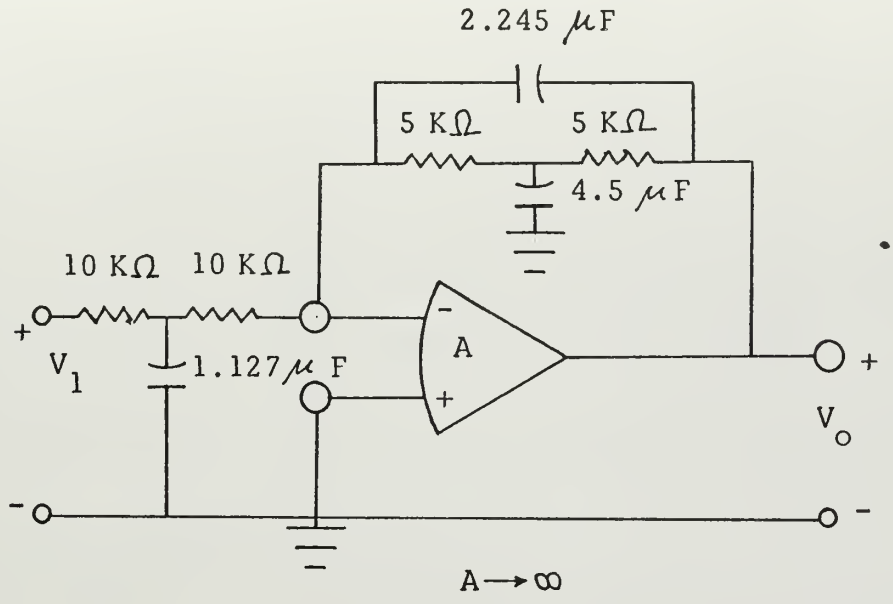

Figure 4-6. Circuit realization of Example 4-1

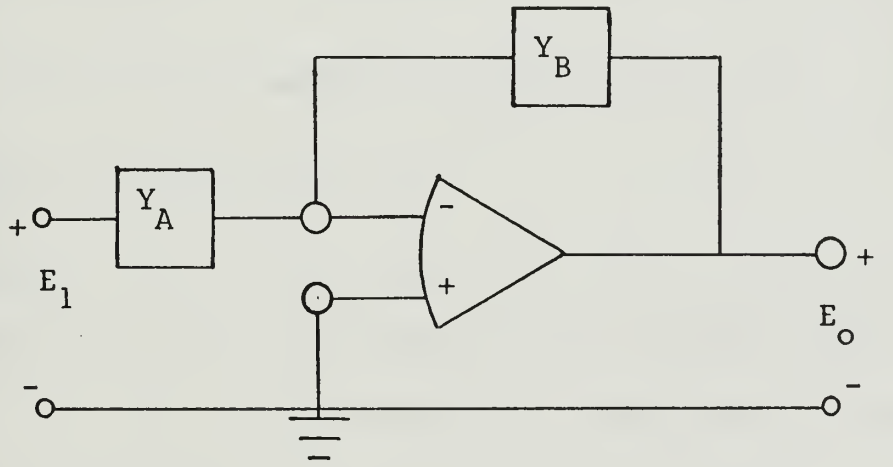

Figure 4-7. Active network configuration of Mathews and Seifert

$$A_2 = A_1$$

$$T_1 = 2.245 \times 10^{-2} \qquad (4\text{-}23)$$

$$T_2 = 1.127 \times 10^{-2} = T \quad .$$

Applying the relations in Figures 4-5a and 4-5b and arbitrarily choosing $R_1 = 10\ K\Omega$ give the component values for the two networks:

$$R_2 = R_1/2 = 5\ K\Omega$$

$$C = \frac{1.127 \times 10^{-2}}{10^4} = 1.127\ \mu F$$

$$C_1 = \frac{4 \times 1.127 \times 10^{-2}}{10^4} = 4.5\ \mu F$$

$$C_2 = \frac{2.245 \times 10^{-2}}{10^4} = 2.245\ \mu F \qquad (4\text{-}24)$$

and the resulting circuit realization is shown in Figure 4-6.

C. MATHEWS AND SEIFERT [1955]

Mathews and Seifert presented a paper [Ref. 14] which described three systematic synthesis methods for realizing complex transfer functions. The first of these belongs to the single-feedback realization category of this chapter.

Mathews and Seifert approached the synthesis problem in two ways.

Using the basic feedback configuration shown in Figure 4-7, they assumed an infinite-gain amplifier and initially treated $Y_A(s)$ and $Y_B(s)$ as <u>two-terminal</u> RC driving-point admittance networks to come up with the open-circuit voltage transfer function:

$$\frac{E_o(s)}{E_1(s)} = -\frac{Y_A(s)}{Y_B(s)} \quad . \tag{4-25}$$

Consequently, the poles and zeros of each $Y_A(s)$ and $Y_B(s)$ must alternate along the negative real axis of the complex-frequency plane and the lowest critical frequency of each must be a zero. In effect, the poles and zeros of the transfer function must all lie on the negative real axis. However, since the transfer function poles are the poles of $Y_A(s)$ and the zeros of $Y_B(s)$ and since the transfer function zeros are the zeros of $Y_A(s)$ and the poles of $Y_B(s)$, two transfer function poles or two zeros may occur together and the transfer function lowest critical frequency may be a pole. This situation is shown in Figure 4-8. One has, in effect, a realizable transfer function so long as all transfer function poles and zeros are restricted to lie along the negative real axis including the origin. A given transfer function can, therefore, be written as

$$\frac{E_o(s)}{E_1(s)} = -\frac{N(s)/Q(s)}{D(s)/Q(s)} \quad , \tag{4-26}$$

where $N(s)/Q(s) = Y_A(s)$ and $D(s)/Q(s) = Y_B(s)$ and where $Q(s)$ is selected so that both $Y_A(s)$ and $Y_B(s)$ can be realized as two-terminal RC driving-point admittance networks. The synthesis of $Y_A(s)$ and $Y_B(s)$ may now be carried out individually.

One method of synthesis is a partial-fraction expansion [Ref. 15] of $Y_A(s)$ and $Y_B(s)$ as indicated by $Y(s)$ below:

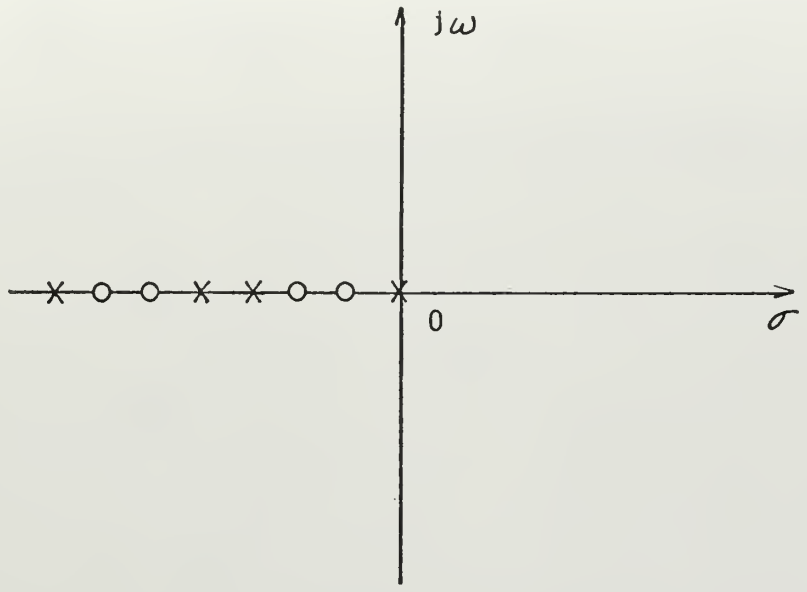

Figure 4-8. Location of poles and zeros for 2-terminal RC network configuration

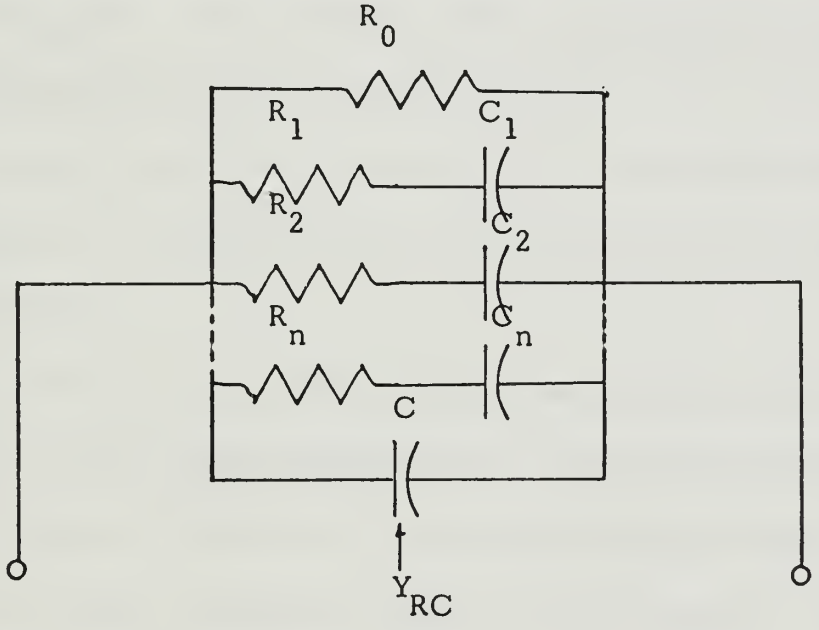

Figure 4-9. Second Foster form realization of an RC admittance function

$$\frac{Y(s)}{s} = \frac{K_o}{s} + \frac{K_1}{s+\sigma_1} + \ldots\ldots + K_\infty \quad . \tag{4-27}$$

Subsequent multiplication by s of each term in the right-hand side of equation (4-27) gives

$$Y(s) = K_o + \sum_{i=1}^{n} \frac{K_i s}{s+\sigma_i} + K_\infty s \quad , \tag{4-28a}$$

or

$$Y_{RC}(s) = K_o + \sum_{i=1}^{n} \frac{1}{\frac{1}{K_i} + \frac{\sigma_i}{K_i s}} + K_\infty s \quad , \tag{4-28b}$$

where $K_o = 1/R_o$, $K_\infty = C_\infty$ and each $1/K_i = R_i$ and each $K_i/\sigma_i = C_i$ in units of ohms for the R's and farads for the C's.

The resulting network for $Y_A(s)$ and $Y_B(s)$ is the configuration shown in Figure 4-9. Note that this is the second Foster form for an RC admittance function.

To give this synthesis method a more general application, Mathews and Seifert substituted <u>three-terminal</u> networks for the two-terminal networks, as shown in Figure 4-3. The transfer function of such a configuration was already developed in Section A of this chapter. The relation, assuming reciprocal networks, is

$$\frac{E_o(s)}{E_1(s)} = -\frac{y_{12A}(s)}{y_{12B}(s)} \quad , \tag{4-29}$$

where $y_{12A}(s)$ and $y_{12B}(s)$ are transfer admittance functions. The transfer admittance of a three-terminal RC network can have only simple poles [Ref. 16] which must lie on the negative real axis of the complex-frequency plane excluding the origin but may have zeros which lie anywhere in the complex-frequency plane except on the positive real axis. Since these zeros need not be simple, the transfer function in equation (4-29) is perfectly general.

The realization of a desired transfer function using the configuration in Figure 4-3 then boils down to synthesizing the transfer admittances in equation (4-29).

Several procedures [Refs. 17-19] are available for synthesizing such transfer admittances but for an example, the method of Guillemin [Ref. 17] will be used.

Example 4-2. Realize the high-pass transfer function derived in Example 2-3:

$$H(s) = - \frac{s^2}{s^2 + 57.24\, s + 5576.46} \quad . \tag{4-30}$$

The transfer function, H(s), in equation (4-29) may now be expressed as

$$H(s) = - \frac{N(s)/Q(s)}{D(s)/Q(s)} \quad , \tag{4-31}$$

where

$$y_{12A}(s) = - N(s)/Q(s) \tag{4-32a}$$

$$y_{12B}(s) = - D(s)/Q(s) \quad . \tag{4-32b}$$

For $y_{12A}(s)$ and $y_{12B}(s)$ to be realizable, the roots of Q(s) must be restricted to the negative real axis. Hence, Q(s) is judiciously [1] chosen to be

$$Q(s) = (s + 50)\ (s + 150) \quad , \tag{4-33}$$

such that

$$y_{12A}(s) = - \frac{s^2}{(s + 50)\ (s + 150)} \quad , \tag{4-34a}$$

$$y_{12B}(s) = - \frac{(5576.46 + 57.24\ s + s^2)}{(s + 50)\ (s + 150)} \quad . \tag{4-34b}$$

By Guillemin's procedure, driving-point admittance functions are then chosen with the same poles as the transfer admittances, $y_{12A}(s)$ and $y_{12B}(s)$. These driving-point admittances are then expanded into RC ladder networks in such a manner as to realize the zeros of the transfer admittances. For convenience, let

$$y_{11A}(s) = y_{11B}(s) = \frac{(s + 10)\ (s + 97.5)}{(s + 50)\ (s + 150)} \quad . \tag{4-35}$$

For reasons that will become apparent, $y_{12B}(s)$ is then decomposed as follows:

$$y_{12B}(s) = - \frac{(5576.46 + 57.24\ s)}{(s + 50)\ (s + 150)} - \frac{s^2}{(s + 50)\ (s + 150)} \quad , \tag{4-36}$$

such that

---

[1] The choice is arbitrary but it can happen that for a particular choice, the spread in the calculated element values becomes too wide to be practical.

$$y_{12B1}(s) = - \frac{(5576.46 + 57.24\ s)}{(s + 50)\ (s + 150)} \quad , \tag{4-37a}$$

$$y_{12B2}(s) = - \frac{s^2}{(s + 50)\ (s + 150)} \quad , \tag{4-37b}$$

$y_{11B}(s)$ is now expanded [Ref. 20] to realize the zeros of $y_{12B1}(s)$ at $s = -97.5$ and at $s = -\infty$:

$$y_{11B}(s) = y_{11B1}(s)$$

$$= \frac{1}{\frac{28.5}{s + 97.5} + 1 + \frac{1}{0.0156\ s + \frac{1}{6.4}}} \quad . \tag{4-38}$$

The resulting network, N_{B1}, is shown in Figure 4-10.

Again $y_{11B}(s)$ is expanded to realize the two zeros of $y_{12B2}(s)$ at $s = 0$:

$$y_{11B}(s) = y_{11B2}(s)$$

$$= \frac{1}{7.7} + \frac{1}{\frac{1}{0.0109\ s} + \frac{1}{\frac{1}{1.47} + \frac{1}{\frac{1}{0.00158\ s} + 6.3}}} \quad . \tag{4-39}$$

The resulting network, N_{B2}, is shown in Figure 4-11.

Before these two networks, N_{B1} and N_{B2}, can be connected in parallel to realize $y_{12B}(s)$, it is first necessary to adjust their individual admittance levels. From Figure 4-10, $y_{12B1}(s) = -1/7.693 = -0.13$ at $s = 0$ and equation (4-37a) gives $y_{12B1}(s) = -0.746$ at $s = 0$. A multiplier K_{B1} for the network, N_{B1}, is therefore

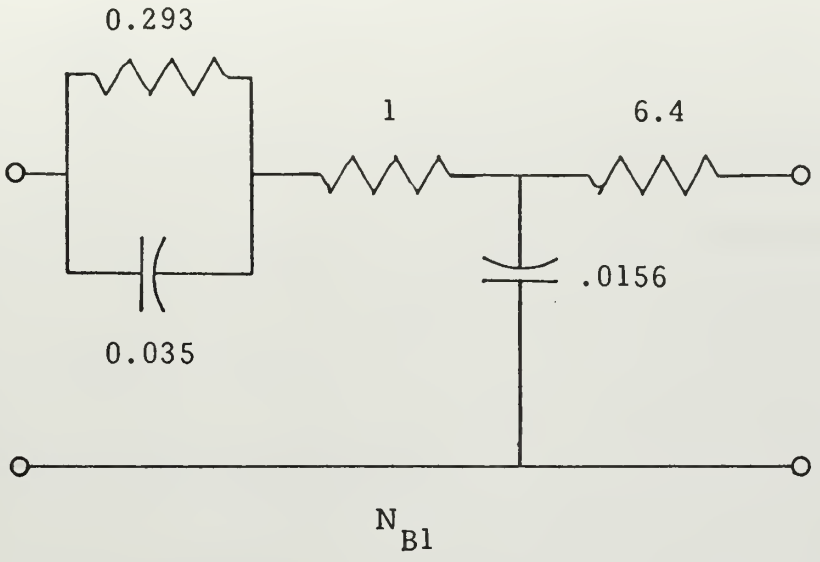

Figure 4-10. Circuit realization of $y_{12B1}(s)$ and $y_{11B1}(s)$

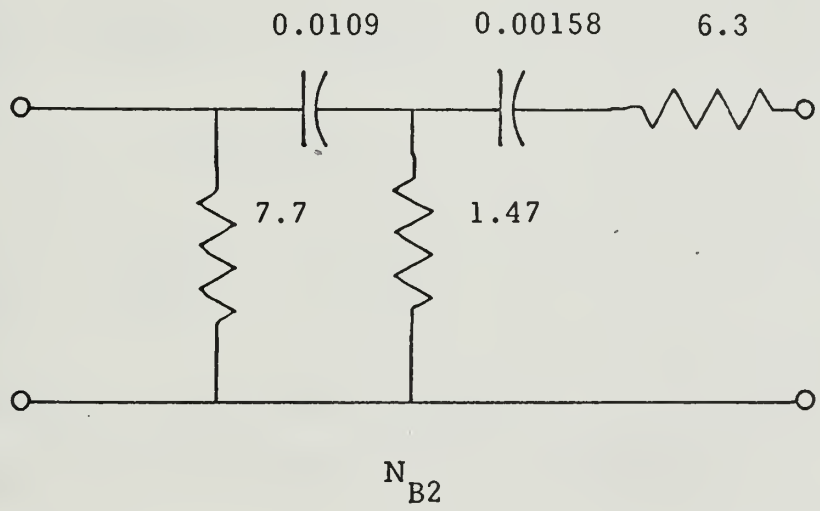

Figure 4-11. Circuit realization of $y_{12B2}(s)$ and $y_{11B2}(s)$

$$K_{B1} = \frac{0.13}{0.746} = 0.174 \quad . \tag{4-40}$$

For N_{B2}, $y_{12B2}(s) = -1/.63 = -0.159$ at $s = -\infty$ from Figure 4-11. From equation (4-37b), $y_{12B2}(s) = -1$ at $s = -\infty$. Consequently,

$$K_{B2} = \frac{0.159}{1} = 0.159 \quad . \tag{4-41}$$

K_B is then determined from the relation

$$\frac{1}{K_B} = \frac{1}{K_{B1}} + \frac{1}{K_{B2}} \tag{4-42}$$

to be $K_B = 0.0832$.

The admittance level of N_{B1} is now multiplied by

$$\frac{K_B}{K_{B1}} = \frac{0.0832}{0.174} = 0.478 \quad , \tag{4-43}$$

and that of N_{B2} is multiplied by

$$\frac{K_B}{K_{B2}} = \frac{0.0832}{0.159} = 0.523 \quad . \tag{4-44}$$

The realization of $y_{12A}(s)$ can be observed to be exactly the network, N_{B2}, except that the admittance level is multiplied by

$$K_A = K_{B2} = 0.159 \quad . \tag{4-45}$$

The complete network realization is shown in Figure 4-12. Note that the transfer function, H(s), in equation (4-30) is realized within the constant multiplier:

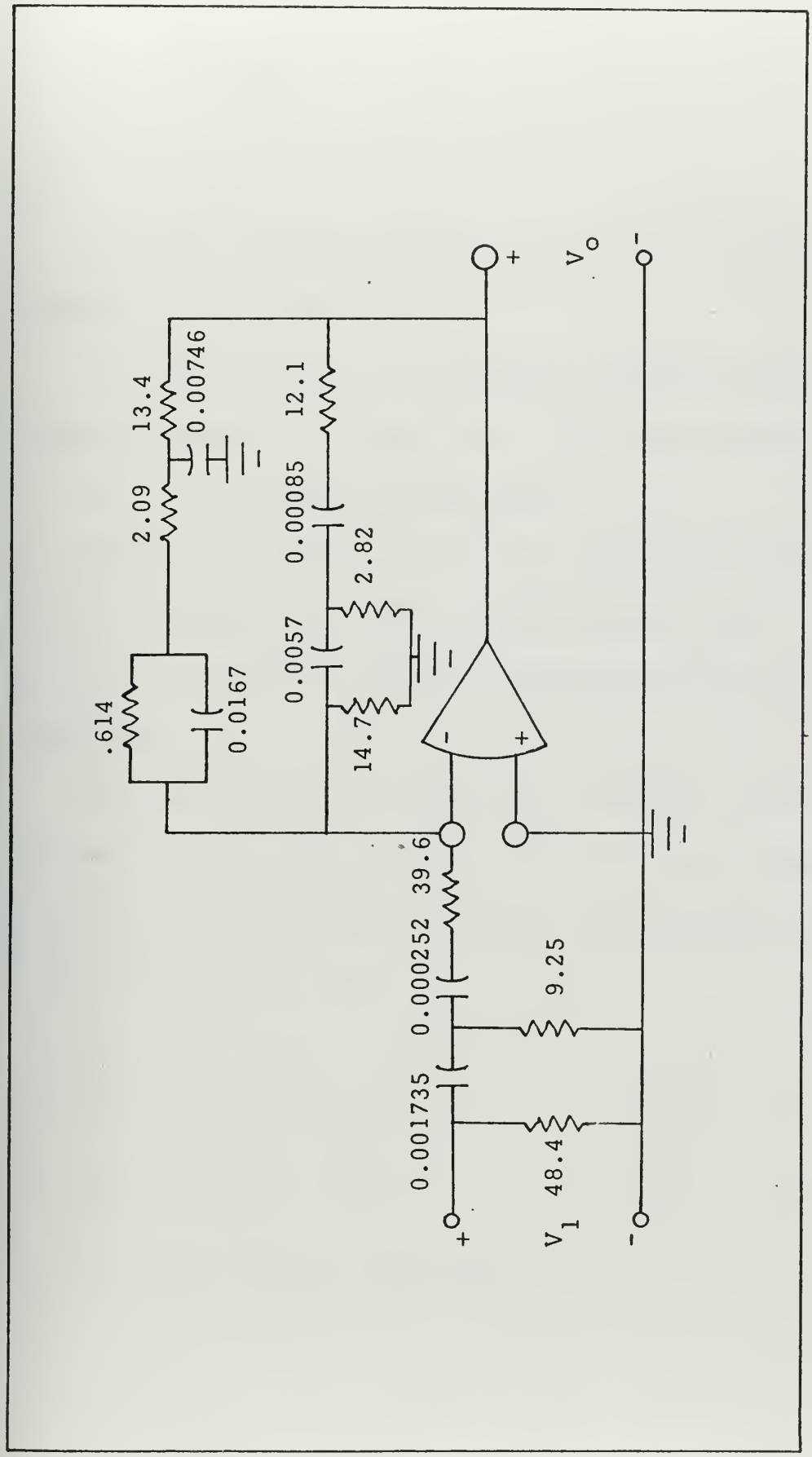

Figure 4-12. Circuit realization of Example 4-2

$$\frac{K_A}{K_B} = \frac{0.159}{0.0832} = 1.91 \quad . \tag{4-46}$$

D. PAUL [1963]

Paul [Ref. 21] sought to correct two limitations of the synthesis method of Mathews and Seifert:

1. No capability for independent adjustment of each transfer function coefficient, or, alternatively, of each pole and zero.

2. Wide spread of element values.

Using as a starting point the basic network configuration of Figure 4-3 and its corresponding voltage transfer function, $H(s) = - y_{21A}(s)/y_{12B}(s)$, he proposed the adjustable network configuration shown in Figure 4-13.

It can be noted that the three basic T-networks, shown in Figure 4-14 and governed by the relations in Table 4-2, are all integrated in both the input and the feedback networks. The configuration in Figure 4-13 is a special case where

$$N_1 = N_2 = 1$$

$$N_1 = R_C/2R_A = 1$$

$$N_2 = 2R_C/R_B = 1$$

$$\tau = C_A R_C = 2C_B R_C = 1/2\ C_C R_C \quad . \tag{4-47}$$

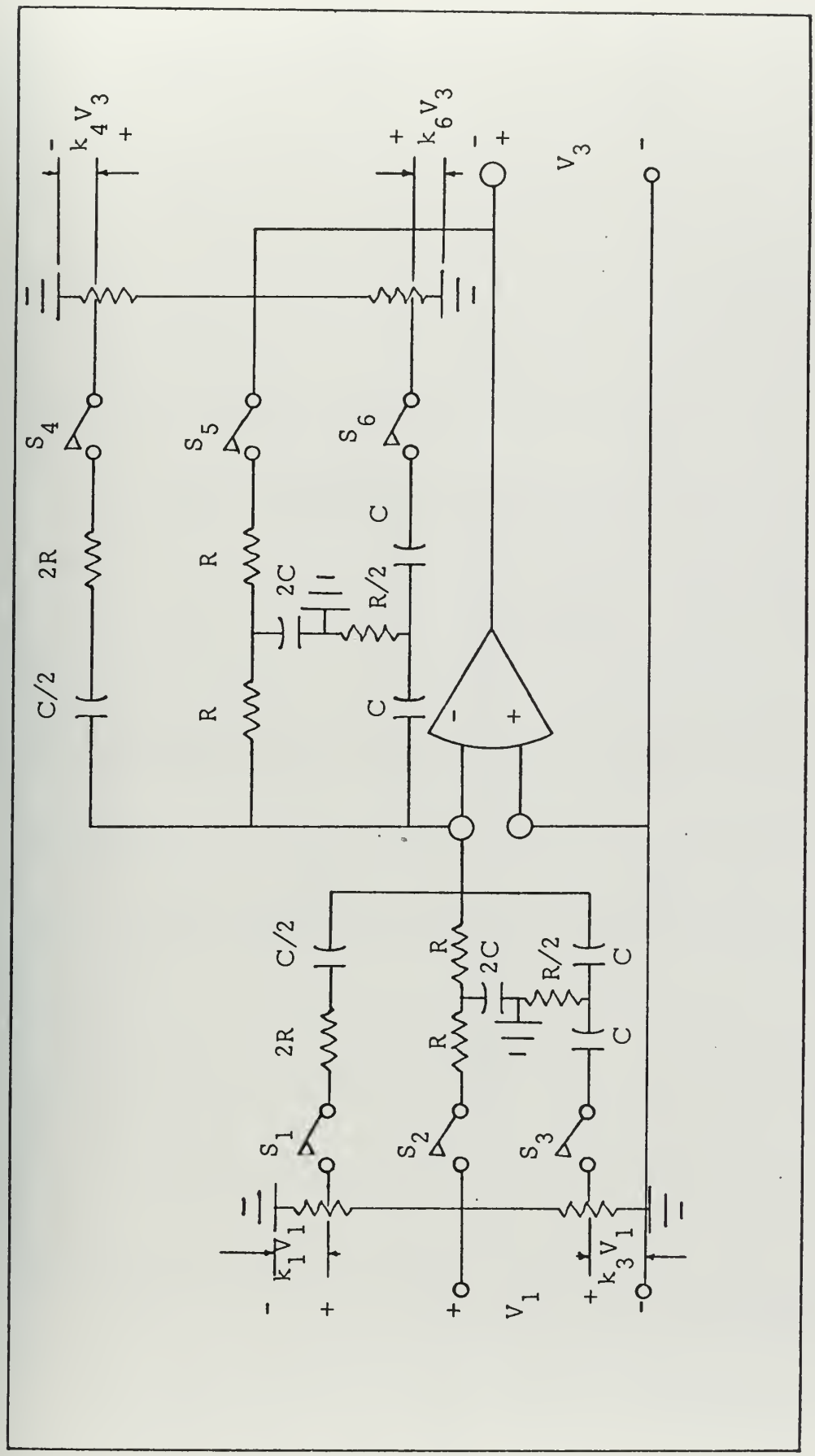

Figure 4-13. Paul's active network configuration

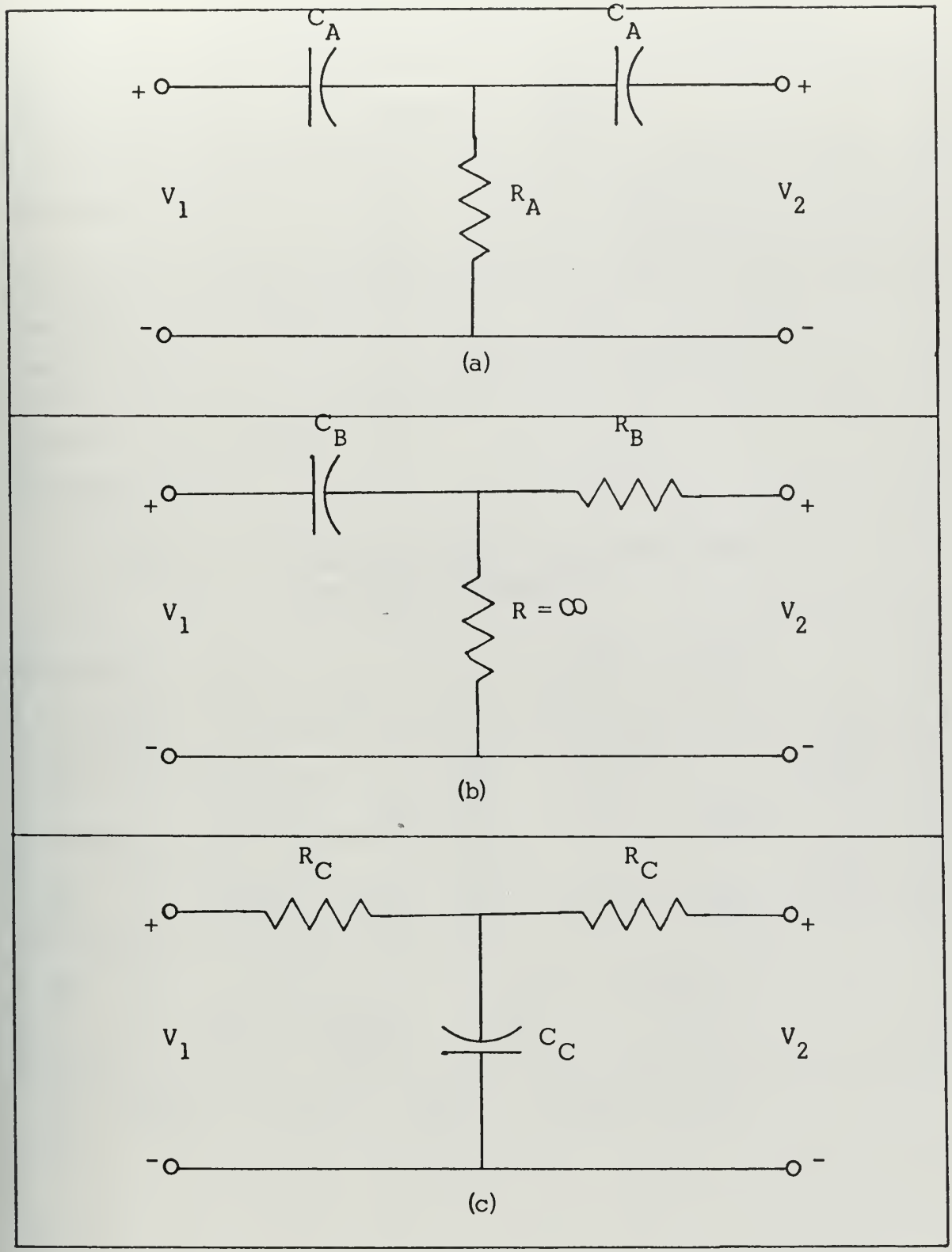

Figure 4-14. Type 1 T-Networks for Paul's configuration

Table 4-1. Some Transfer Functions Realizable by Figure 4-13

Network Conditions	$H(s) = \dfrac{V_o(s)}{V_1(s)}$
All switches closed	$-\dfrac{1 + k_1 s\tau + k_3 s^2\tau^2}{1 + k_4 s\tau + k_6 s^2\tau^2}$
Switches 1,2,4,5,6 closed Switch 3 open	$-\dfrac{1 + k_1 s\tau}{1 + k_4 s\tau + k_6 s^2\tau^2}$
Switches 1,2,4,5 closed Switches 3,6 open	$-\dfrac{1 + k_1 s\tau}{1 + k_4 s\tau}$

Table 4-2. Transfer Admittance Relationship of the Three Type 1 T-Networks

Network	$y_{21}(s) = -y_{12}(s)$
(a)	$\dfrac{s^2 C_A{}^2 R_A}{1+s2C_A R_A} = \dfrac{1}{2R_C}\left(\dfrac{R_C}{2R_A}\ \dfrac{s^2\tau^2}{1+s\tau}\right) = \dfrac{1}{2R_C}\left(\dfrac{N_1 s^2\tau^2}{1+s\tau}\right)$
(b)	$\dfrac{sC_B}{1+s\,C_B R_B} = \dfrac{1}{2R_C}\left(\dfrac{2R_C}{R_B}\ \dfrac{s\tau}{1+s\tau}\right) = \dfrac{1}{2R_C}\left(\dfrac{N_2 s\tau}{1+s\tau}\right)$
(c)	$\dfrac{1}{2R_C\left(1+\dfrac{sC_C R_C}{2}\right)} = \dfrac{1}{R_C}\left(\dfrac{1}{1+s\tau}\right)$

where $\tau = 2C_A R_A = C_B R_B = 1/2C_C R_C = CR$

If

$$C_A = 2C_B = 1/2\ C_C = C$$

$$R_C = 1/2\ R_B = 2R_A = R \quad , \tag{4-48}$$

then

$$\tau = CR \quad . \tag{4-49}$$

Some transfer function forms possible for the configuration in Figure 4-13 are given in Table 4-1.

Another special variation for the configuration shown in Figure 4-13 is the case where

$$N_1 = 1 \qquad N_2 = 2$$

$$N_1 = R_C/2R_A = 1$$

$$N_2 = 2R_C/R_B = 2$$

$$\tau = C_A R_C = C_B R_C = 1/2\ C_C R_C \quad . \tag{4-50}$$

If

$$C_A = C_B = 1/2\ C_C = C$$

$$R_C = R_B = 2R_A = R \quad , \tag{4-51}$$

then

$$\tau = CR \quad . \tag{4-52}$$

In this case, the transfer function forms tabulated in Table 4-1 result with every sT term in both numerator and denominator replaced by 2sT.

If, instead of three standard T-networks, an RC configuration, such as the one shown in Figure 4-15, is used as both the input and feedback networks, the transfer admittance of each network can be shown to be

$$y_{21}(s) = \frac{(1 + sCR_1)(1 + sCR_4)}{[2 + sC(R_1 + R_2)][R_3 + R_4 + sCR_3R_4] + [2 + sC(R_3 + R_4)][R_1 + R_2 + sCR_1R_2]} \quad (4\text{-}53)$$

and the resulting voltage transfer function is

$$H(s) = -\frac{(1 + sCR_A)(1 + sCR_D)}{(1 + sCR_B)(1 + sCR_C)} = -\frac{(1 + s\tau_A)(1 + s\tau_D)}{(1 + s\tau_B)(1 + s\tau_C)}, \quad (4\text{-}54)$$

where, in relation to the network in Figure 4-15, for the input network,

$$R_1 = R_A$$

$$R_2 = R_B$$

$$R_3 = R_C$$

$$R_4 = R_D, \quad (4\text{-}55)$$

and for the feedback network,

$$R_1 = R_B$$

$$R_2 = R_A$$

$$R_3 = R_D$$

$$R_4 = R_C. \quad (4\text{-}56)$$

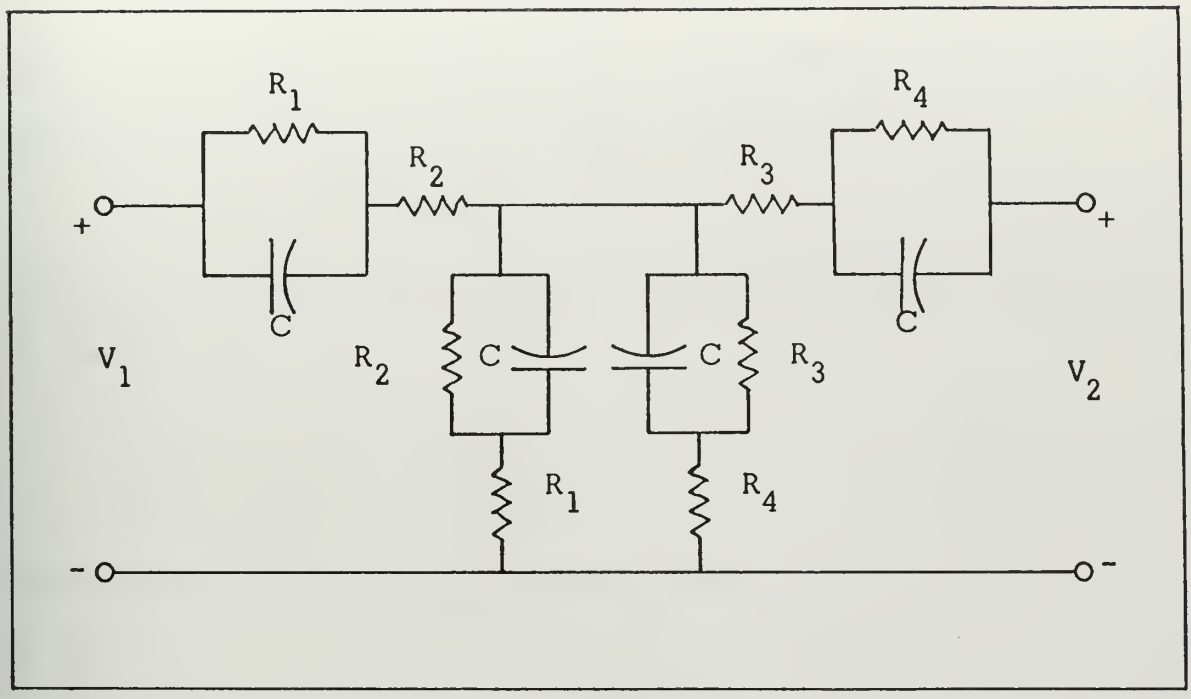

Figure 4-15. Type 2 T-Network for Paul's configuration

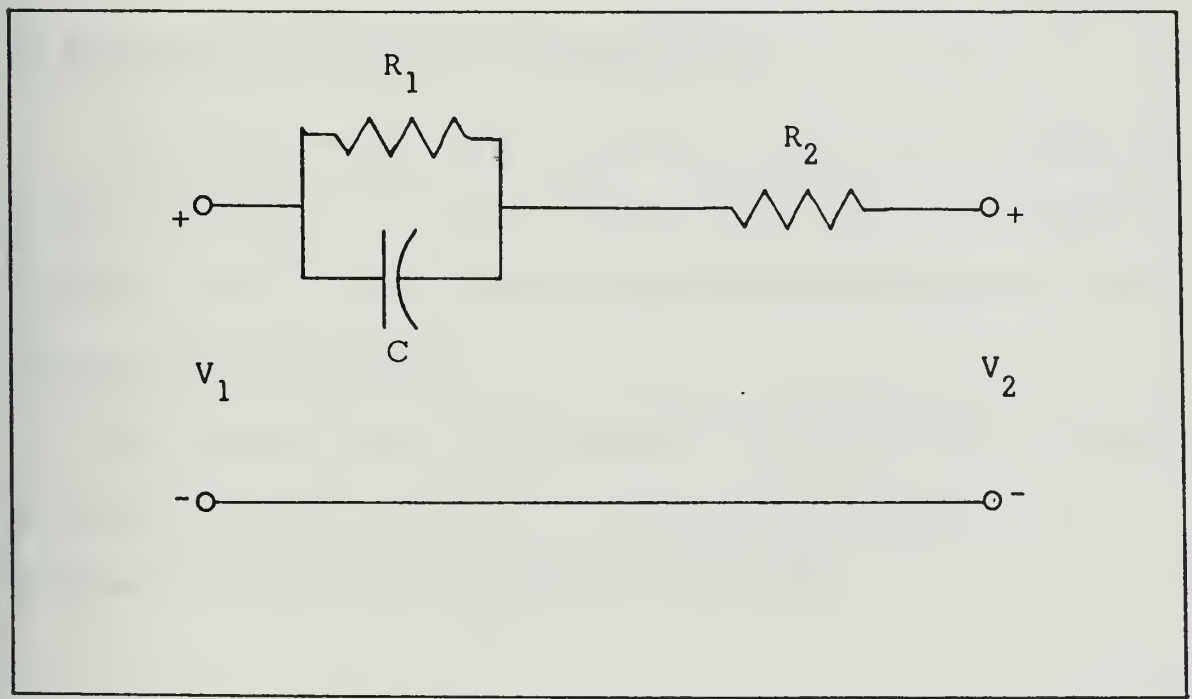

Figure 4-16. Type 3 Network for Paul's configuration

Note that independent adjustment of the time-constants, τ, is possible by adjusting the relevant set of resistors and capacitors.

If the network configuration, shown in Figure 4-16, is used as both the input and the feedback networks, the transfer admittance can be shown to be

$$y_{21}(s) = \frac{1 + sCR_1}{R_1 + R_2 + sCR_1R_2} \quad , \tag{4-57}$$

and the overall active voltage transfer function is

$$H(s) = - \frac{1 + sCR_A}{1 + sCR_B} = - \frac{1 + s\tau_A}{1 + s\tau_B} \quad . \tag{4-58}$$

In relation to Figure 4-16, for the input network, $R_1 = R_A$ and $R_2 = R_B$; for the feedback network, $R_1 = R_B$ and $R_2 = R_A$.

The transfer function forms generated by the network configurations of Paul would ideally be used for realizing higher-order filter transfer functions, broken up into biquadratic polynomials and cascaded to form the desired transfer function.

Two networks that would be especially useful for such realizations are shown in Figures 4-17 and 4-18. The network in Figure 4-17 is designed to simulate transfer functions of the form

$$H(s) = - \frac{1}{1 + s\tau} \quad , \tag{4-59}$$

where $\tau = RC$. That in Figure 4-18 simulates transfer functions of the form

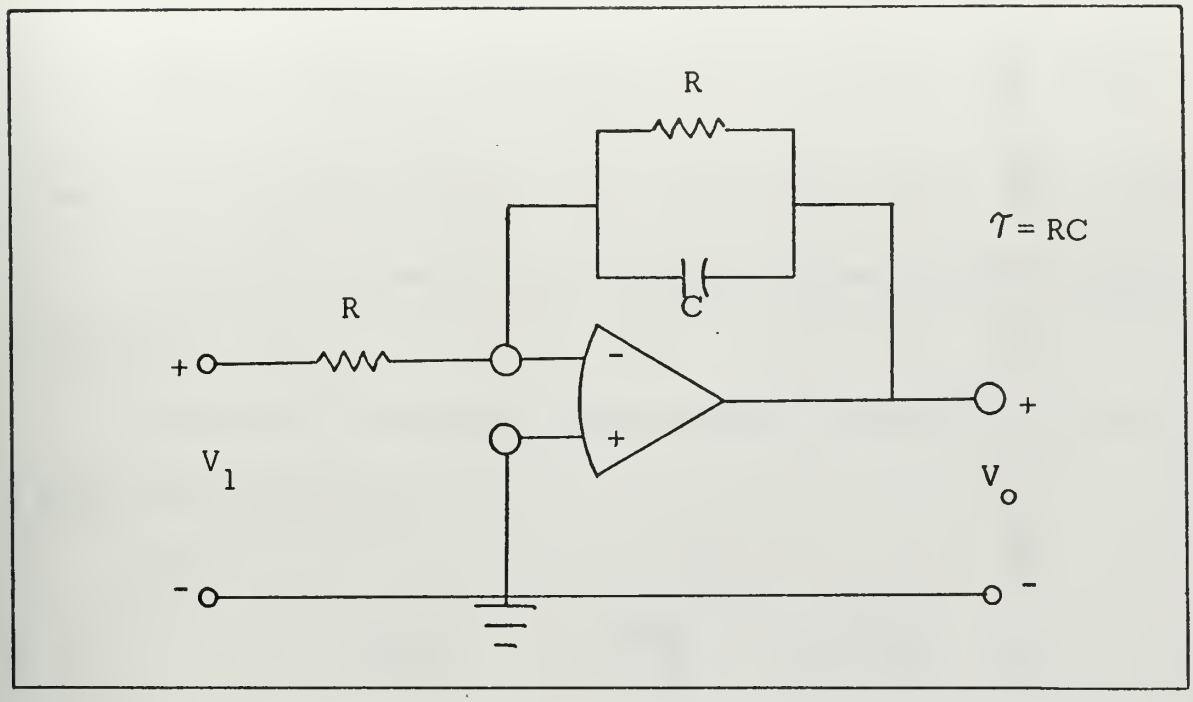

Figure 4-17. Paul's circuit to simulate $V_o(s)/V_1(s) = -1/(1 + s\tau)$

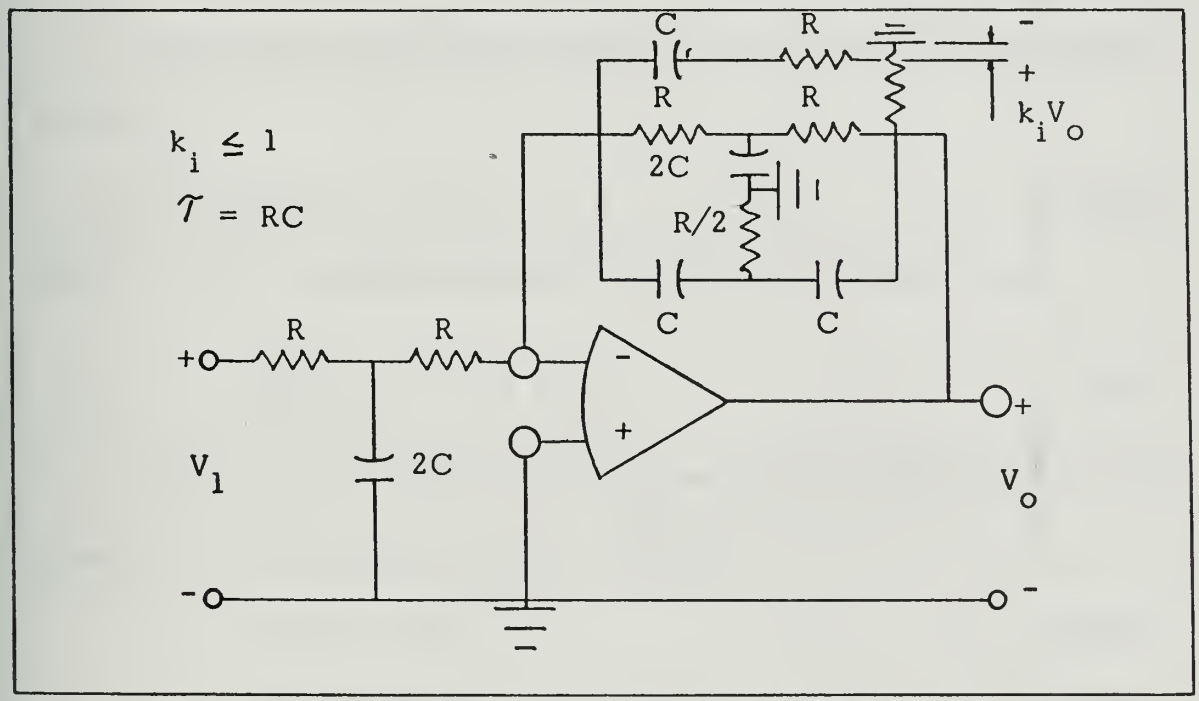

Figure 4-18. Paul's circuit to simulate $V_o(s)/V_1(s) = -1/(1+k_i 2s\tau + s^2\tau^2)$

$$H(s) = - \frac{1}{1 + 2k_i s\tau + s^2\tau^2} , \qquad (4\text{-}60)$$

where $k_i \leq 1$. These two networks will be used in the example to follow.

Example 4-3. Realize the fifth-order Butterworth transfer function of Example 2-2.

Reduced to a form suitable for simulation by Figures 4-17 and 4-18, the transfer function is

$$H(s) = \frac{-1}{1 + \frac{s}{62.83}} \cdot \frac{1}{1 + \frac{0.618}{62.83} s + \frac{s^2}{(62.83)^2}} \cdot \frac{1}{1 + \frac{1.618}{62.83} s + \frac{s^2}{(62.83)^2}} . \qquad (4\text{-}61)$$

Comparison of the first product term with equation (4-59) yields the relation

$$\tau = 1/62.83 \qquad (4\text{-}62)$$

For $C = 1\ \mu F$, the corresponding value of R is determined to be

$$R = \frac{10^6}{62.83} = 15.9\ K\Omega . \qquad (4\text{-}63)$$

Comparing the second and third product terms with equation (4-60) gives the following potentiometer settings:

$$k_1 = 0.618/2 = 0.309 \qquad (4\text{-}64)$$

$$k_2 = 1.618/2 = 0.809 . \qquad (4\text{-}65)$$

The final circuit realization is shown in Figure 4-19.

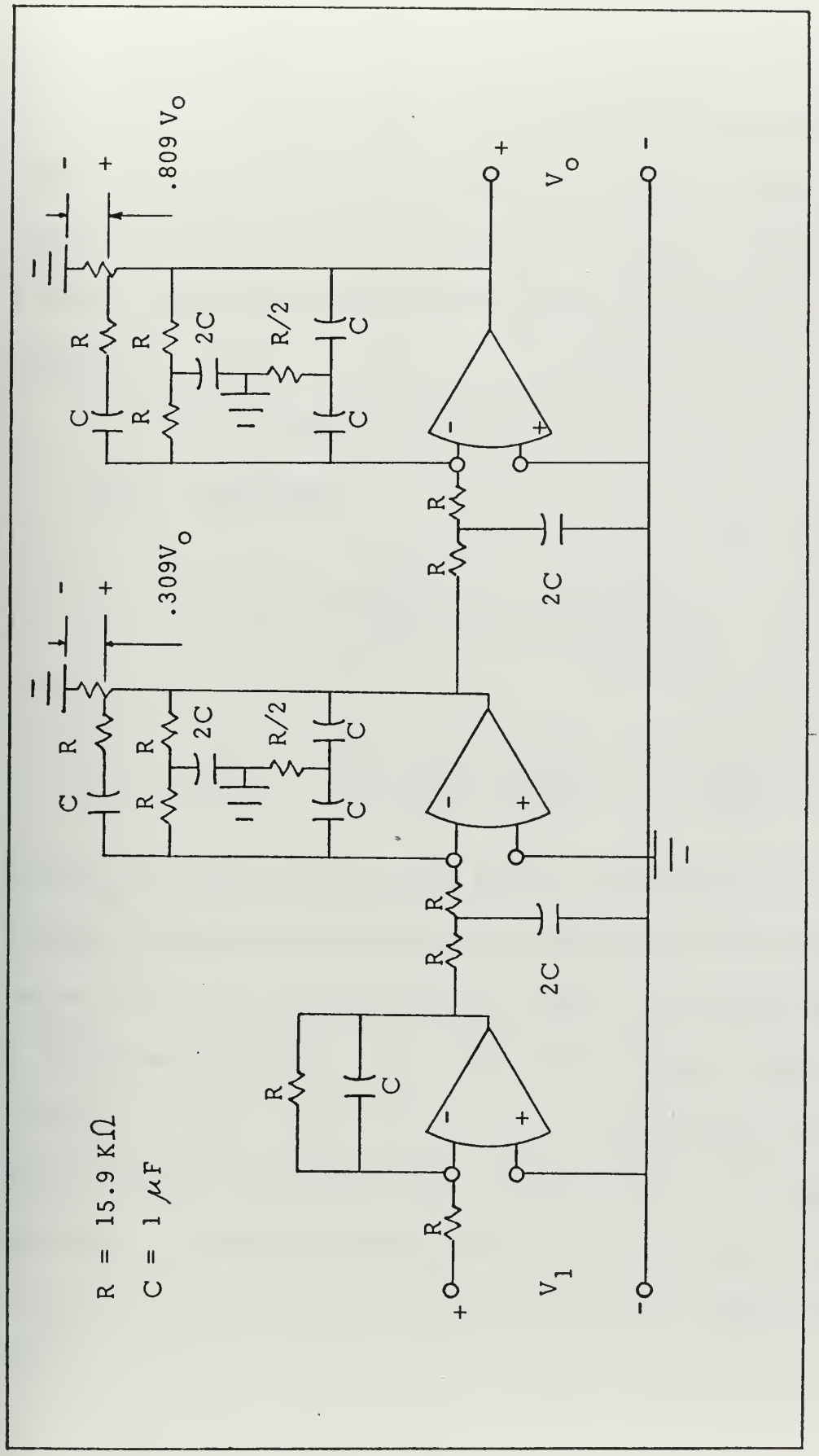

Figure 4-19. Circuit realization of Example 4-3

E. HAKIM [1964]

Hakim [Ref. 22] considered the realization of minimum phase transfer functions. His method essentially follows the same line of approach as that of Mathews and Seifert. His method of development, however, is more detailed and gives a clearer picture of the synthesis procedure.

If the general transfer function is

$$H(s) = - N(s)/D(s)$$

$$= - \frac{a_m s^m + a_{m-1} s^{m-1} + ... + a_1 s + a_o}{b_n s^n + b_{n-1} s^{n-1} + ... + b_1 s + b_o}$$

$$= - \frac{a_m}{b_n} \cdot \frac{(s + \alpha_1)(s + \alpha_2) \ldots (s + \alpha_m)}{(s + \beta_1)(s + \beta_2) .... (s + \beta_n)} , \qquad (4\text{-}66)$$

where a_o to a_m and b_o to b_n are all positive real coefficients and where the negative sign has been introduced in anticipation of the phase inversion caused by operational amplifier action, for the transfer function to be physically realizable, the order m of the numerator polynomial N(s) must be less than or equal to the order n of the denominator polynomial D(s). Stability considerations restrict all the poles $-\beta_1$ to $-\beta_n$ to the left half of the complex-frequency plane. If all the zeros $-\alpha_1$ to $-\alpha_m$ are also restricted to the left half of the plane, then the transfer function is said to be minimum phase.

For the feedback network configuration in Figure 4-3, the open-circuit voltage transfer function has been shown to be

$$H(s) = \frac{E_o(s)}{E_1(s)} = - \frac{y_{21A}(s)}{y_{12B}(s)} \quad . \tag{4-67}$$

If the transfer admittance functions, $y_{21A}(s)$ and $y_{12B}(s)$ are to be realized by RC networks, an auxiliary polynomial Q(s) has to be chosen with roots restricted to the negative real axis such that $Q(s) = (s + \sigma_1)(s + \sigma_2) \ldots . (s + \sigma_n)$ where σ_1 to σ_n are real positive numbers.

Equation (4-66) may be written as

$$H(s) = - \frac{N(s)/Q(s)}{D(s)/Q(s)} \tag{4-68}$$

and, equating equations (4-67) and (4-68),

$$y_{21A}(s) = - N(s)/Q(s)$$

$$y_{12B}(s) = - D(s)/Q(s) \quad . \tag{4-69}$$

Assuming the transfer function, H(s), has a pair of complex conjugate poles or zeros, $y_{21A}(s)$ and $y_{12B}(s)$ can be realized using Guillemin's procedure [Ref. 17]. Equation (4-69) may now be written as

$$y_{21A}(s) = - \frac{a_m s^m + a_{m-1} s^{m-1} + \ldots . + a_1 s + a_o}{(s + \sigma_1)(s + \sigma_2) \ldots . (s + \sigma_n)} \tag{4-70a}$$

$$y_{12B}(s) = - \frac{b_n s^n + b_{n-1} s^{n-1} + ... + b_1 s + b_o}{(s + \sigma_1)(s + \sigma_2).... (s + \sigma_n)} \qquad (4\text{-}70b)$$

Following Guillemin's procedure, short-circuit driving-point admittances are arbitrarily chosen. For convenience, let

$$y_{22A}(s) = y_{11B}(s) = \frac{(s + \delta_1)(s + \delta_2) \ldots (s + \delta_n)}{(s + \sigma_1)(s + \sigma_2) \ldots (s + \sigma_n)} , \qquad (4\text{-}71)$$

where δ_1 to δ_n are all positive numbers. Since N_A and N_B are to be RC networks, the poles and zeros of equation (4-71) must alternate and the lowest critical frequency must be a zero.

Synthesis of each network may now follow. For $y_{21A}(s)$, N(s) is first decomposed such that

$$N(s) = n_1(s) + n_2(s) = \ldots + n_r(s) \quad , \qquad (4\text{-}72a)$$

where

$$n_1(s) = a_o + a_1 s$$

$$n_2(s) = a_2 s^2 + a_3 s^3$$

.

.

$$n_r(s) = a_{n-1} s^{n-1} + a_n s^n \quad . \qquad (4\text{-}72b)$$

The last polynomial $n_r(s)$ contains one or two terms depending on whether the order n of N(s) is odd or even.

$$K_A y_{21A}(s) = \frac{K_A}{K_{A1}} y_{21A1}(s) + \frac{K_A}{K_{A2}} y_{21A2}(s) + \ldots.$$

$$\ldots. + \frac{K_A}{K_{Ar}} y_{21Ar}(s) \quad , \qquad (4\text{-}75)$$

and if the resulting scaled ladder realizations of each of these components are connected in parallel at their input and output ports, the resulting two-port network will realize the short-circuit admittance $y_{22A}(s)$ and the required zeros of $y_{21A}(s)$.

The transfer admittance $y_{12B}(s)$ is realized in a similar manner. The resulting network is shown in Figure 4-20.

Although basically the same method has been used in Section C to realize a high-pass transfer function, another example using Hakim's method to realize a low-pass filter will be given for purposes of comparison with other low-pass realizations.

Example 4-4. Realize the Butterworth low-pass transfer function of Example 2-1.

The transfer function

$$H(s) = - \frac{3947.84}{s^2 + 88.84\, s + 3947.84} \qquad (4\text{-}76)$$

is first divided in both numerator and denominator by a judiciously chosen $Q(s) = (s + 30)\ (s + 60)$ so that

$$y_{21A}(s) = - \frac{3947.84}{(s + 30)\ (s + 60)} \qquad (4\text{-}77a)$$

and

$$y_{12B}(s) = - \frac{3947.84 + 88.84\,s}{(s + 30)\,(s + 60)} - \frac{s^2}{(s + 30)\,(s + 60)} , \quad (4\text{-}77b)$$

where

$$y_{12B1}(s) = - \frac{3947.84 + 99.84\,s}{(s + 30)\,(s + 60)} \quad (4\text{-}78a)$$

and

$$y_{12B2}(s) = - \frac{s^2}{(s + 30)\,(s + 60)} . \quad (4\text{-}78b)$$

Driving-point admittances are then chosen. For convenience, let

$$y_{22A}(s) = y_{11B}(s) = \frac{(s + 10)\,(s + 44.5)}{(s + 30)\,(s + 60)} . \quad (4\text{-}79)$$

$y_{11B}(s)$ is first expanded into a ladder network in such a manner as to realize the zeros of $y_{12B1}(s)$ at $s = -44.5$ and at $s = -\infty$:

$$y_{11B}(s) = y_{11B1}(s)$$

$$= \cfrac{1}{\cfrac{6.51}{s + 44.5} + 1 + \cfrac{1}{\cfrac{s}{28.99} + \cfrac{1}{2.899}}} . \quad (4\text{-}80)$$

The network realization, N_{B1}, is shown in Figure 4-21.

$y_{11B}(s)$ is next expanded to realize the two zeros of $y_{12B2}(s)$ at $s = 0$:

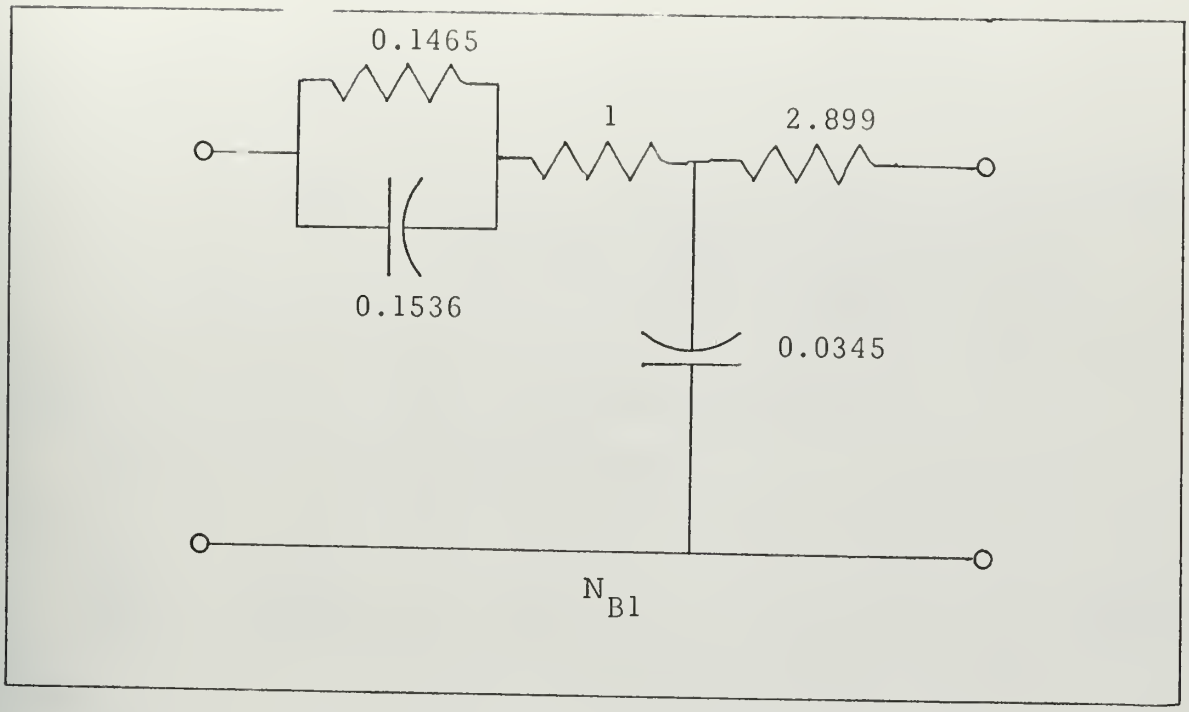

Figure 4-21. Circuit realization of $y_{12B1}(s)$ and $y_{11B1}(s)$

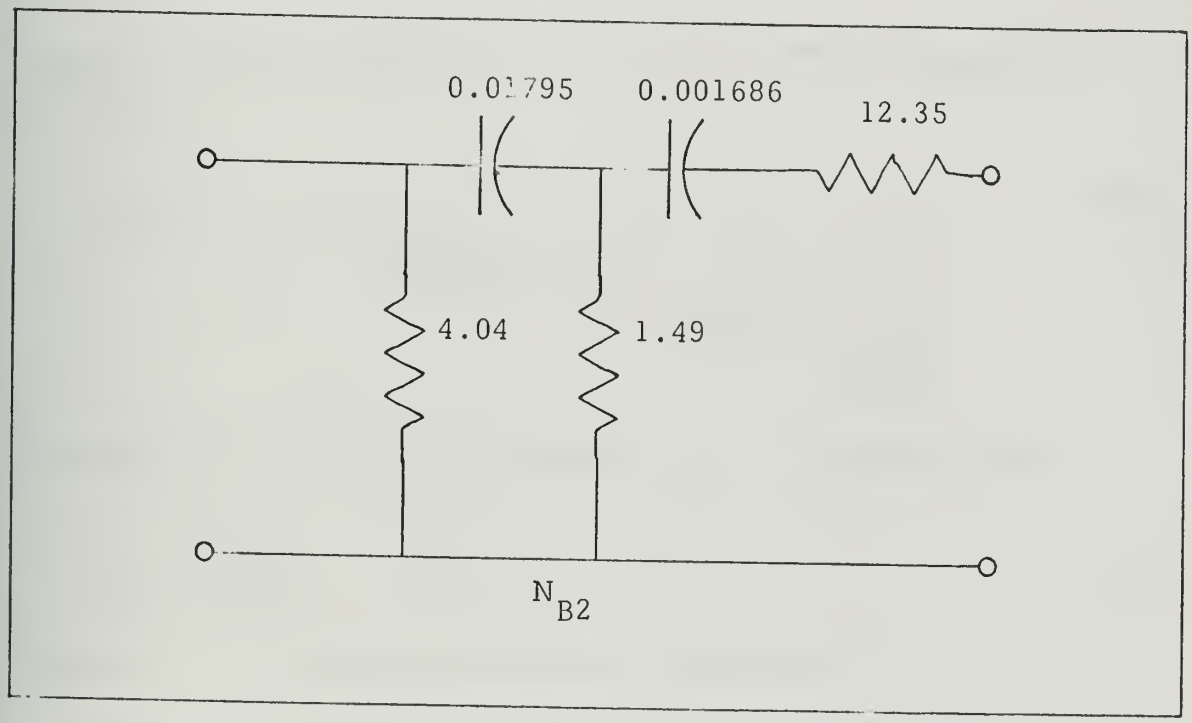

Figure 4-22. Circuit realization of $y_{12B2}(s)$ and $y_{11B2}(s)$

$$y_{11B}(s) = y_{11B2}(s)$$

$$= \frac{1}{4.04} + \cfrac{1}{\cfrac{1}{0.01795s} + \cfrac{1}{\cfrac{1}{1.49} + \cfrac{1}{\cfrac{1}{1.686s} + 12.35}}}} \quad (4\text{-}81)$$

The network realization, N_{B2}, is shown in Figure 4-22.

Scaling factors are determined to be

$$\frac{K_B}{K_{B1}} = \frac{0.0471}{0.1127} = 0.418 \quad (4\text{-}82a)$$

and

$$\frac{K_B}{K_{B2}} = \frac{0.0471}{0.081} = 0.582 \quad (4\text{-}82b)$$

$y_{22A}(s)$ is then expanded to realize the double zeros of $y_{21A}(s)$ at $s = -\infty$:

$$y_{22A}(s) = \cfrac{1}{1 + \cfrac{1}{0.0282s + \cfrac{1}{2.18 + \cfrac{1}{0.0423s + \cfrac{1}{0.865}}}}} \quad . \quad (4\text{-}83)$$

The scaling factor for the input network, N_A, is calculated to be

$$K_A = \frac{0.247}{2.195} = 0.1125 \quad . \quad (4\text{-}84)$$

The final circuit realization is shown in Figure 4-23.

The transfer function in equation (4-76) is realized within a constant multiplier

$$\frac{K_A}{K_B} = \frac{0.1125}{0.0471} = 2.39 \quad . \quad (4\text{-}85)$$

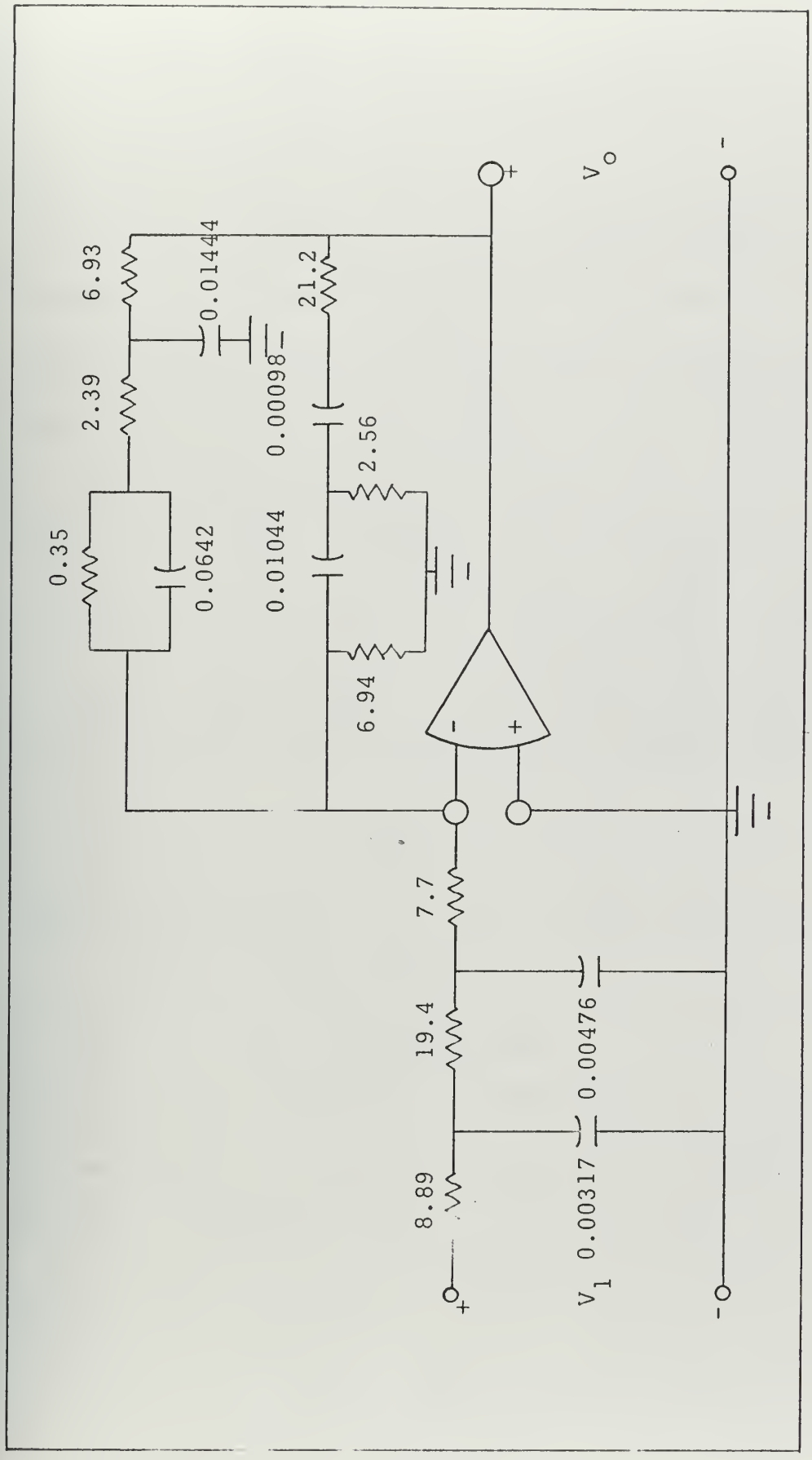

Figure 4-23. Circuit realization of Example 4-4

F. MUIR AND ROBINSON [1968]

One method proposed by Muir and Robinson [Ref. 23] utilizes three operational amplifiers to realize a second-order transfer function. A three-amplifier realization of a low-pass filter is shown in Figure 4-24. The basic building block for this configuration is a single operational amplifier feedback circuit, shown in Figure 4-25, with the familair voltage transfer function, $H(s) = -Y_1/Y_2$.

If the currents at the input of each operational amplifier of Figure 4-24 are added, assuming $A \longrightarrow \infty$, the resulting equations are

$$V_1 g_6 + V_o g_3 + V_A g_4 = 0 \qquad (4\text{-}86a)$$

$$V_A g_1 + V_B (g_2 + sC_2) = 0 \qquad (4\text{-}86b)$$

$$V_B g_5 + V_o sC_1 = 0 \quad . \qquad (4\text{-}86c)$$

Solving the above equations simultaneously yields the following voltage transfer function:

$$\frac{V_o}{V_1} = - \frac{g_1 g_5 g_6 / g_4 C_1 C_2}{s^2 + (g_2/C_2)\, s + (g_1 g_3 g_5 / g_4 C_1 C_2)} \quad . \qquad (4\text{-}87)$$

If equation (4-87) is identified with the prototype low-pass filter transfer function in equation (2-16),

$$\frac{V_o}{V_1} = - \frac{H \omega_o^{\,2}}{s^2 + a \omega_o s + \omega_o^{\,2}} \quad , \qquad (4\text{-}88)$$

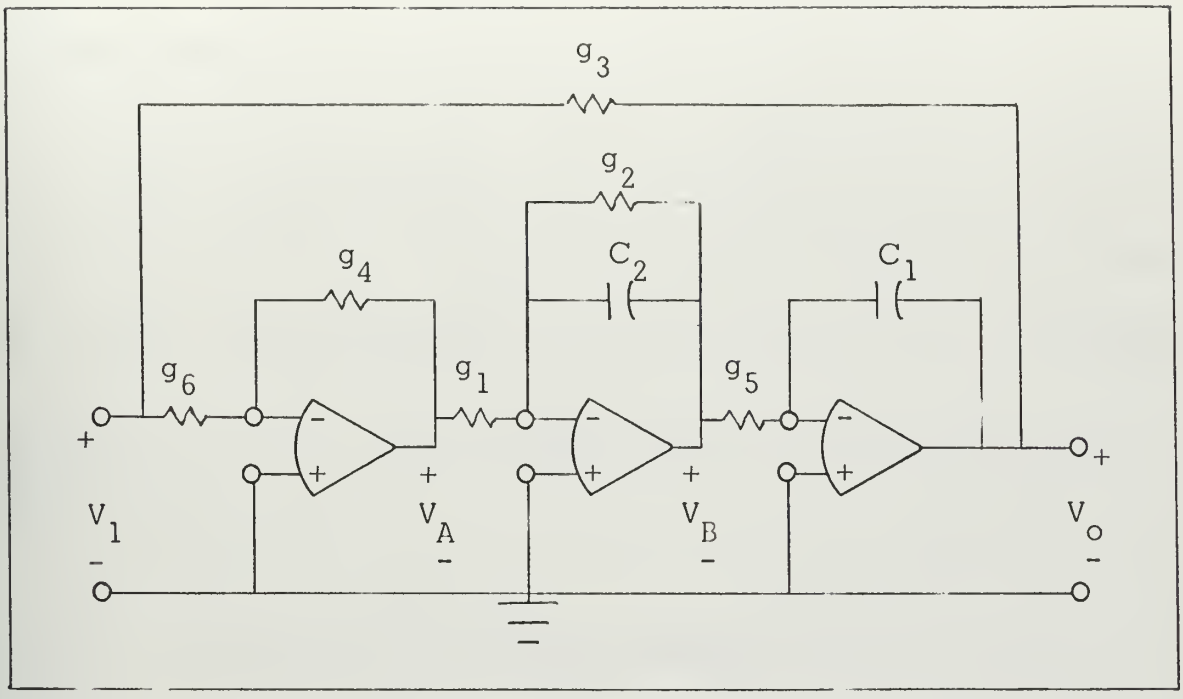

Figure 4-24. Active network configuration of Muir and Robinson

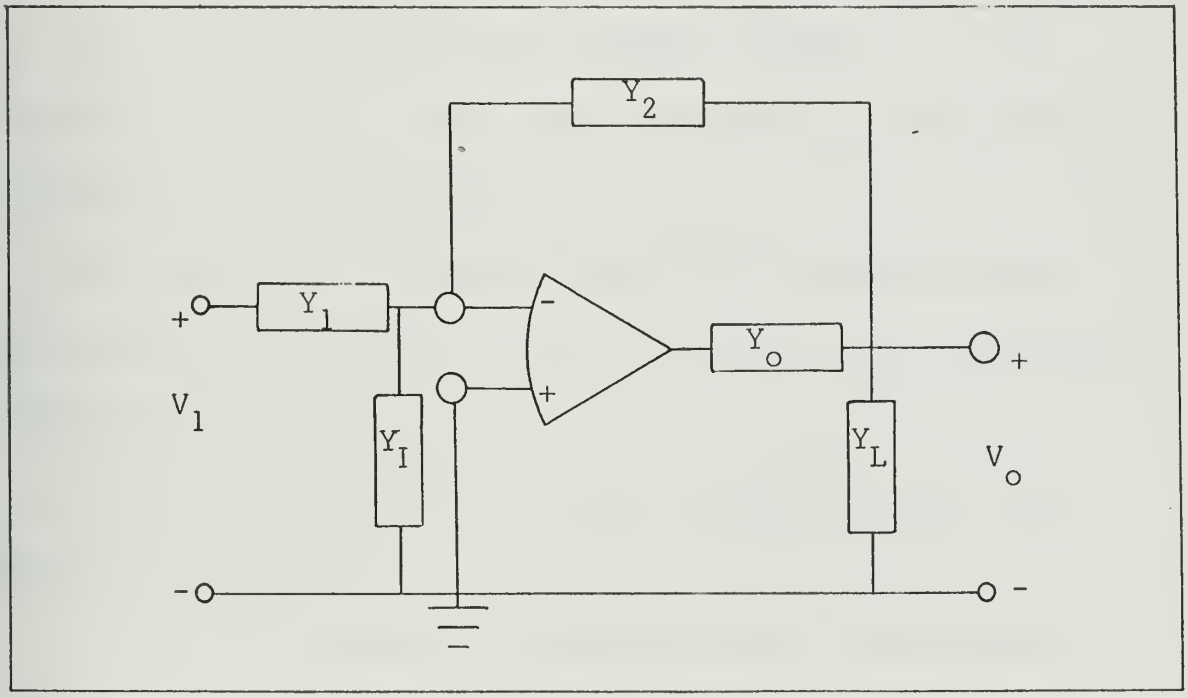

Figure 4-25. Basic circuit block used in triple amplifier realization of transfer functions

it can be seen that

$$H\,\omega_o^2 = g_1 g_5 g_6 / g_4 C_1 C_2 \qquad (4\text{-}89a)$$

$$a\,\omega_o = g_2 / C_2 \qquad (4\text{-}89b)$$

$$\omega_o^2 = g_1 g_3 g_5 / g_4 C_1 C_2 \quad . \qquad (4\text{-}89c)$$

To realize a desired low-pass transfer function, it is only necessary to make the following steps:

1. Select C_1, C_2 and g_3.
2. Determine g_2 from equation (4-89b).
3. Let $g_3 = g_4$.
4. Employ the relation $\frac{g_1}{C_2} = \frac{g_5}{C_1} = \omega_o$ to obtain g_1 and g_5.
5. Finally compute g_6 from equation (4-89a).

High-pass, bandpass and band-reject configurations, similar to Figure 4-24 may be obtained from Ref. 23.

Note that in the realization of higher-order transfer functions, the configuration of Figure 4-24 reverts to the status of a second-order building block.

Example 4-5. Realize the low-pass Butterworth filter transfer function of Example 2-1.

Following the design procedure steps laid out in this section, let

$$C_1 = C_2 = 1\,\mu F \qquad (4\text{-}90a)$$

$$R_3 = R_4 = 100\ K\Omega \quad . \qquad (4\text{-}90b)$$

From the relation, $g_2/C_2 = 88.84$, R_2 is calculated to be

$$R_2 = 11.27\ K\Omega \quad . \tag{4-91}$$

Knowing $\omega_o = 62.83$ rad/sec, R_1 and R_5 are determined to be

$$R_1 = R_5 = \frac{10^6}{62.83} = 15.9\ K\Omega \quad . \tag{4-92}$$

Finally, R_6 is calculated from equation (4-89a) to be

$$R_6 = \frac{1}{g_4} \cdot \frac{g_1 g_5}{C_1 C_2} \cdot \frac{1}{H\,\omega_o^2} = R_4 = 100\ K\Omega \tag{4-93}$$

since $H = 1$.

The final circuit realization is shown in Figure 4-26.

G. ADVANTAGES AND DISADVANTAGES

Compared to comparable realizations falling under the other categories in this paper, single-feedback realizations will be observed to require considerably more elements. This can be noted especially in the method of Hakim, where the number of ladder networks increases with the order of the transfer function. This disadvantage is due to having to realize the input and the feedback networks separately, each network with its own set of natural frequencies. Because of this same reason, however, such realizations determine transfer function pole locations by the zeros of the two passive networks, rather than by the gain of the operational amplifier, and hence, are quite stable.

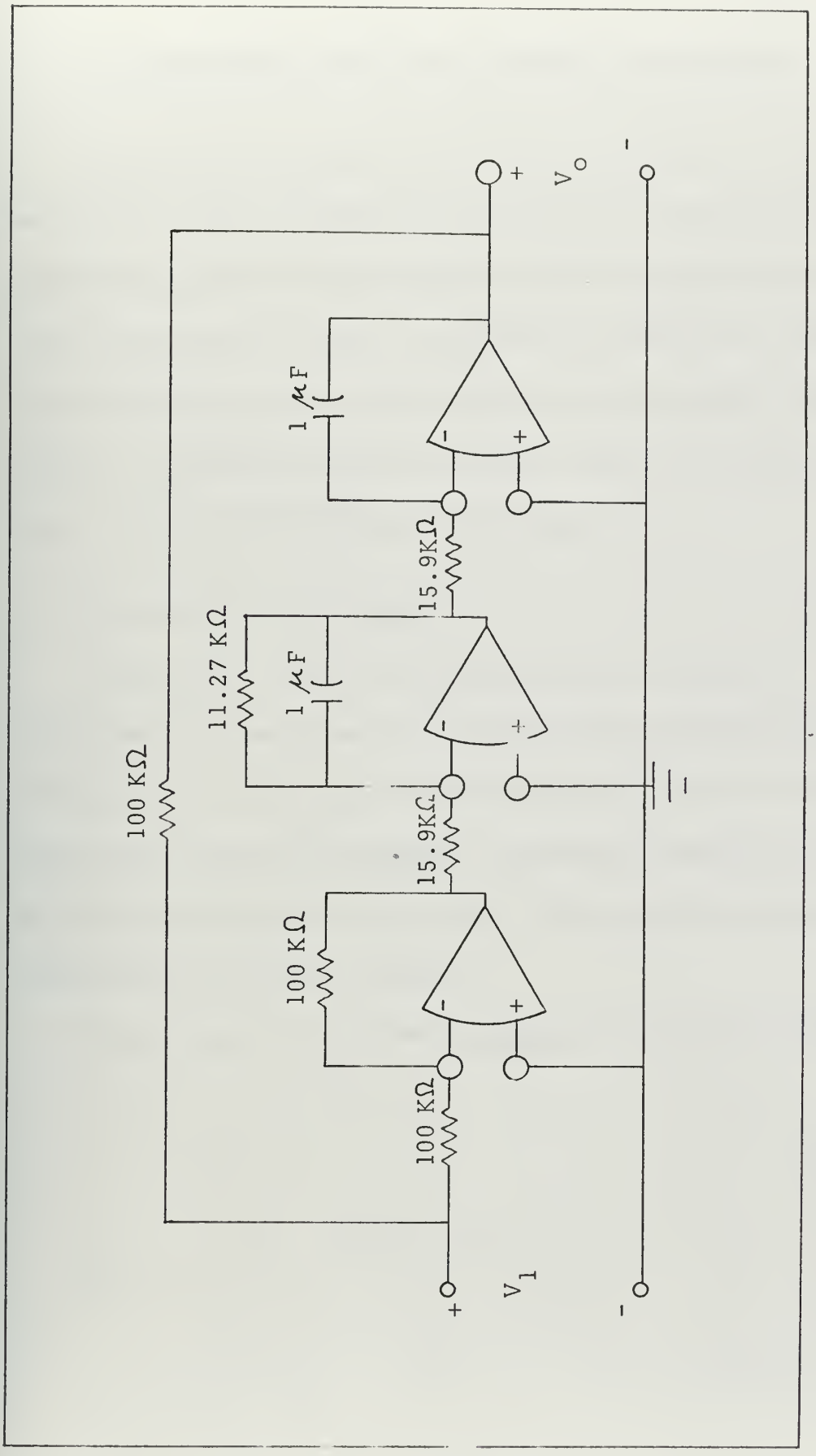

Figure 4-26. Circuit realization of Example 4-5

V. INFINITE-GAIN MULTIPLE-FEEDBACK REALIZATIONS

This chapter contains the significant contributions falling under the general category of Infinite-Gain Multiple-Feedback Realizations. The difference between this category and that in Chapter IV is that, as the classification implies, the feedback connections are made to more than one point in the input network from the output of the operational amplifier. Realizations falling under this category will thus be of the general network configuration shown in Figure 5-1.

A. THEORETICAL DEVELOPMENT

Consider the network configuration shown in Figure 5-2. This is the second-order prototype of the general multiple-feedback configuration in Figure 5-1. Consisting of five two-terminal admittances and one infinite-gain operational amplifier, this network would be an ideal choice for illustrating Nathan's method [Ref. 12] for analyzing networks constrained by an operational amplifier.

The Y matrix for the network without the operational amplifier is

$$
[Y] = \begin{array}{c} \begin{array}{cccc} 1 & 2 & 3 & 5 \end{array} \\ \left[\begin{array}{cccc} Y_1 & -Y_1 & 0 & 0 \\ -Y_1 & (Y_1+Y_2+Y_3+Y_4) & -Y_3 & -Y_4 \\ 0 & -Y_3 & (Y_3+Y_5) & -Y_5 \\ 0 & -Y_4 & -Y_5 & (Y_4+Y_5) \end{array}\right] \begin{array}{c} 1 \\ 2 \\ 3 \\ 4 \end{array} \end{array} \qquad (5\text{-}1)
$$

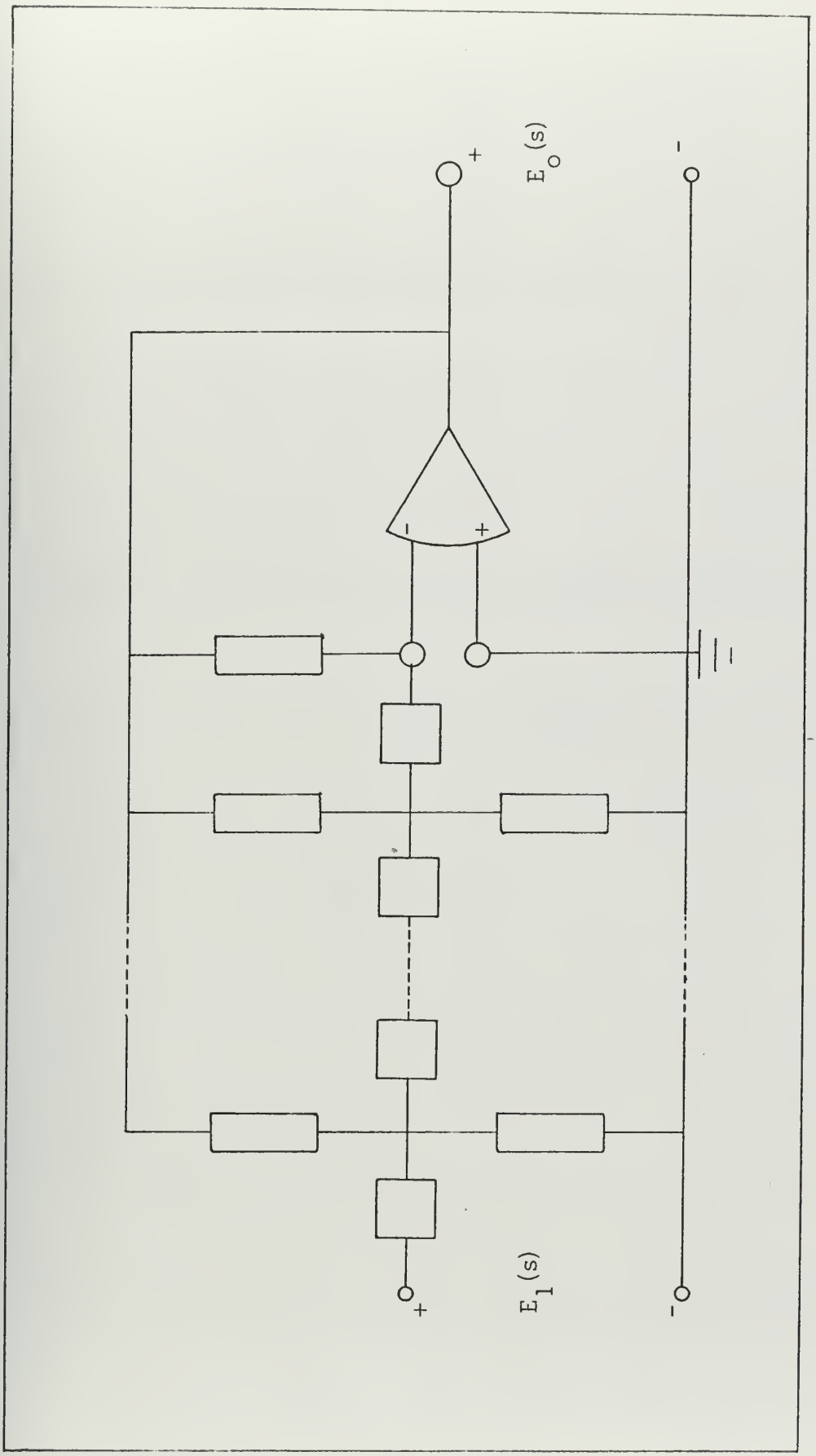

Figure 5-1. General infinite-gain multiple-feedback configuration

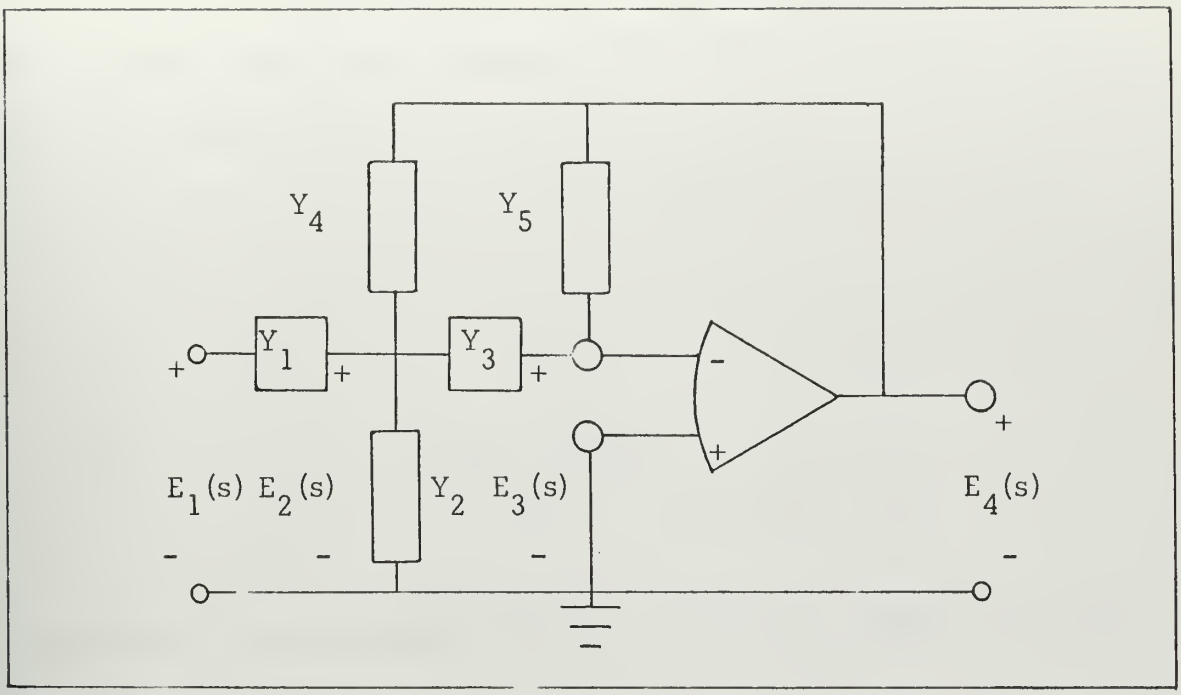

Figure 5-2. Second-order prototype of multiple-feedback configuration

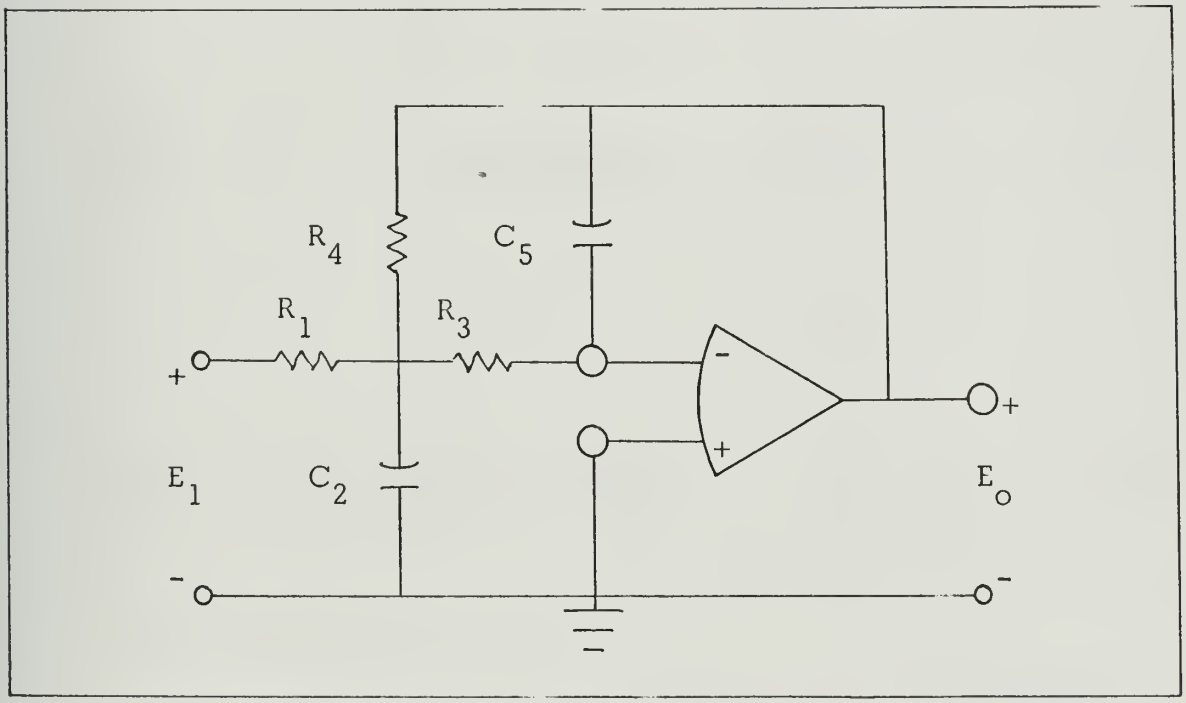

Figure 5-3. Second-order low-pass filter network of Rauch and Nichols

In accordance with Nathan's procedure, the desired matrix, [Y'], for the network <u>with</u> the operational amplifier is obtained by deleting the fourth row and the third column from the Y matrix in equation (5-1):

$$[Y'] = \begin{matrix} \\ 1 \\ -Y_1 \\ 2 \\ 0 \\ 3 \end{matrix} \begin{matrix} \begin{matrix} 1 & \quad 2 & \quad 4 \end{matrix} \\ \begin{bmatrix} Y_1 & -Y_1 & 0 \\ -Y_1 & (Y_1+Y_2+Y_3+Y_4) & -Y_4 \\ 0 & -Y_3 & -Y_5 \end{bmatrix} \end{matrix} \qquad (5\text{-}2)$$

To obtain the voltage transfer function, $E_4(s)/E_1(s)$, equation (C-7) in Appendix C is applied:

$$\frac{E_4(s)}{E_1(s)} = \frac{Y^{14}}{Y^{11}} = \frac{\begin{vmatrix} -Y_1 & (Y_1+Y_2+Y_3+Y_4) \\ 0 & -Y_3 \end{vmatrix}}{\begin{vmatrix} (Y_1+Y_2+Y_3+Y_4) & -Y_4 \\ -Y_3 & -Y_5 \end{vmatrix}} \qquad (5\text{-}3a)$$

or

$$H(s) = \frac{-Y_1Y_3}{Y_5(Y_1+Y_2+Y_3+Y_4) + Y_3Y_4} \quad . \qquad (5\text{-}3b)$$

B. RAUCH AND NICHOLS [1956]

Using equation (5-3) as the basic equation, Rauch and Nichols [Ref. 24] developed what was to be referred to as the "Rauch" filter. The filter network, shown in Figure 5-3, is the low-pass version of the general second-order prototype in Figure 5-2.

The transfer function corresponding to the network in Figure 5-3 is

$$H(s) = - \frac{G_1 G_3}{s^2 C_2 C_5 + s C_5 (G_1 + G_3 + G_4) + G_3 G_4} \qquad (5\text{-}4a)$$

or, in a more convenient form,

$$H(s) = - \frac{\frac{1}{R_1 R_3 C_2 C_5}}{s^2 + \frac{R_3 R_4 + R_1 R_4 + R_1 R_3}{C_2 R_1 R_3 R_4} s + \frac{1}{C_2 C_5 R_3 R_4}} \qquad (5\text{-}4b)$$

The synthesis procedure then becomes a matter of equating the coefficients of the desired second-order low-pass transfer function of the form of equation (2-16) to the element coefficients of equation (5-4b).

An example of this procedure is given in Example 5-1.

Example 5-1. Realize the low-pass transfer function in Example 2-1 using a second-order Rauch filter.

The transfer function, repeated here for convenience, is

$$H(s) = - \frac{3947.84}{s^2 + 88.84\, s + 3947.84} \; . \qquad (5\text{-}5)$$

Equating coefficients of equations (5-4b) and (5-5) yields

$$\frac{R_3 R_4 + R_1 R_4 + R_1 R_3}{C_2 R_1 R_3 R_4} = 88.84 \qquad (5\text{-}6a)$$

and

$$1/C_2 C_5 R_3 R_4 = 3947.84 \; . \qquad (5\text{-}6b)$$

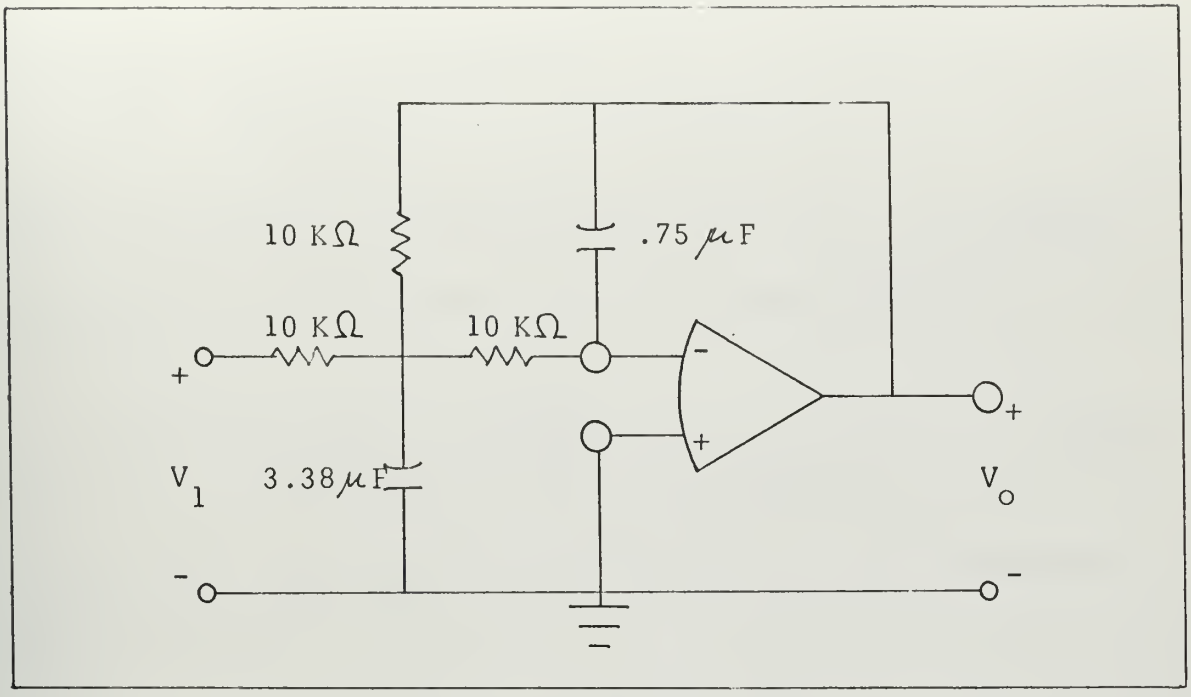

Figure 5-4. Circuit realization of Example 5-1

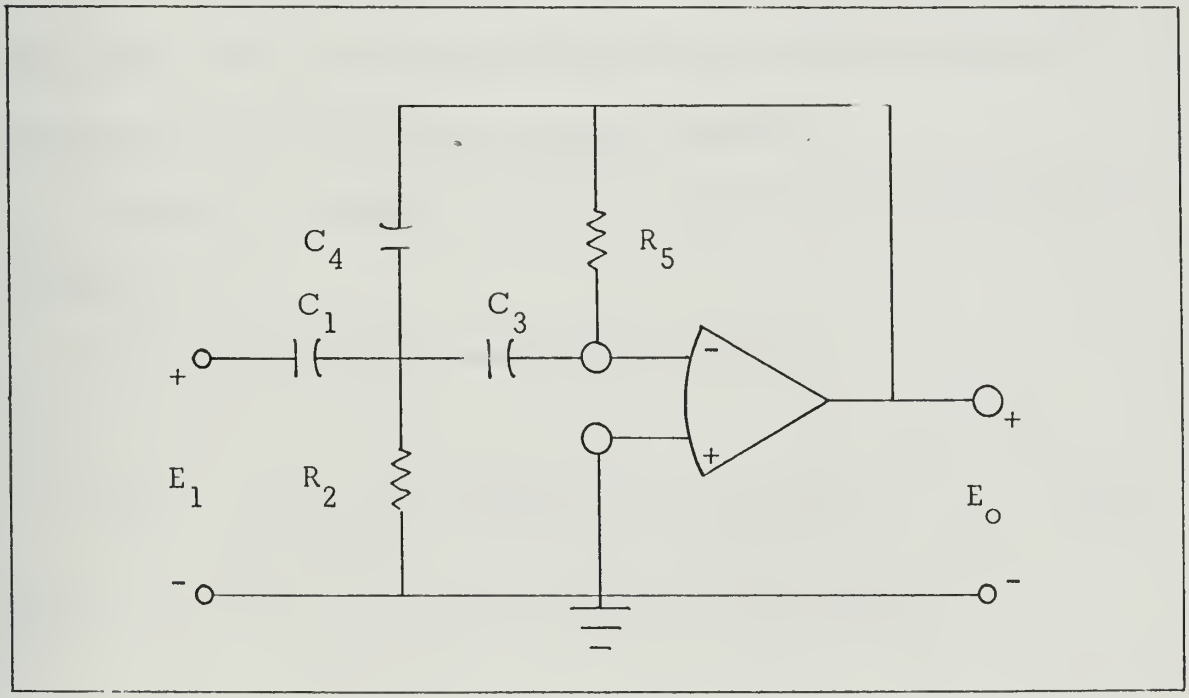

Figure 5-5. High-pass active network configuration of Bridgman and Brennan

$$H(s) = \frac{s^2 C_1 C_3 R_2 R_5}{s^2 R_2 R_5 C_3 C_4 + s R_2 (C_1 + C_3 + C_4) + 1} , \qquad (5\text{-}10)$$

and the two bandpass arrangements shown in Figure 5-6. If Z_1 and Z_5 are capacitors as shown in Figure 5-6a, the transfer function is

$$H(s) = \frac{s C_1 R_4}{s^2 C_1 C_5 R_3 R_4 + s C_5 (R_3 + R_4 + R_3 R_4 / R_2) + 1} . \qquad (5\text{-}11)$$

If Z_3 and Z_4 are capacitors as shown in Figure 5-6b, the corresponding transfer function is

$$H(s) = \frac{s C_3 R_2 R_5}{s^2 R_1 R_3 R_4 C_2 C_5 + s R_1 R_2 (C_3 + C_4) + (R_1 + R_2)} . \qquad (5\text{-}12)$$

Again element values for a desired second-order transfer function are determined using the coefficient-matching approach.

Example 5-2. Realize the Chebyshev high-pass transfer function of Example 2-3.

The transfer function is converted to the form

$$H(s) = \frac{s^2/5576.46}{(s^2/5576.46) + (57.24/5576.46)\, s + 1} . \qquad (5\text{-}13)$$

Equating coefficients of equations (5-10) and (5-13) gives

$$C_1 C_3 R_2 R_5 = 1/5576.46 \qquad (5\text{-}14a)$$

$$C_3 C_4 R_2 R_5 = 1/5576.46 \qquad (5\text{-}14b)$$

$$R_2 (C_1 + C_3 + C_4) = 57.24/5576.46 . \qquad (5\text{-}14c)$$

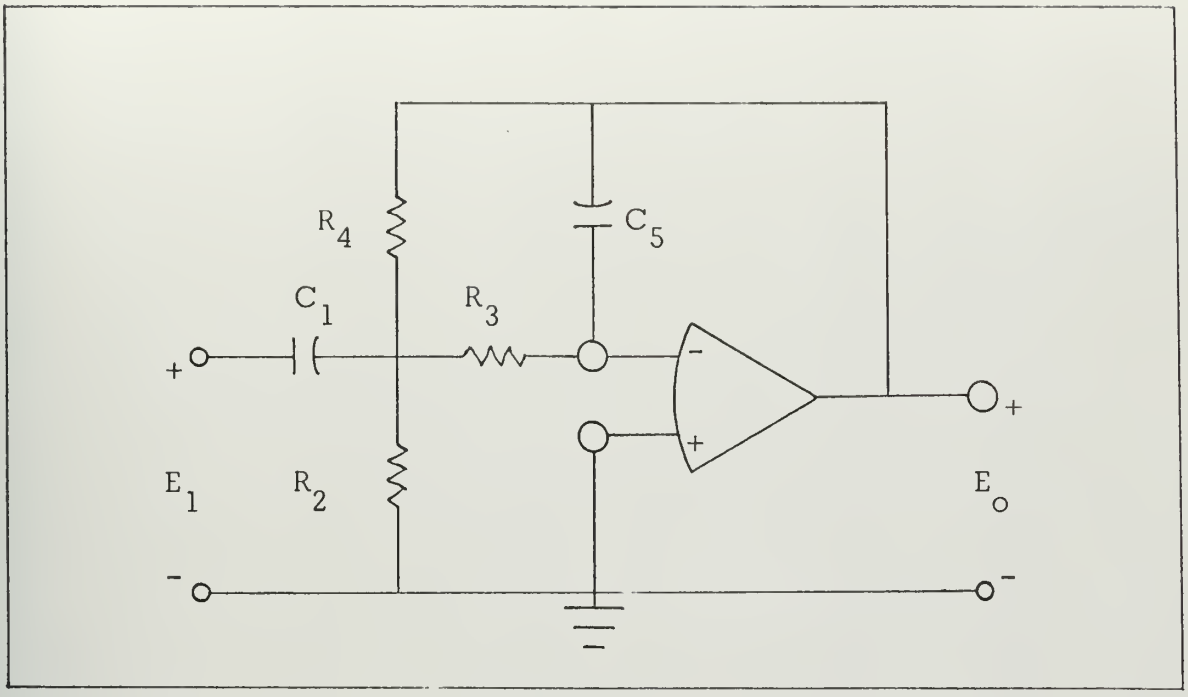

Figure 5-6a. Bandpass configuration No. 1 of Bridgman and Brennan

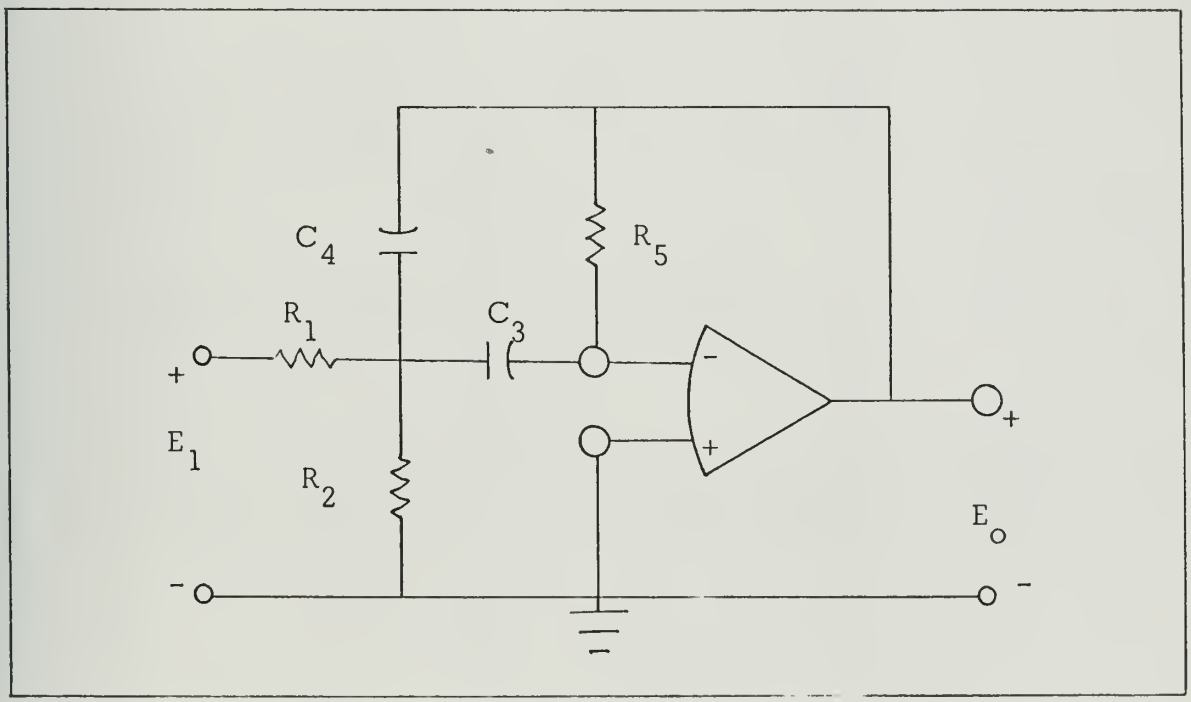

Figure 5-6b. Bandpass configuration No. 2 of Bridgman and Brennan

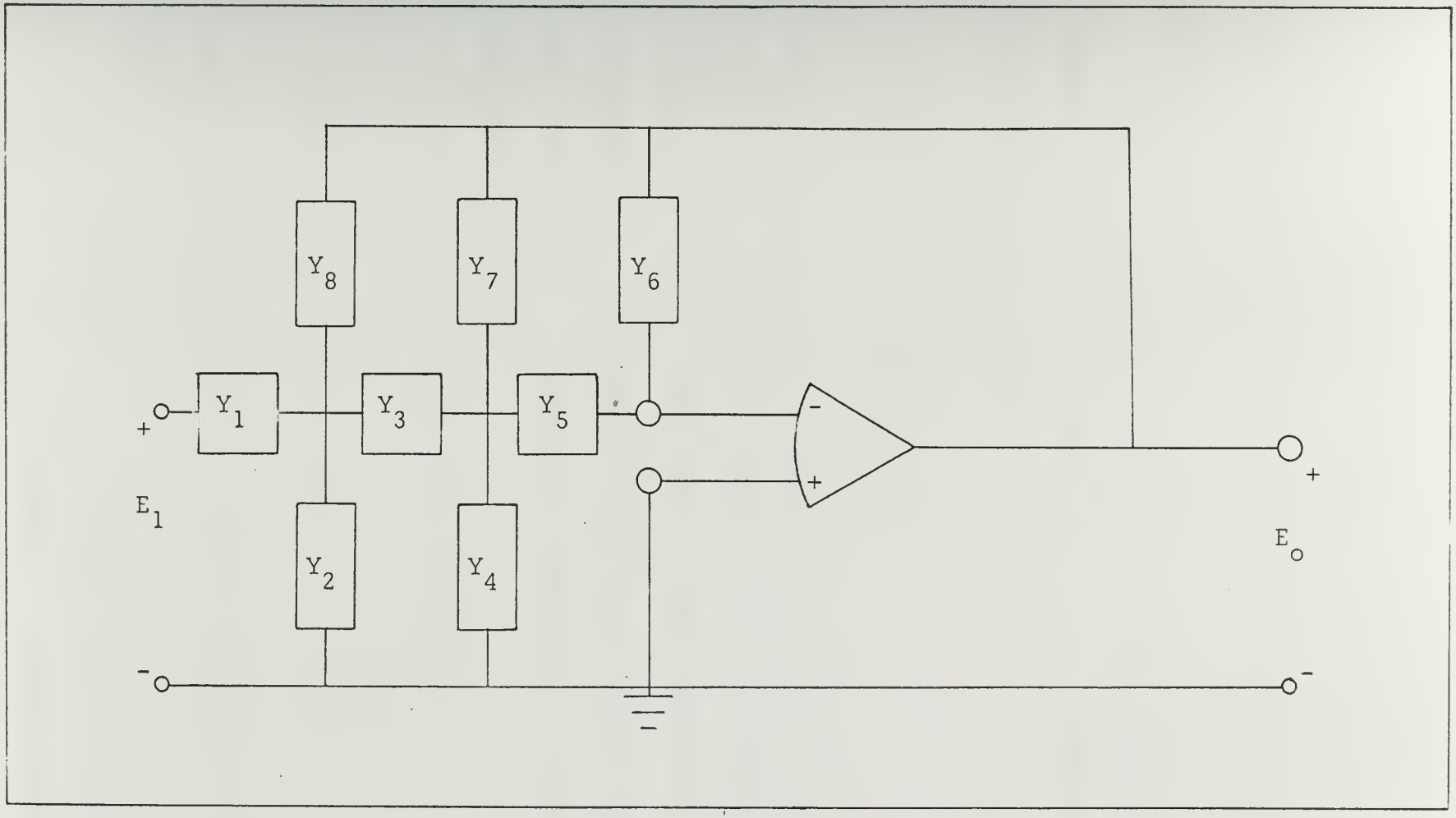

Figure 5-7. Wadhwa's third-order active network configuration

$$H(s) = - \frac{a_2 s^2 + a_1 s + a_o}{b_3 s^3 + b_2 s^2 + b_1 s + 1} \quad , \tag{5-18}$$

where all numerator and denominator polynomial coefficients are positive and real.

Wadhwa investigated the realization of three separate cases of equation (5-18). The first of these [Ref. 26] is the realization of the case where $a_2 = a_1 = 0$ such that

$$H(s) = - \frac{a_o}{b_3 s^3 + b_2 s^2 + b_1 s + 1} \quad . \tag{5-19}$$

Three possible arrangements of resistors and capacitors to realize equation (5-19) are shown in Ref. 26 with their corresponding relations between transfer function coefficients and network elements. One such arrangement with its corresponding coefficient-component relations is shown in Figure 5-8. This particular arrangement is an extension of the second-order Rauch filter.

For the realization of the special case where

$$H(s) = - \frac{a_1 s}{b_3 s^3 + b_2 s^2 + b_1 s + 1} \quad , \tag{5-20}$$

three possible combinations of resistors and capacitors are shown in Ref. 27.

One combination which is an extension of the network in Figure 5-6a is shown in Figure 5-9. Its coefficient-component relations have

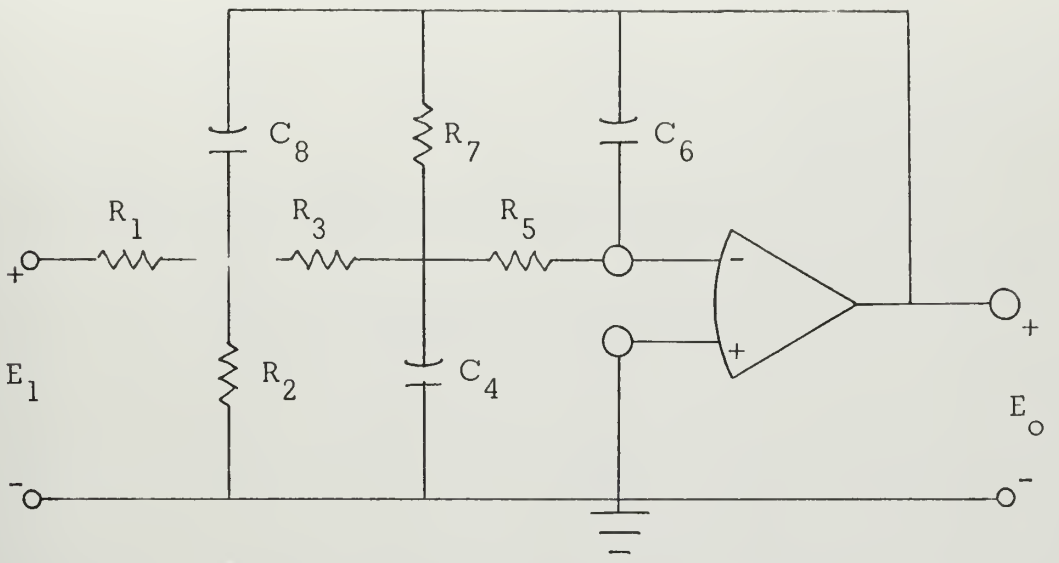

$$a_0 = b_0/3$$

$$b_1 = 1/3\ [(5b_0+1)RC_6 + (b_0+1)RC_8]$$

$$b_2 = 1/3\ RC_6\,[3b_0RC_4 + (2b_0+1)RC_8]$$

$$b_3 = \frac{b_0}{3}\ R^3C_4C_6C_8$$

$$R_1 = R_2 = R_3 = R_5 = R$$

$$R_7 = b_0R$$

$$b_1 > \frac{b_3}{b_2}\ (b_0+1)$$

Figure 5-8. Wadhwa's configuration to simulate $H(s) = -a_0/(b_3s^3 + b_2s^2 + b_1s + 1)$

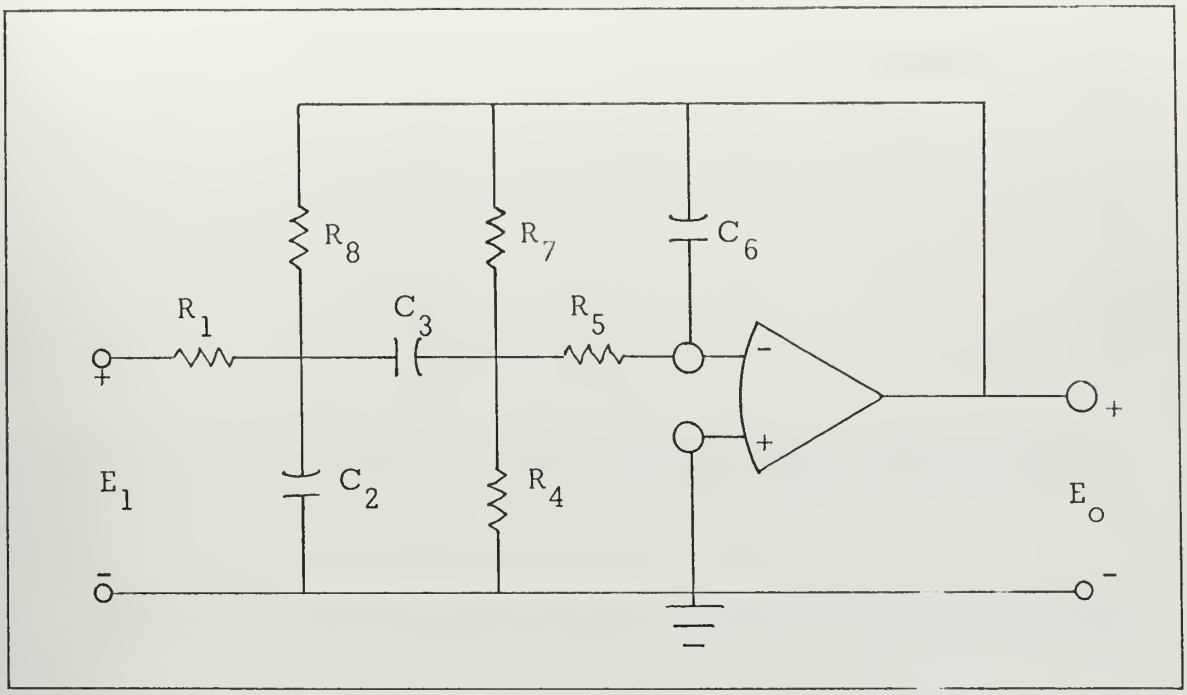

Figure 5-9. Wadhwa's active network configuration to simulate $H(s) = -a_1 s/(b_3 s^3 + b_2 s^2 + b_1 s + 1)$

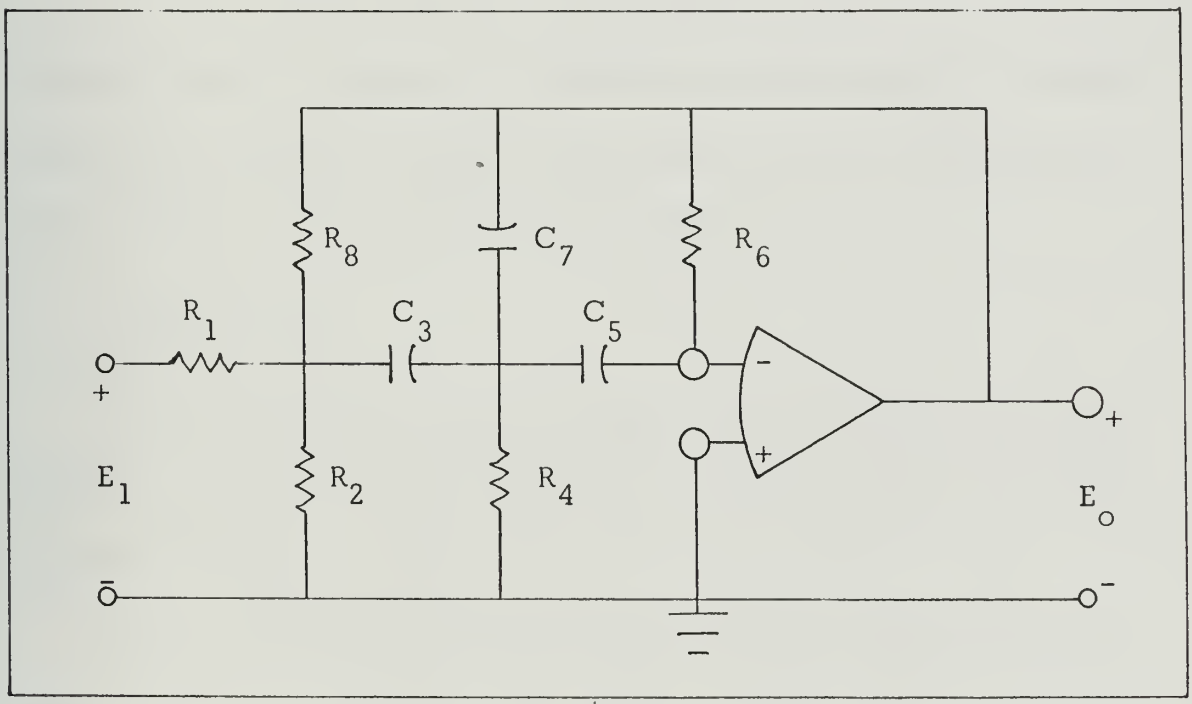

Figure 5-10. Wadhwa's active network configuration to simulate $H(s) = -a_2 s^2/(b_3 s^3 + b_2 s^2 + b_1 s + 1)$

been intentionally omitted because the realization conditions become too complicated to be of any illustrative value.

Finally, Ref. 28 treats the realization of the special case where

$$H(s) = - \frac{a_2 s^2}{b_3 s^3 + b_2 s^2 + b_1 s + 1} \quad . \tag{5-21}$$

One of the three possible combinations discussed is shown in Figure 5-10.

Realizations of still higher-order transfer functions generalized by

$$H(s) = - \frac{a_o (a_{n-1} s^{n-1} + a_{n-2} s^{n-2} + \ldots + a_1 s + 1)}{b_n s^n + b_{n-1} s^{n-1} + \ldots + b_2 s^2 + b_1 s + 1} \tag{5-22}$$

following the same approach of coefficient-matching subject to certain realization conditions have been described in Ref. 29. The details of these, however, will not be included in this paper.

E. FOSTER [1965]

Foster [Ref. 30] developed a method of realizing low-pass filter transfer functions of orders higher than the third by using Rauch's two- and three-pole filter configurations.

Basically, if a fourth-order low-pass filter is desired, the corresponding transfer function is realized by cascading two two-pole Rauch filters. If a fifth-order filter is desired, a three-pole and a two-pole filters are cascaded.

In general, if an odd-order low-pass filter is desired, a three-pole Rauch filter followed by as many two-pole filters as necessary effects the realization. If an even-order filter is required, the necessary number of two-pole Rauch filters is used.

The two-pole or the second-order Rauch filter has already been developed in Section B of this chapter. The third-order Rauch filter is shown in Figure 5-11. Its transfer function is

$$\frac{E_o(s)}{E_1(s)} = \frac{-1/R_1R_3R_5C_2C_4C_6}{s^3 + \left(\frac{R_3R_7 + R_3R_5 + R_5R_7}{R_3R_5R_7C_4} + \frac{R_1 + R_3}{R_1R_3C_2}\right)s^2 + \left(\frac{R_5R_7 + R_3R_7 + R_3R_5 + R_1R_7 + R_1R_5}{R_1R_3R_5R_7C_2C_4} + \frac{1}{R_5R_7C_4C_6}\right)s + \left(\frac{R_1 + R_3}{R_1R_3R_5R_7C_2C_4C_6}\right)} \quad . \quad (5\text{-}23)$$

A third-order low-pass filter may then be realized by equating the coefficients of its transfer function to the coefficients of equation (5-17). It is normally convenient in this kind of procedure to make all resistors of the same value, choosing the resistor value to come up with practical capacitor values.

Using equal resistors for both two- and three-pole Rauch configurations, Foster simplified the realization of higher-order low-pass filters by tabulating normalized capacitor values for Butterworth, Bessel, and Chebyshev filters up to order 10. A portion of the capacitor table

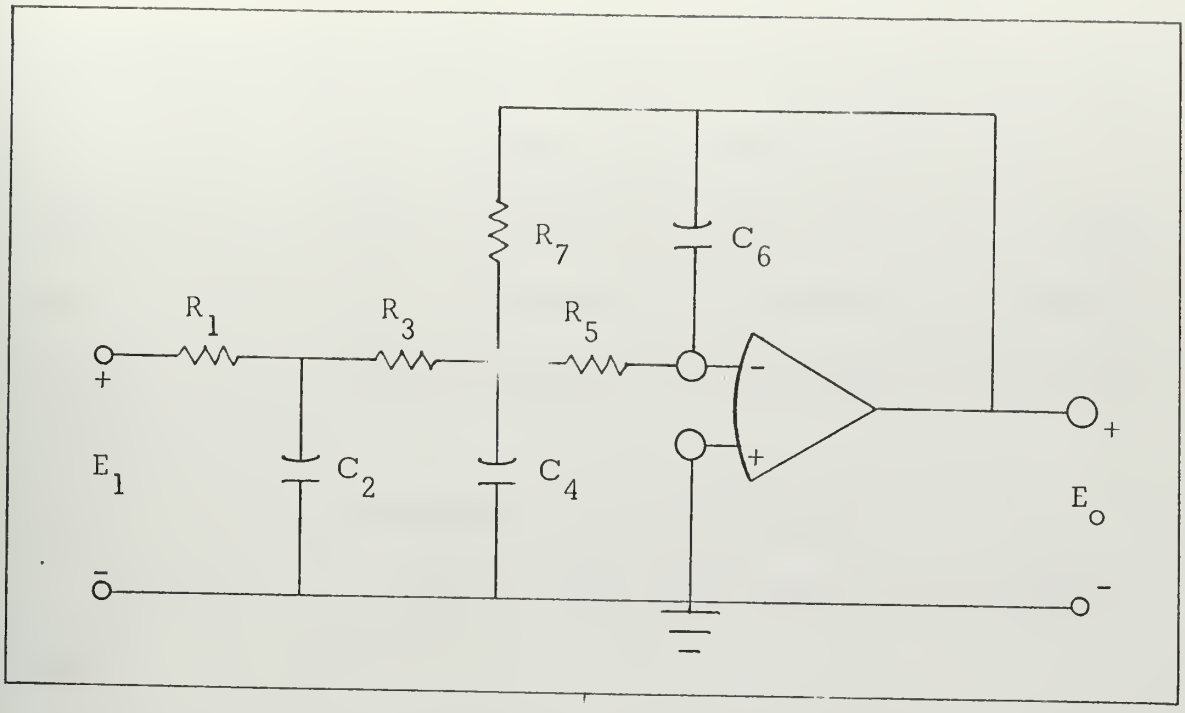

Figure 5-11. Third-order Rauch active filter

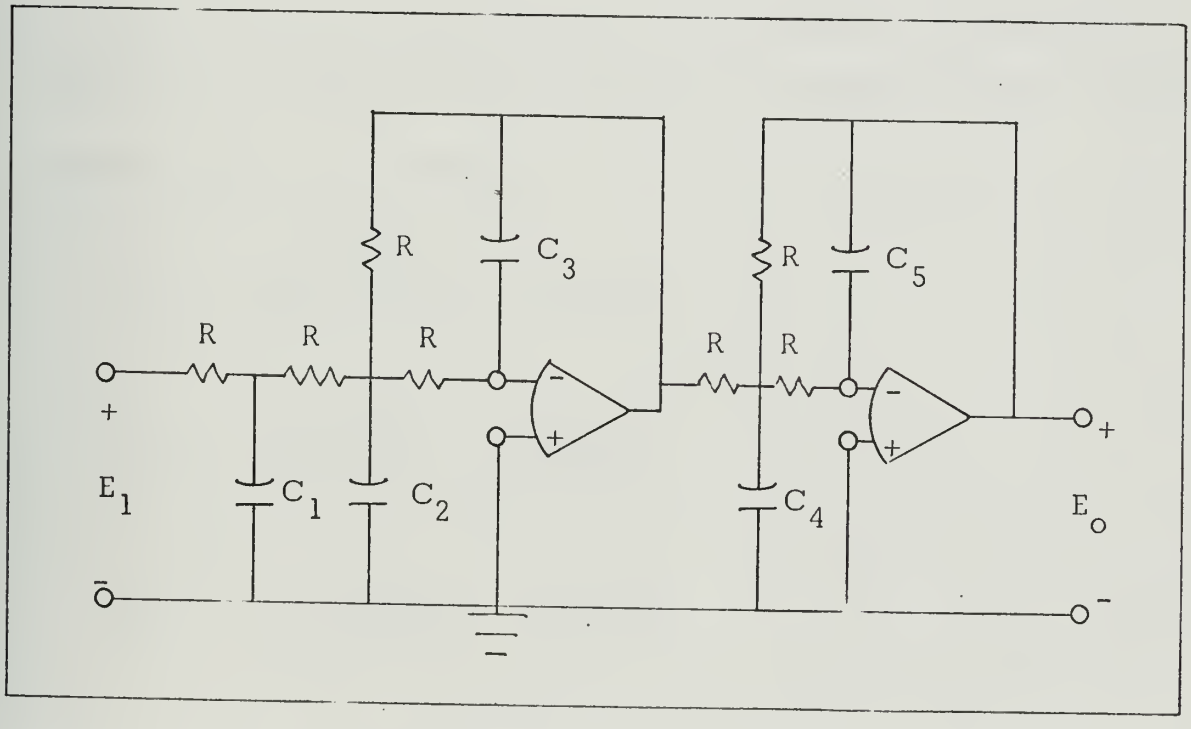

Figure 5-12. Circuit realization of Example 5-3

for Butterworth filters is shown in Table 5-1. The values in the tables are expressed in farads. To denormalize, each capacitor value is divided by $R\omega_o$, where R is the chosen resistor value and ω_o is the angular cutoff frequency. A good practice in choosing R is to check if dividing the largest and the smallest capacitor values by $R\omega_o$ results in practical values.

To illustrate this method, an example follows.

Example 5-3. Realize the fifth-order Butterworth filter transfer function in Example 2-2.

The angular cutoff frequency of the desired filter is $\omega_o = 62.83$ rad/sec. From Table 5-1, it is noted that the largest capacitor value is 4.31481 farads and the smallest is 0.21386 farad. An appropriate value for R is therefore 10 KΩ so that $R\omega_o = 6.283 \times 10^5$. The required capacitor values are therefore:

$$C_1 = \frac{2.16471}{6.283 \times 10^5} = 3.45\,\mu F$$

$$C_2 = \frac{4.31481}{6.283 \times 10^5} = 6.87\,\mu F$$

$$C_3 = \frac{0.21386}{6.283 \times 10^5} = 0.340\,\mu F \qquad (5\text{-}24)$$

$$C_4 = \frac{1.85410}{6.283 \times 10^5} = 2.960\,\mu F$$

Table 5-1. Normalized Capacitor Values for Butterworth Filter

n	C_1	C_2	C_3	C_4	C_5
1	1.00000				
2	2.12132	0.47140			
3	2.37484	2.59100	0.32503		
4	3.91969	0.25512	1.62359	0.61592	
5	2.16741	4.31481	0.21386	1.85410	0.53935

$$C_5 = \frac{0.53935}{6.283 \times 10^5} = 0.859\ \mu F$$

The resulting filter network is shown in Figure 5-12.

F. HOLT AND SEWELL [1965]

The method of design proposed by Holt and Sewell [Ref. 31] differs somewhat from the basic multiple-feedback configuration shown in Figure 5-1 in that it involves two cascaded sections shown in Figure 5-13. However, the active section includes an infinite-gain operational amplifier and a multiloop feedback circuit, as shown in Figure 5-14, and hence, belongs under the multiple-feedback classification.

The method is limited to the realization of biquadratic functions having transmission zeros on the imaginary axis of the s-plane. Such functions are known as Cauer or elliptic functions, having low-pass transfer functions of the form:

$$H(s) = \frac{s^2 + a_o}{s^2 + b_1 s + b_o} \quad . \tag{5-25}$$

The active circuit of Figure 5-14 is used to produce the transfer function

$$H_1(s) = \frac{s^2 + A_1 s + A_o}{s^2 + b_1 s + b_o} \quad , \tag{5-26}$$

and the passive section is used to produce the transfer function

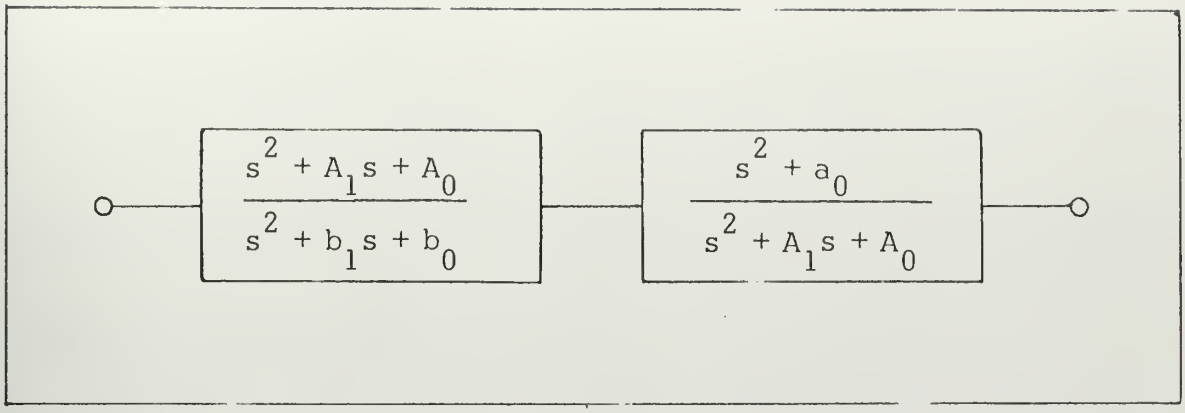

Figure 5-13. Configuration of Holt and Sewell

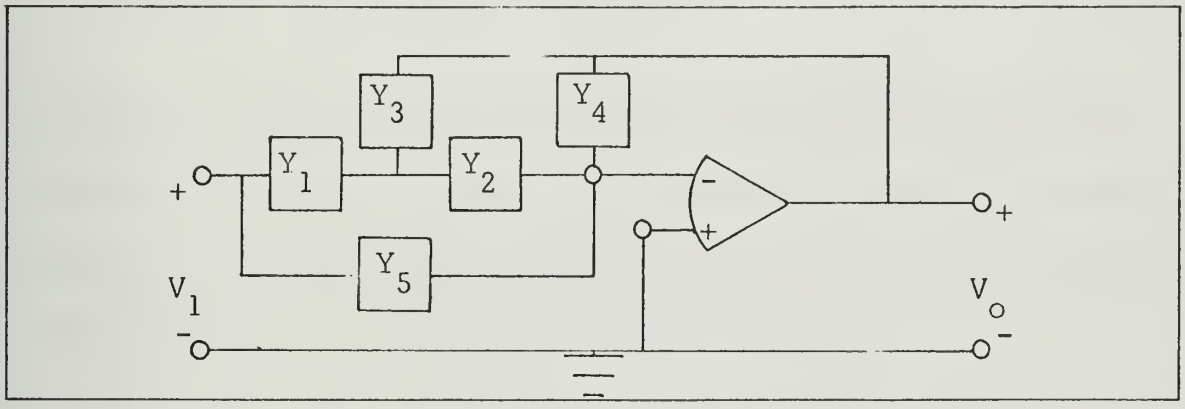

Figure 5-14. Active section of Holt and Sewell

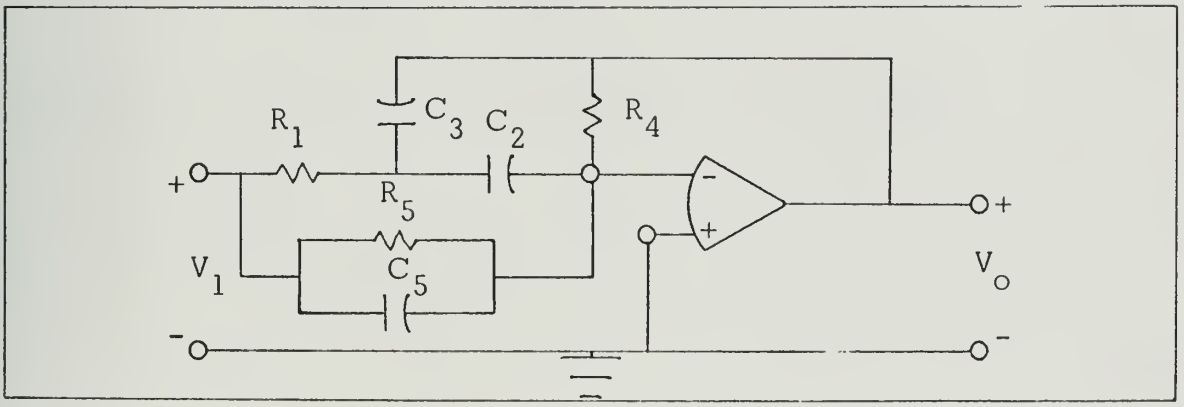

Figure 5-15. Active network of Holt and Sewell to realize

$$H_1(s) = \frac{s^2 + A_1 s + A_0}{s^2 + b_1 s + b_0}$$

$$H_2(s) = \frac{s^2 + a_o}{s^2 + A_1 s + A_o} \quad . \tag{5-27}$$

The active and passive sections are then cascaded to yield the required transfer function in equation (5-25).

Analysis of the operational amplifier section yields the transfer function

$$H_1(s) = - \frac{Y_1 Y_2 + Y_5 (Y_1 + Y_2 + Y_3)}{Y_2 Y_3 + Y_4 (Y_1 + Y_2 + Y_3)} \quad . \tag{5-28}$$

One possible combination of elements that would give the desired form of equation (5-26) is for Y_1 and Y_4 to be resistors, Y_2 and Y_3 capacitors and Y_5 to be a resistor and a capacitor in parallel, as shown in Figure 5-15. The transfer function in terms of the elements is

$$H(s) = - \frac{\frac{1}{R_1 R_5} + \left(\frac{C_2 + C_5}{R_1} + \frac{C_2 + C_3}{R_5} \right) s + C_5 (C_2 + C_3) s^2}{\frac{1}{R_1 R_4} + \left(\frac{C_2 + C_3}{R_4} \right) s + C_2 C_3 s^2} \tag{5-29}$$

Equating coefficients of equations (5-26) and (5-29) gives:

$$\begin{aligned} b_o &= 1/R_1 R_4 \\ b_1 &= (C_2 + C_3)/R_4 \\ 1 &= C_2 C_3 \quad . \end{aligned} \tag{5-30}$$

If

$$C_2 = C_3 = C_5 = C = 1 \quad , \tag{5-31}$$

the resulting resistor values are

$$R_1 = b_1/2b_o$$

$$R_4 = 2/b_1 \quad . \tag{5-32}$$

If $R_5 = 1$, equation (5-29) becomes

$$H_1(s) = \frac{2\left[\frac{b_o}{b_1} + \left(\frac{2b_o}{b_1} + 1\right)s + s^2\right]}{b_o + b_1 s + s^2} \quad . \tag{5-33}$$

The passive network following the active section has to produce the following transfer function:

$$H_2(s) = -\frac{s^2 + a_o}{s^2 + \left(\frac{2b_o}{b_1} + 1\right)s + \frac{b_o}{b_1}} \quad . \tag{5-34}$$

Equation (5-34) may be synthesized following Guillemin's parallel-ladder method [Ref. 20] provided it has only real poles, or expressed in terms of its denominator coefficients, provided that

$$\left(\frac{2b_o}{b_1} + 1\right)^2 > \frac{4b_o}{b_1} \quad . \tag{5-35}$$

If the desired transfer function of the form of equation (5-25) satisfies this realization condition, the cascaded sections of Holt and Sewell may be used.

Example 5-4. Realize the first product term of the transfer function in Example 2-6.

The product term

$$H(s) = \frac{s^2 + 3908.36}{s^2 + 5.51\,s + 3420.98} \tag{5-36}$$

is first checked to determine if it satisfies the realization condition of equation (5-35). With $b_o = 3420.98$ and $b_1 = 5.51$, it can be seen that equation (5-36) does satisfy the realization condition.

From equation (5-33), the active section transfer function is

$$H_1(s) = -\frac{2(s^2 + 1243\,s + 621)}{s^2 + 5.51\,s + 3420.98} \quad . \tag{5-37}$$

The passive section transfer function, from equation (5-34), is

$$H_2(s) = -\frac{s^2 + 3908.35}{s^2 + 1243\,s + 621} \quad , \tag{5-38}$$

where $a_o = 3908.36$.

Equations (5-33) and (5-34) were determined by setting $C_2 = C_3 = C_5 = 1$ and $R_5 = 1$ in the active section, so that all that remains to specify the active section completely is to determine R_4 and R_1 as follows:

$$R_4 = 2/b_1 = 0.363 \tag{5-39a}$$

$$R_1 = b_1/2b_o = 0.805 \times 10^{-3} \quad , \tag{5-39b}$$

where C's are in farads and R's in ohms.

The synthesis of the passive transfer function, $H_2(s)$, involves choosing an appropriate Q(s). In this case, one choice is

$$Q(s) = (s + 2)\ (s + 1500) \quad , \tag{5-40}$$

such that

$$H_2(s) = - \frac{\dfrac{s^2 + 3908.36}{(s + 2)\ (s + 1500)}}{\dfrac{s^2 + 1243\ s + 621}{(s + 2)\ (s + 1500)}} \quad , \tag{5-41}$$

where

$$y_{12P}(s) = - \frac{s^2 + 3908.36}{(s + 2)\ (s + 1500)} \tag{5-42a}$$

$$y_{22P}(s) = \frac{s^2 + 1243\ s + 621}{(s + 2)\ (s + 1500)} \quad . \tag{5-42b}$$

$y_{22P}(s)$ can now be expanded so as to realize the double zeros of $y_{12P1}(s) = - s^2/(s + 2)\ (s + 1500)$ at $s = 0$:

$$y_{22P1}(s) = - \frac{1}{4.83} + \cfrac{1}{\dfrac{1}{0.310s} + \cfrac{1}{\dfrac{1}{1.61} + \cfrac{1}{\dfrac{1}{0.000115s} + 5.81}}}$$

$y_{22P}(s)$ can then be expanded to realize the double zeros of $y_{12P2}(s) = - 3908.36/(s + 2)\ (s + 1500)$ at $s = - \infty$:

$$Y_{22P2}(s) = \cfrac{1}{1 + \cfrac{1}{\cfrac{s}{259} + \cfrac{1}{0.21 + \cfrac{1}{0.55s + \cfrac{1}{3.62}}}}} \quad . \quad (5\text{-}44)$$

To be able to connect the two ladder-network components of $y_{12P}(s)$, shown in Figure 5-16, their admittance levels have to be individually adjusted by the following scaling factors:

$$\frac{K_P}{K_{P1}} = \frac{0.0276}{0.207} = 0.1333 \qquad (5\text{-}45a)$$

$$\frac{K_P}{K_{P2}} = \frac{0.0276}{0.0329} = 0.839 \qquad (5\text{-}45b)$$

The complete normalized circuit realization is shown in Figure 5-17. Both the active and the passive sections may be independently de-normalized to give practical element values.

G. ADVANTAGES AND DISADVANTAGES

For second-order functions, this category of realizations has the distinct advantage of usually requiring a minimum number of elements. For instance, in the realization of the low-pass transfer function of Example 2-1, Hakim's method of realization, belonging to the single-feedback category, required one operational amplifier, nine resistors and six capacitors. The Rauch filter, belonging to this category, required one operational amplifier, three resistors and two capacitors. For higher-order cases, Wadhwa and Aggarwal have shown that realization

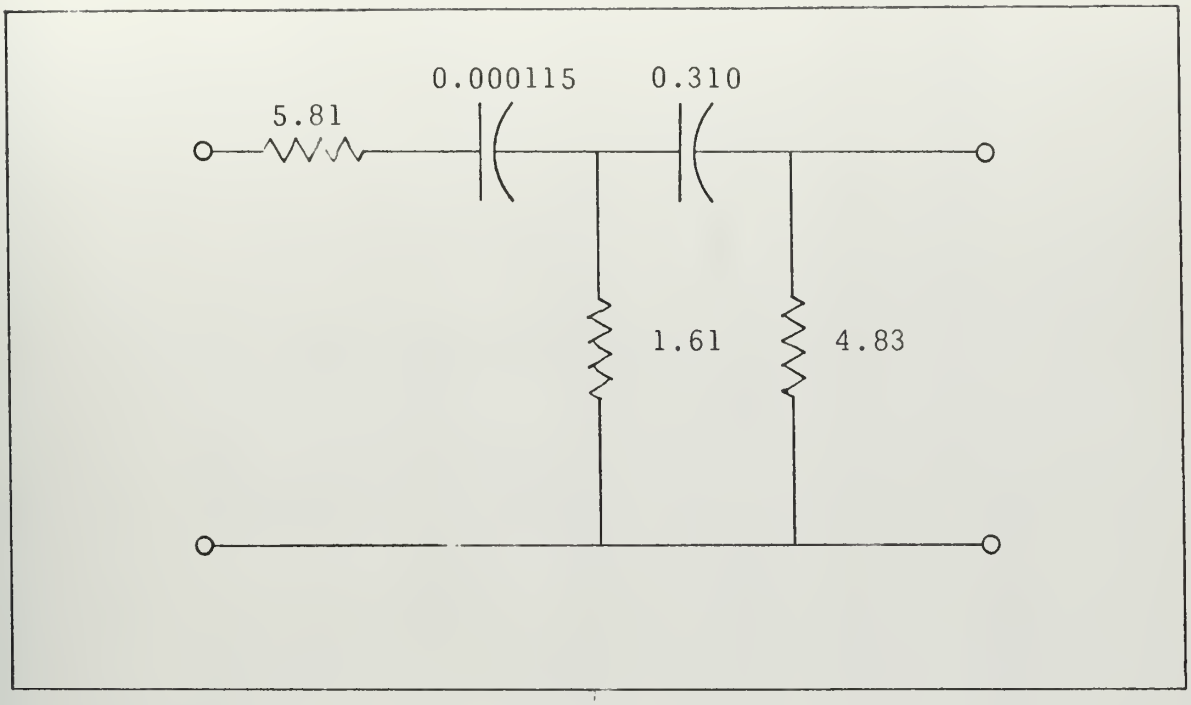

Figure 5-16a. Network realization of $y_{12P1}(s)$ and $y_{22P1}(s)$

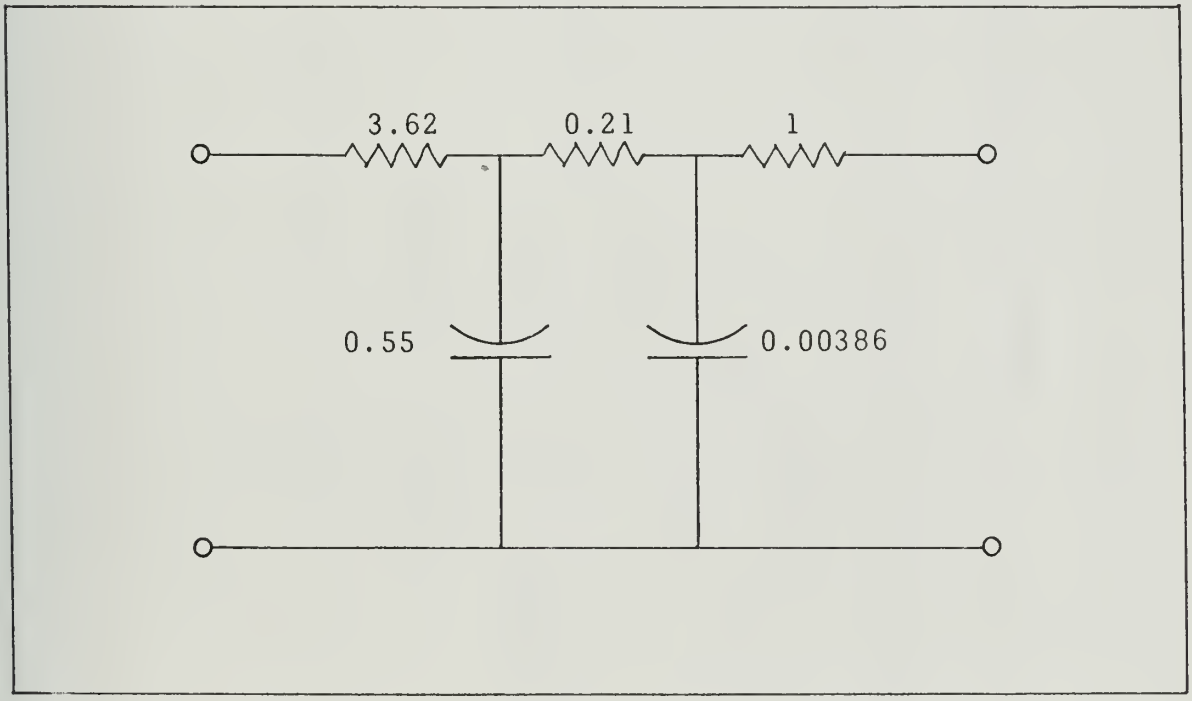

Figure 5-16b. Network realization of $y_{12P2}(s)$ and $y_{22P2}(s)$

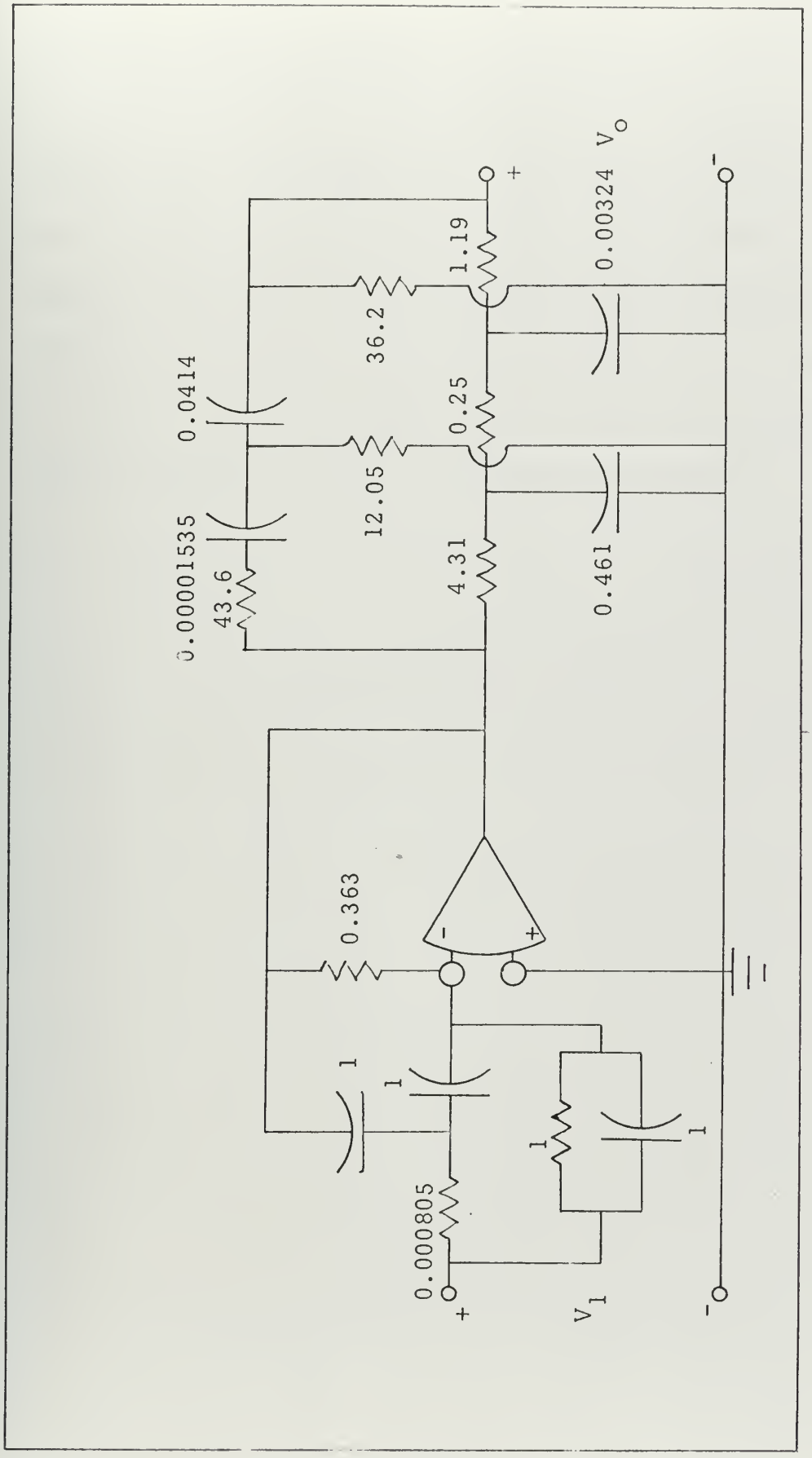

Figure 5-17. Circuit realization of Example 5-4

of such functions is possible by simply extending the basic second-order prototype configuration but the determination of the element values becomes increasingly complicated with increasing order because of the nonlinear nature of the relating equations. Such higher-order cases can easily be realized by factoring them into first- and second-order product terms and cascading the realizations of these terms. Cascading terms is possible without appreciable interaction because the output impedance of each realization is that of the operational amplifier.

VI. INFINITE-GAIN GENERAL REALIZATION TECHNIQUES

Two general realization procedures using infinite-gain operational amplifiers are presented in this chapter. They are general in the sense that they can realize any rational function of any order. As opposed to the realization techniques of the last two chapters, these two procedures are not limited by the restrictions on the passive RC configurations that make up their input and feedback networks.

A. LOVERING [1965]

The general circuit proposed by Lovering [Ref. 32] is shown in Figure 6-1. Since the two operational amplifiers are assumed to have gain approaching infinity, the current summation at each of their summing points may be written directly as:

$$V_1 Y_1 + V Y_3 + V_o Y_4 = 0 \tag{6-1}$$

$$V_1 Y_2 + V Y_5 + V_o Y_6 = 0 \quad . \tag{6-2}$$

If $Y_3 = Y_5$, subtracting equation (6-2) from equation (6-1) yields

$$V_1 (Y_1 - Y_2) + V_o (Y_4 - Y_6) = 0. \tag{6-3}$$

Putting equation (6-3) in transfer function form gives

$$\frac{V_o}{V_1} = \frac{Y_1 - Y_2}{Y_6 - Y_4} = H(s) \quad . \tag{6-4}$$

Since the general transfer function may be expressed in the form

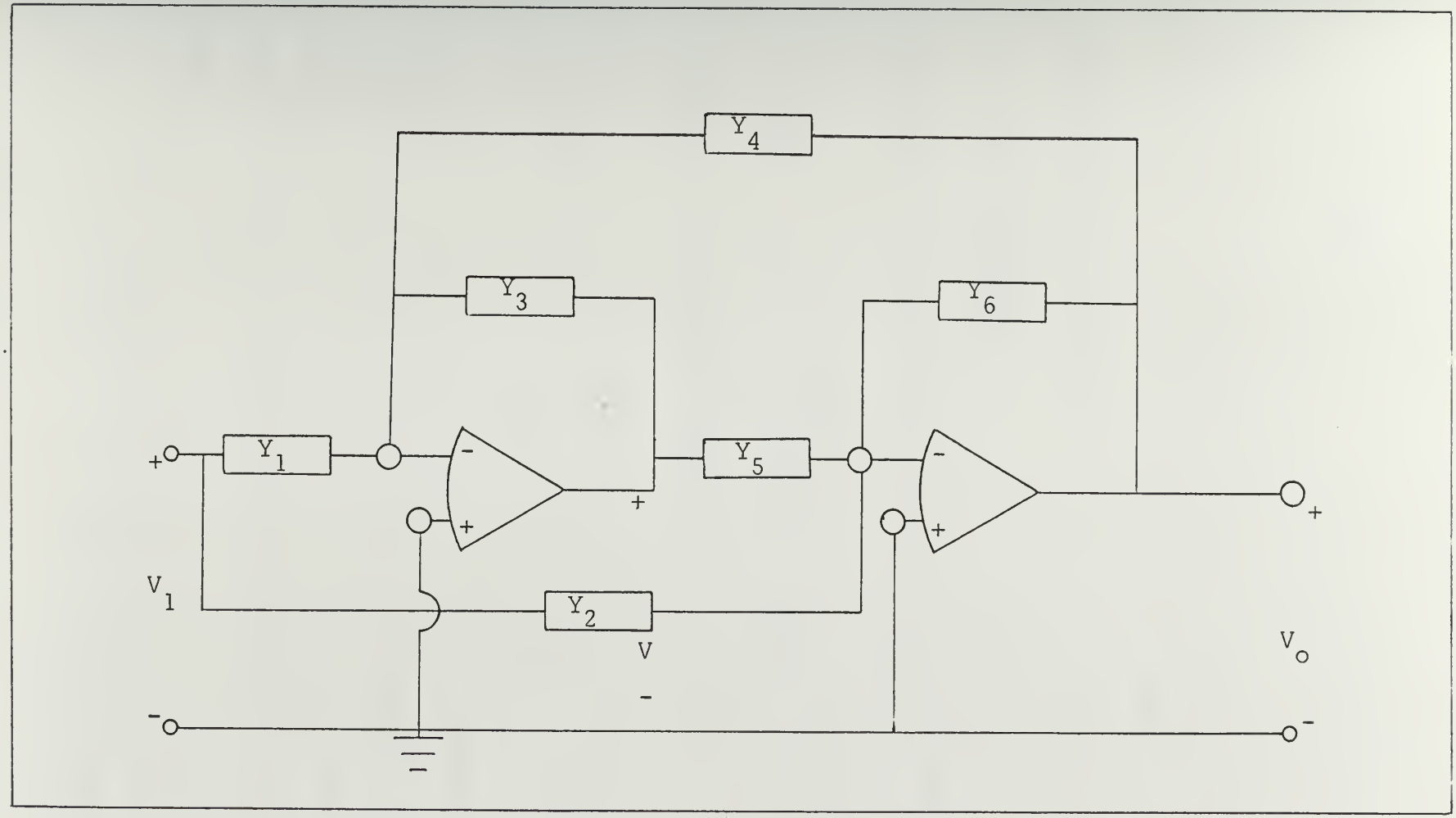

Figure 6-1. Lovering's active network configuration

$$H(s) = \frac{N(s)}{D(s)} \quad , \tag{6-5}$$

if both numerator and denominator are divided by a polynomial, Q(s), having simple roots restricted to the negative real axis and whose degree is one less than that of N(s) or D(s), whichever is greater, the transfer function may then be written as

$$H(s) = \frac{N(s)/Q(s)}{D(s)/Q(s)} \quad . \tag{6-6}$$

If N(s)/Q(s) is expanded [Ref. 15] in the partial-fraction form

$$\frac{N(s)}{D(s)} = K_o + \sum_{i=1}^{n} \frac{K_i s}{s + \sigma_i} + K_\infty s \quad , \tag{6-7a}$$

or, expressed in terms of R's and C's,

$$Y_{RC}(s) = \frac{1}{R_o} + \sum_{i=1}^{n} \frac{1}{\frac{1}{R_i} + \frac{1}{C_i s}} + C_\infty s \quad , \tag{6-7b}$$

the result is a string of positive and negative terms because the vatious K's are all real but may be positive or negative. If $Y_1 - Y_2$ in equation (6-4) is now equated to N(s)/Q(s), Y_1 can directly be associated with all the positive terms in equation (6-7) and Y_2 with all the negative terms.

A similar expansion of D(s)/Q(s) can then be carried out and all the positive terms of the resulting expansion can be equated to Y_6 and all the negative terms to Y_4.

An example of this procedure will clarify the steps indicated.

Example 6-1. Realize the low-pass Butterworth transfer function of Example 2-1:

$$H(s) = \frac{3947.84}{s^2 + 88.84\,s + 3947.84} = \frac{N(s)}{D(s)} \quad . \tag{6-8}$$

If the dividing polynomial is chosen to be $Q(s) = s + 100$, the resulting numerator rational polynomial can be expanded as

$$\frac{H(s)}{Q(s)} = 39.48 - \frac{39.48s}{s + 100} \quad . \tag{6-9}$$

Similarly, the denominator rational polynomial can be expanded to produce

$$\frac{D(s)}{Q(s)} = 39.48 + s - \frac{50.64s}{s + 100} \quad . \tag{6-10}$$

Equating equation (6-9) to $Y_1 - Y_2$ and equation (6-10) to $Y_6 - Y_4$ the following relations can be made:

$$Y_1 = 39.48 \tag{6-11a}$$

$$Y_2 = \frac{39.48s}{s + 100} \quad . \tag{6-11b}$$

$$Y_6 = 39.48 + s \tag{6-11c}$$

$$Y_4 = \frac{50.64s}{s + 100} \quad . \tag{6-11d}$$

The following element values can then be calculated:

$R_1 = 0.0253$ ohm

$R_2 = 0.0253$ ohm

$C_2 = 0.3948$ farad

$R_6 = 0.0253$ ohm

$C_6 = 1$ farad

$R_4 = 0.01971$ ohm

$C_4 = 0.5064$ farad . (6-12)

If a scaling factor of 10^5 is applied to the values in equation (6-12), the following component values result:

$R_1 = 2.53\ K\Omega$

$R_2 = 2.53\ K\Omega$

$C_2 = 3.948\ \mu F$

$R_6 = 2.53\ K\Omega$

$C_6 = 10\ \mu F$

$R_4 = 1.971\ K\Omega$

$C_4 = 5.064\ \mu F$. (6-13)

R_3 and R_5 may conveniently be chosen to be $1\ K\Omega$.

The complete realization is shown in Figure 6-2.

To illustrate the property that this procedure can indeed realize any transfer function, even with poles and zeros in the right half of the complex-frequency plane, consider the next example.

Example 6-2. Realize the transfer function

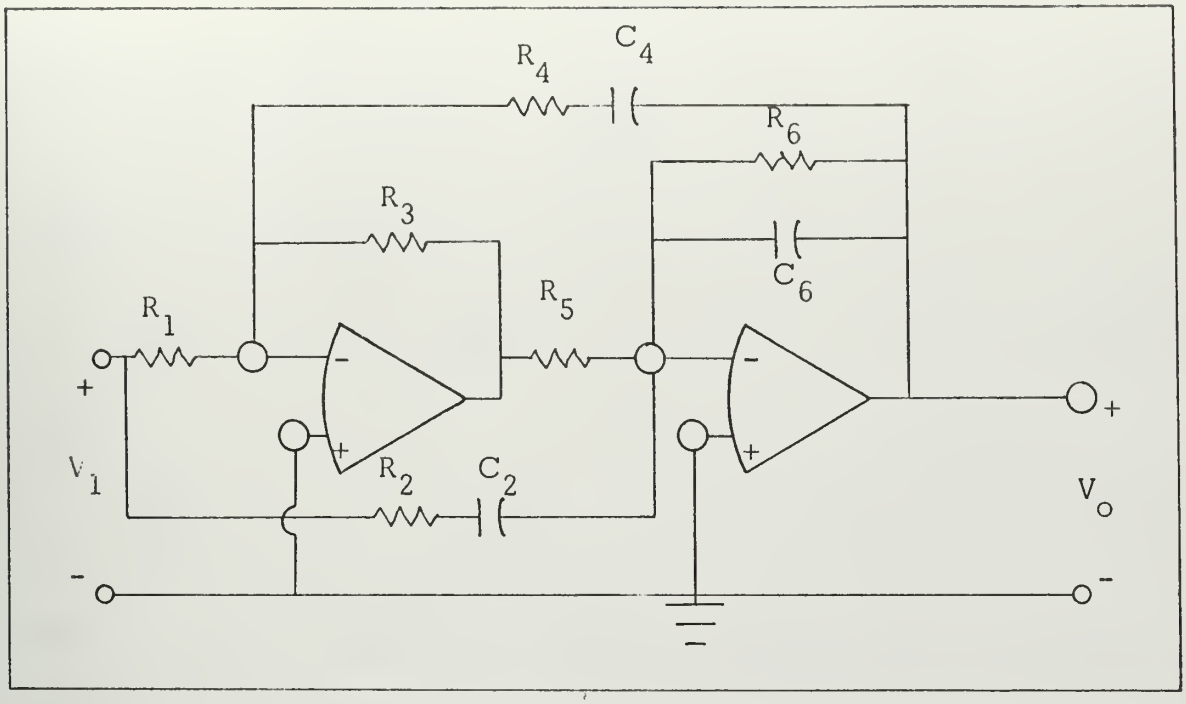

Figure 6-2. Circuit realization of Example 6-1

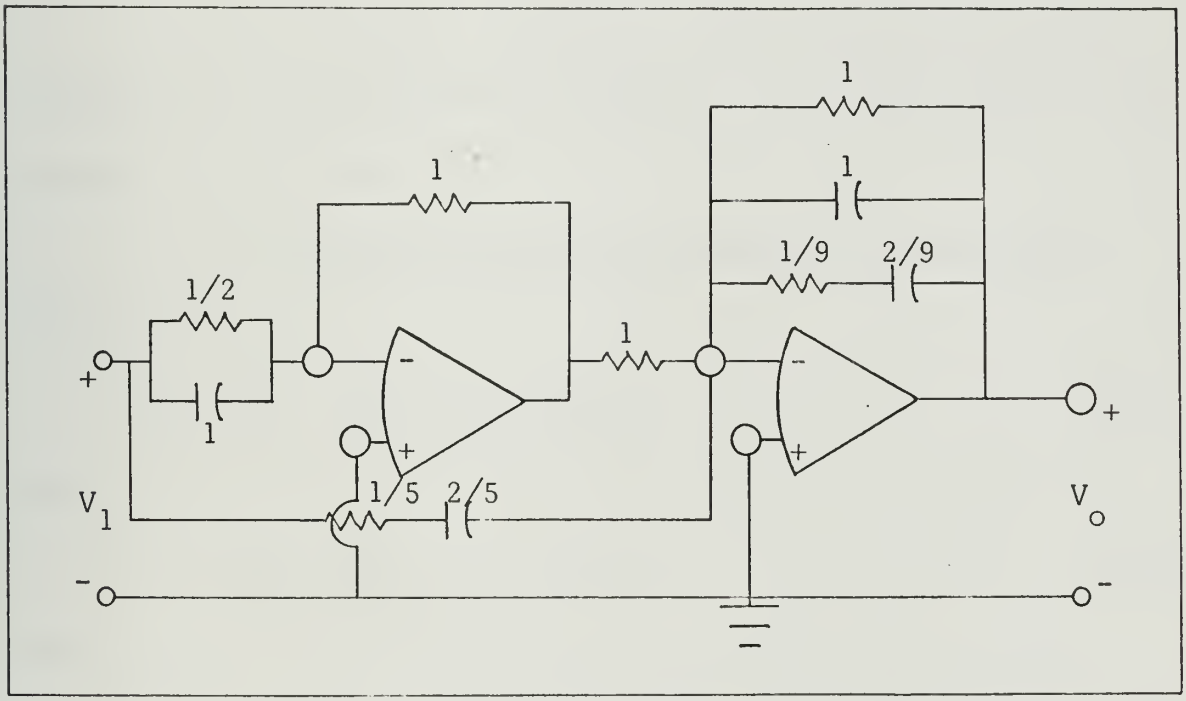

Figure 6-3. Circuit realization of Example 6-2

$$H(s) = \frac{s^2 - s + 4}{s^2 + 12s + 2} = \frac{N(s)}{D(s)} \quad . \tag{6-14}$$

If $Q(s) = s + 2$ is chosen,

$$\frac{N(s)}{Q(s)} = 2 + s - \frac{5s}{s + 2} \quad , \tag{6-15a}$$

and

$$\frac{D(s)}{Q(s)} = 1 + s + \frac{9s}{s + 2} \quad . \tag{6-15b}$$

If R_3 and R_5 are chosen to be 1 ohm, the normalized circuit realization is shown in Figure 6-3.

B. BRUGLER [1966]

Brugler [Ref. 33] used a differential-input operational amplifier to develop his general realization technique. The configuration he used is shown in Figure 6-4.

A current summation at the two input nodes of the operational amplifier gives:

$$(V_1 - V_A)Y_1 - V_A Y_2 - (V_A - V_o)Y_3 = 0 \quad , \tag{6-16}$$

and

$$(V_1 - V_B)Y_4 - V_B Y_5 - (V_B - V_o)Y_6 = 0 \quad . \tag{6-17}$$

Solving equations (6-16) and (6-17) in terms of V_A and V_B results in:

$$V_A = \frac{V_1 Y_1 + V_o Y_3}{Y_1 + Y_2 + Y_3} \quad , \tag{6-18}$$

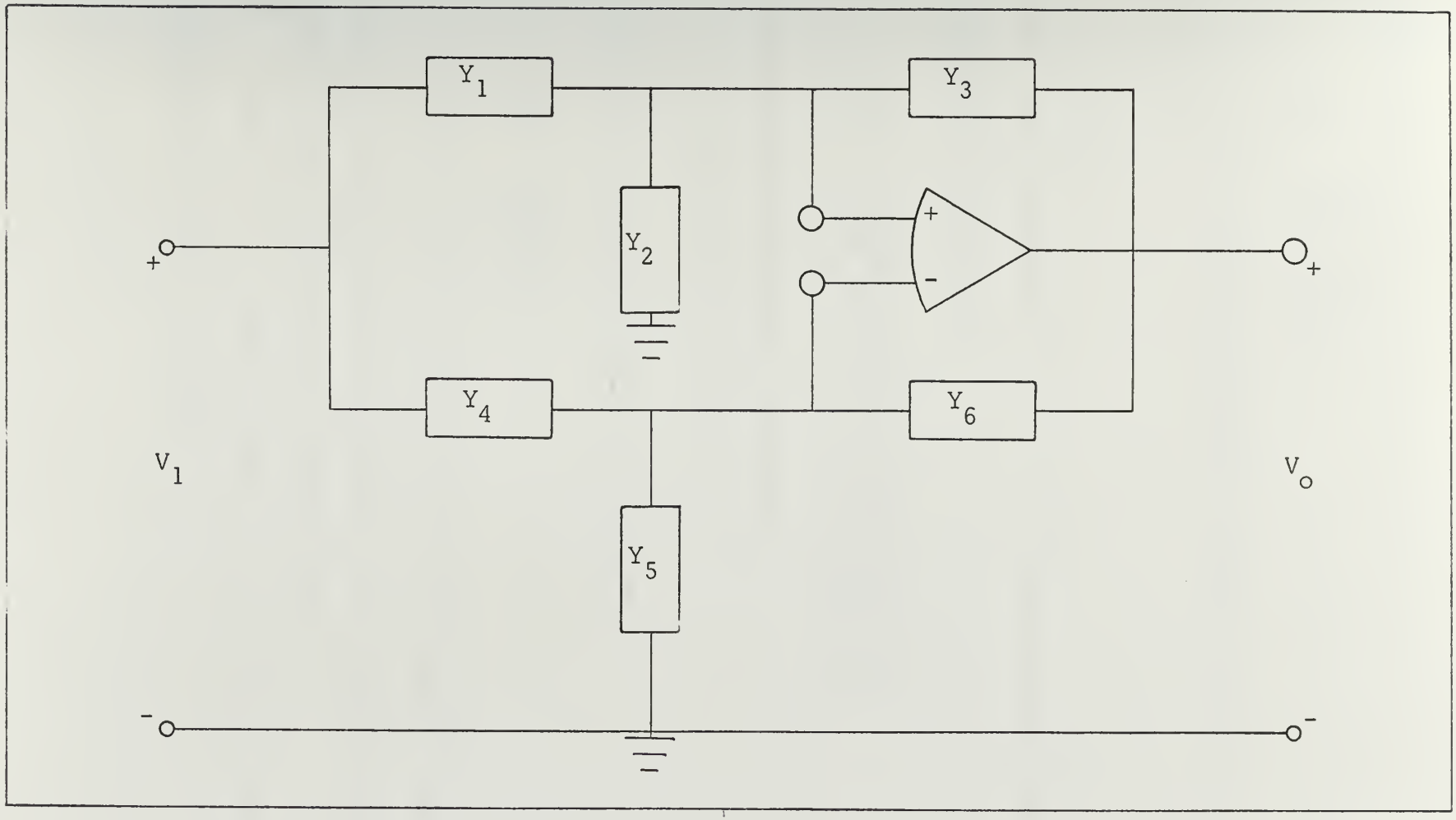

Figure 6-4. Brugler's active network configuration

and

$$V_B = \frac{V_1 Y_4 + V_o Y_6}{Y_4 + Y_5 + Y_6} \quad . \tag{6-19}$$

But since an infinite-gain operational amplifier forces its two inputs to be equal,

$$V_A = V_B \quad . \tag{6-20}$$

So, equating equations (6-18) and (6-19) gives the transfer function of the circuit in Figure 6-4:

$$\frac{V_o}{V_1} = \frac{Y_1 (Y_4 + Y_5 + Y_6) - Y_4 (Y_1 + Y_2 + Y_3)}{Y_6 (Y_1 + Y_2 + Y_3) - Y_3 (Y_4 + Y_5 + Y_6)} \quad . \tag{6-21}$$

If a simplifying condition is now applied,

$$Y_1 + Y_2 + Y_3 = Y_4 + Y_5 + Y_6 \quad , \tag{6-22}$$

the transfer function in equation (6-9) becomes

$$\frac{V_o}{V_1} = \frac{Y_1 - Y_4}{Y_6 - Y_3} \quad . \tag{6-23}$$

Equation (6-23) is exactly the form of the transfer function of Lovering's general circuit and exactly the same realization techniques can be applied to generate the required elements.

With Y_1, Y_4, Y_6, and Y_3 known, equation (6-22) can now be used to determine Y_2 and Y_5 by setting

$$Y_2 = Y_4 + Y_6 \quad , \tag{6-24a}$$

$$Y_5 = Y_1 + Y_3 \quad . \tag{6-24b}$$

Common terms in $Y_4 + Y_6$ and $Y_1 + Y_3$ can be subtracted out without violating equation (6-22), thereby simplifying the resulting realizations of Y_2 and Y_5.

An example will illustrate this procedure.

Example 6-3. Realize the Butterworth low-pass transfer function of Example 2-1.

This same transfer function has already been realized using Lovering's method in the previous section and if the same partial-fraction expansion is used for a chosen $Q(s) = s + 100$, the following relations can be made:

$$Y_1 = 39.48 \tag{6-25a}$$

$$Y_4 = \frac{39.48s}{s + 100} \tag{6-25b}$$

$$Y_6 = 39.48 + s \tag{6-25c}$$

$$Y_3 = \frac{50.64s}{s + 100} \quad . \tag{6-25d}$$

If equations (6-24) are now applied, Y_2 and Y_5 are determined to be

$$Y_2 = \frac{39.48s}{s + 100} + 39.48 + s \quad , \tag{6-26a}$$

$$Y_5 = 39.48 + \frac{50.64s}{s + 100} \quad . \tag{6-26b}$$

Note that 39.48 is a common term in equations (6-26a) and (6-26b) and may be subtracted out.

If a scaling factor of 10^5 is now used, the final realization of the desired transfer function is shown in Figure 6-5.

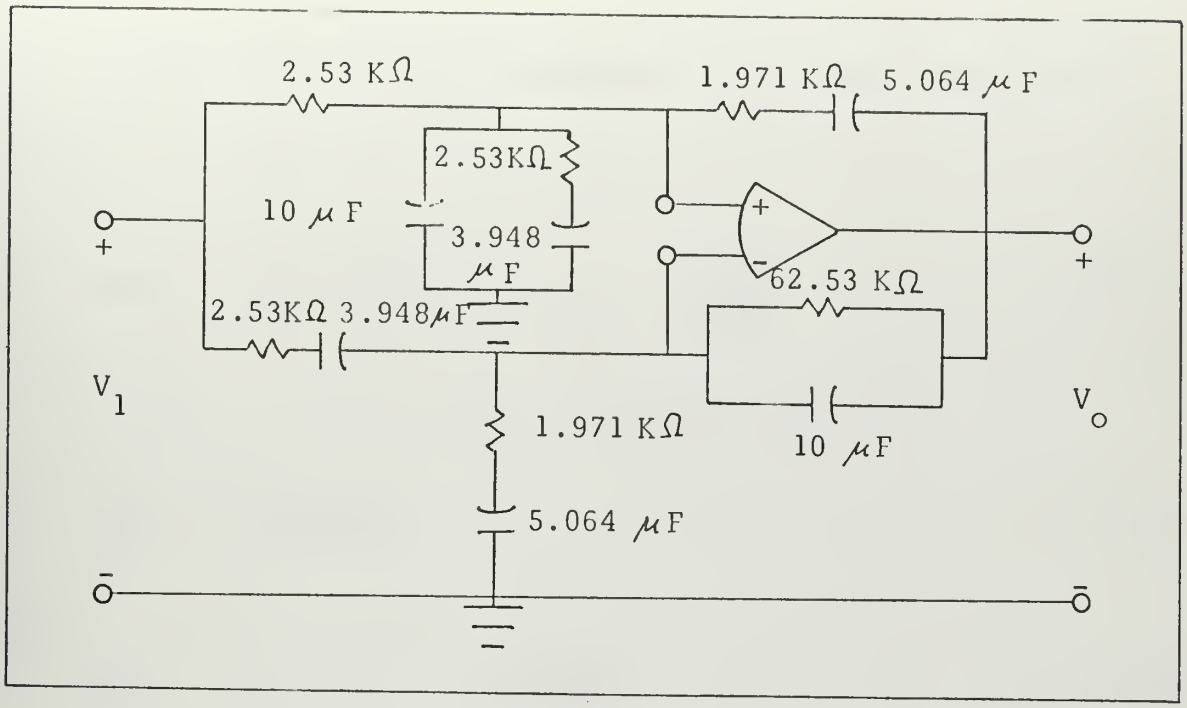

Figure 6-5. Circuit realization of Example 6-3

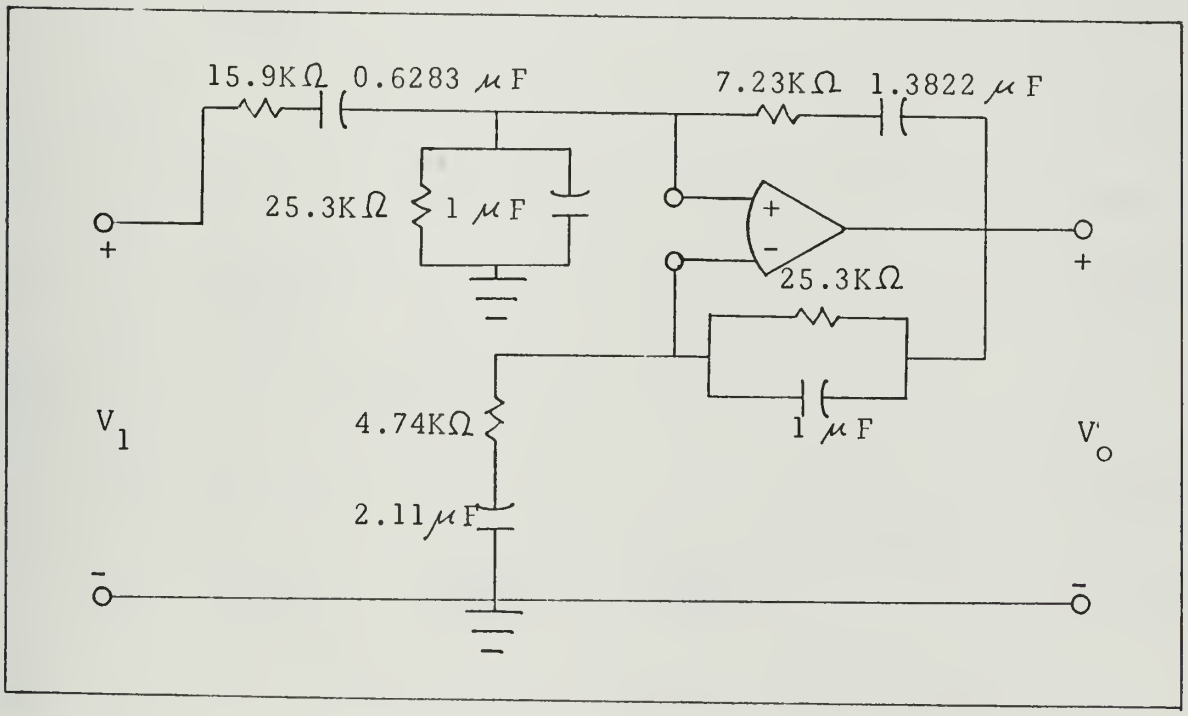

Figure 6-6. Circuit realization of Example 6-4

Example 6-4. Realize the bandpass transfer function of Example 2-4:

$$H(s) = \frac{62.83\,s}{s^2 + 1.257\,s + 3947.84} = \frac{N(s)}{D(s)} \quad . \tag{6-27}$$

If $Q(s) = s + 100$ is chosen, the expanded terms are

$$\frac{N(s)}{Q(s)} = \frac{62.83s}{s + 100} \quad , \tag{6-28a}$$

and

$$\frac{D(s)}{Q(s)} = 39.48 + s - \frac{138.22s}{s + 100} \quad . \tag{6-28b}$$

By association,

$$Y_1 = \frac{62.83s}{s + 100} \tag{6-29a}$$

$$Y_4 = 0 \tag{6-29b}$$

$$Y_6 = 39.48 + s \tag{6-29c}$$

$$Y_3 = \frac{138.22s}{s + 100} \quad . \tag{6-29d}$$

Use of equation (6-24) gives

$$Y_2 = 39.48 + s \tag{6-30a}$$

$$Y_5 = \frac{62.83s}{s + 100} + \frac{138.22s}{s + 100} = \frac{211.05s}{s + 100} \quad . \tag{6-30b}$$

From equations (6-29) and (6-30), the following element values are determined:

$$R_1 = 1/62.83 = 0.0159$$

$$C_1 = 62.83/100 = 0.6283$$

$$R_2 = 1/39.48 = 0.0253$$

$$C_2 = 1$$

$$R_3 = 1/138.22 = 0.00723$$

$$C_3 = 138.22/100 = 1.3822$$

$$R_5 = 1/211.05 = 0.00474$$

$$C_5 = 211.05/100 = 2.1105$$

$$R_6 = 1/39.48 = 0.0253$$

$$C_6 = 1 \quad , \qquad (6\text{-}31)$$

where R's are in ohms and C's in farads.

If a scaling factor of 10^6 is applied to equation (6-31), the resulting circuit realization is shown in Figure 6-6.

C. ADVANTAGES AND DISADVANTAGES

The two procedures discussed in this chapter retain all the advantages associated with techniques using infinite-gain operational amplifiers. The realized circuits are relatively less sensitive to the variations in gain of the active element. Cascading of low-order realizations can be accomplished without appreciable interaction between them because of the operational amplifier's very low output impedance.

And, in addition, these two procedures are capable of realizing any transfer function that a designer might feel is desired. It must be appreciated, however, that the realizations are not necessarily optimum as far as number of required elements is concerned.

VII. INFINITE-GAIN STATE-SPACE REALIZATIONS

Although the idea of realizing high-order transfer functions by factoring them into first- and second-order product terms and realizing these using first- and second-order building-block networks has been mentioned in the previous chapters, it is in this chapter that the practicality and the advantages of such an idea are shown in detail.

The realization methods in this chapter make use of state-space concepts to develop the basic second-order building block made up of integrators and summers, both of which use infinite-gain operational amplifiers. Consequently, such realization methods are classified under the category of Infinite-Gain Infinite-Gain Realizations.

A. THEORETICAL DEVELOPMENT

Consider the general open-circuit voltage transfer function

$$\frac{V_o(s)}{V_1(s)} = \frac{a_o + a_1 s + \ldots + a_{n-1} s^{n-1} + a_n s^n}{b_o + b_1 s + \ldots + b_{n-1} s^{n-1} + s^n} \quad . \tag{7-1}$$

A state representation of this transfer function is possible by breaking up equation (7-1) [Ref. 34] as follows:

$$\frac{V_o(s)}{V_1(s)} = \frac{W_F(s)}{V_1(s)} \cdot \frac{V_o(s)}{W_F(s)} \quad , \tag{7-2}$$

where

$$\frac{W_F(s)}{V_1(s)} = \frac{1}{b_o + b_1 s + \ldots + b_{n-1} s^{n-1} + s^n} \qquad (7\text{-}3a)$$

and

$$\frac{V_o(s)}{W_F(s)} = a_o + a_1 s + \ldots + a_{n-1} s^{n-1} + a_n s^n \quad , \qquad (7\text{-}3b)$$

where $W_F(s)$ is the Laplace transform, with initial conditions set equal to zero, of a dummy variable, $w(t)$. Expanding equations (7-3a) and (7-3b) and getting the inverse Laplace transforms of the expanded equations give

$$\frac{d^n w}{dt^n} = - b_{n-1} \frac{d^{n-1} w}{dt^{n-1}} - \ldots - b_1 \frac{dw}{dt} - b_o w + v_1 \qquad (7\text{-}4a)$$

and

$$v_o = a_o w + a_1 \frac{dw}{dt} + \ldots + a_{n-1} \frac{d^{n-1} w}{dt^{n-1}} + a_n \frac{d^n w}{dt^n} \quad , \qquad (7\text{-}4b)$$

where all variables are functions of time.

If $x_1 = w$, $x_2 = \frac{dw}{dt}$, ... , and $u = v_1$ and $y = v_o$, two matrix equations result:

$$\begin{bmatrix} \dot{x}_1 \\ \dot{x}_2 \\ . \\ \dot{x}_{n-1} \\ \dot{x}_n \end{bmatrix} = \begin{bmatrix} 0 & 1 & 0 & \ldots & 0 \\ 0 & 0 & 1 & \ldots & 0 \\ . & . & . & \ldots & . \\ 0 & 0 & 0 & \ldots & 1 \\ -b_o & -b_1 & -b_3 & & -b_{n-1} \end{bmatrix} \begin{bmatrix} x_1 \\ x_2 \\ . \\ x_{n-1} \\ x_n \end{bmatrix} + \begin{bmatrix} 0 \\ 0 \\ . \\ 0 \\ 1 \end{bmatrix} [u] \qquad (7\text{-}5a)$$

and

$$\begin{bmatrix} y \end{bmatrix} = \begin{bmatrix} a_o & a_1 & \cdots & a_{n-1} \end{bmatrix} \begin{bmatrix} x_1 \\ x_2 \\ \cdot \\ x_{n-1} \\ x_n \end{bmatrix} + \begin{bmatrix} 0 & 0 & \cdots & a_n \end{bmatrix} \begin{bmatrix} \dot{x}_1 \\ \dot{x}_2 \\ \cdot \\ \dot{x}_{n-1} \\ \dot{x}_n \end{bmatrix} \qquad (7\text{-}5b)$$

where $\dot{x}_1 = \frac{dx}{dt}$, $\dot{x}_2 = \frac{dx_2}{dt}$, ...

Equation (7-5a) may be written as

$$\underset{\sim}{\dot{x}} = \underset{\sim}{A}\ \underset{\sim}{x} + \underset{\sim}{B}\ \underset{\sim}{u} \quad , \qquad (7\text{-}6)$$

where $\underset{\sim}{x}$ is the state vector, $\underset{\sim}{\dot{x}}$ is the derivative of the state vector, $\underset{\sim}{A}$ is the matrix determined by the properties of the system and $\underset{\sim}{B}\ \underset{\sim}{u}$ represents the inputs to the network.

Equation (7-5b) may be expressed as

$$\underset{\sim}{y} = \underset{\sim}{C}\ \underset{\sim}{x} + \underset{\sim}{D}\ \underset{\sim}{u} \quad . \qquad (7\text{-}7)$$

A signal flow graph can be drawn to represent equations (7-5a) and (7-5b). This is shown in Figure 7-1. Each element of the graph can be realized by an integrator or a summer (inverter), both of which are made up of operational amplifiers, resistors and capacitors, as shown in Figure 7-2.

If a high-order transfer function is to be realized by directly converting its signal flow graph as indicated above, the roots of such

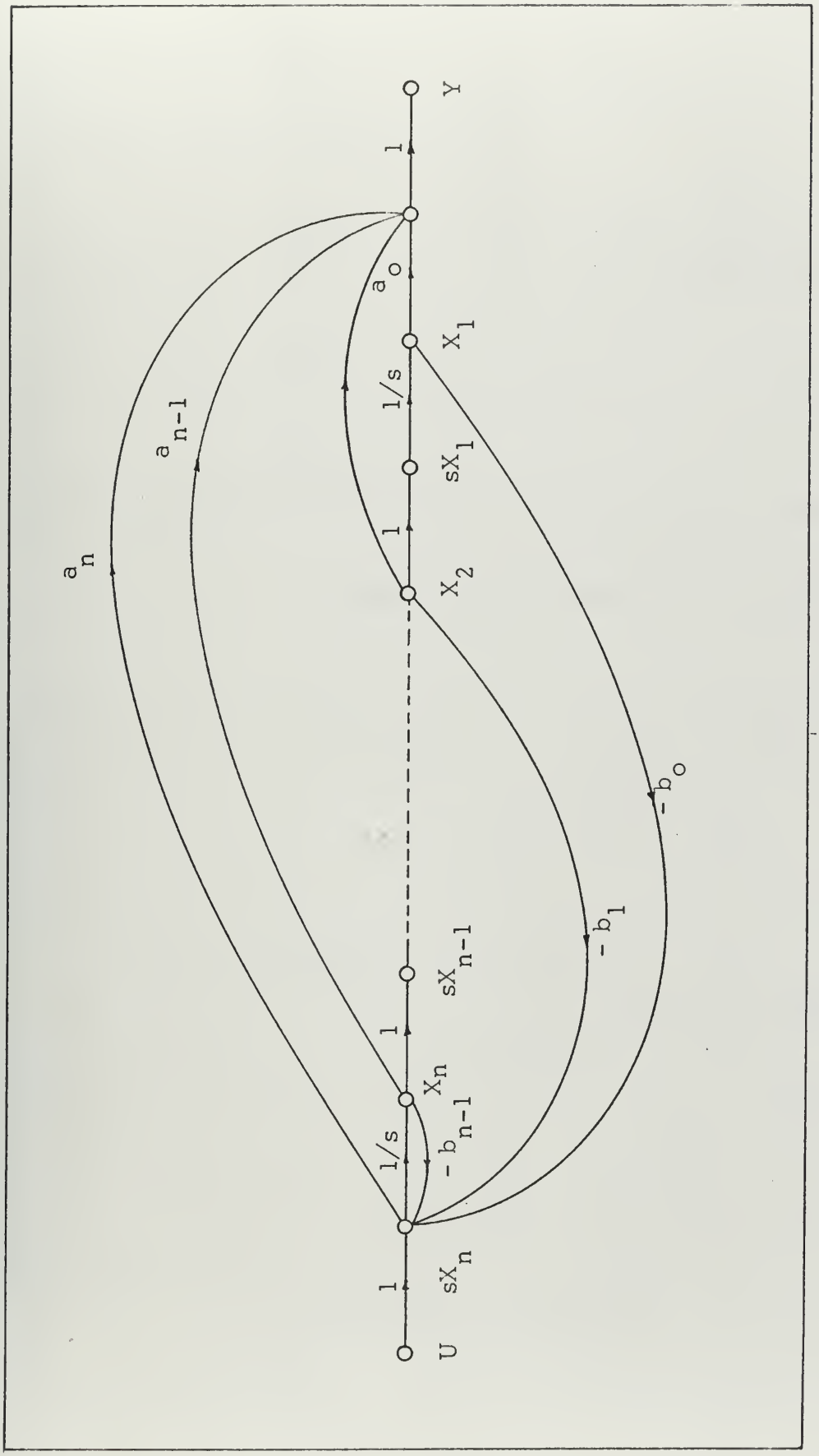

Figure 7-1. Signal flow graph of general nth-order open-circuit voltage transfer function

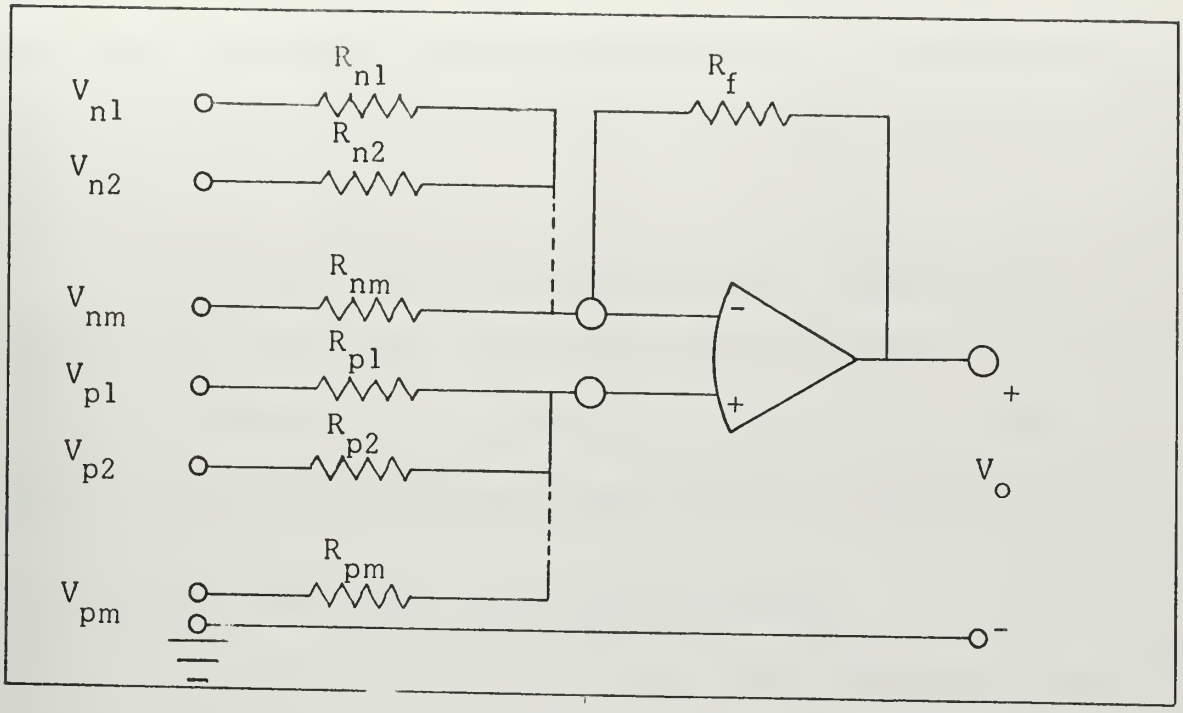

Figure 7-2a. A summer

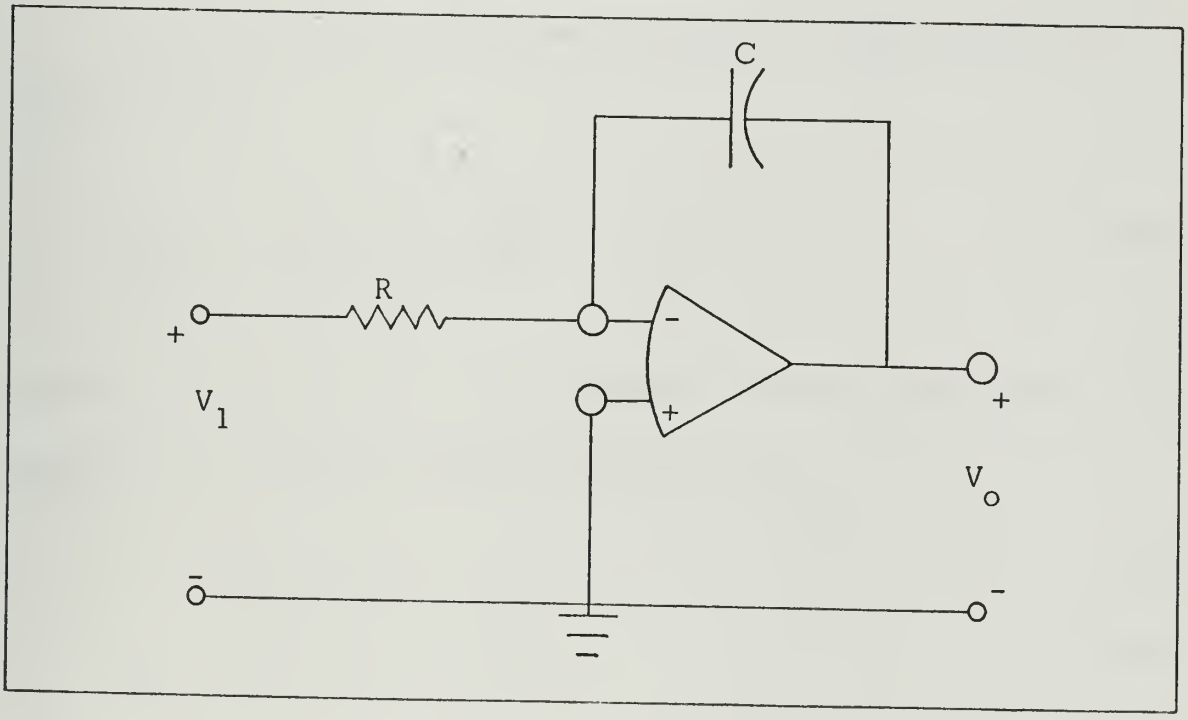

Figure 7-2b. An integrator

high-degree polynomials can become very sensitive to the coefficients, so that very high accuracy is required in the resistive components that determine these coefficients.

For this reason the most practical procedure is to factor the transfer function into first- and second-order product terms. For such terms, the high accuracy is not required and cascading the realizations of these product terms gives the transfer function in insensitive form.

B. KERWIN, HUELSMAN, AND NEWCOMB [1967]

Kerwin, Huelsman, and Newcomb [Ref. 35] recognized the value of the state-space approach and subsequently used its concepts to generate one of the first second-order building blocks.

The general second-order transfer function in equation (2-14) is now considered:

$$\frac{V_2(s)}{V_1(s)} = \frac{a_o + a_1 s + a_2 s^2}{b_o + b_1 s + s^2} \quad . \tag{7-8}$$

If equation (7-8) is expanded as in Section A of this chapter using equation (7-2), the two resulting equations are:

$$\dot{w} = - b_o w - b_1 \dot{w} + v_1 \quad , \tag{7-9a}$$

$$v_2 = a_o w + a_1 \dot{w} + a_2 \ddot{w} \quad . \tag{7-9b}$$

If $w = x_1$, $\dot{w} = x_2$, $v_1 = u$ and $v_2 = y$, Laplace transforming equations (7-9) produces the following state equations:

$$sX_1(s) = X_2(s) \tag{7-10a}$$

$$sX_2(s) = -b_o X_1(s) - b_1 X_2(s) + U(s) \tag{7-10b}$$

$$Y(s) = a_o X_1(s) + a_1 X_2(s) + a_2 sX_2(s) \quad . \tag{7-10c}$$

The signal flow graph corresponding to equations (7-10) is shown in Figure 7-3.

If each element of this second-order signal flow graph were replaced by integrators and summers where appropriate, the resulting circuit would be the second-order building-block network of Kerwin, Huelsman and Newcomb. This is shown in Figure 7-4.

Although four operational amplifiers, ten resistors and two capacitors are required, this network can realize not only the general second-order transfer function in equation (7-8) by taking V_5 as the output voltage, but high-pass, bandpass and low-pass transfer functions as well, using as output V_2, V_3 and V_4 respectively.

By using the output equation of an integrator, which is

$$V_o = - \frac{1}{RC\,s} V_1 \quad , \tag{7-11a}$$

and that of a summer,

$$V_o = \sum_{i=1}^{m} \frac{G_{pi}}{G_p} \left[1 + R_f G_n \right] V_{pi} - \sum_{i=1}^{m} R_f G_n V_{ni} \quad , \tag{7-11b}$$

with Figures 7-2a and 7-2b used as reference figures, where G_p and G_n represent the sum of the input conductances of the positive and

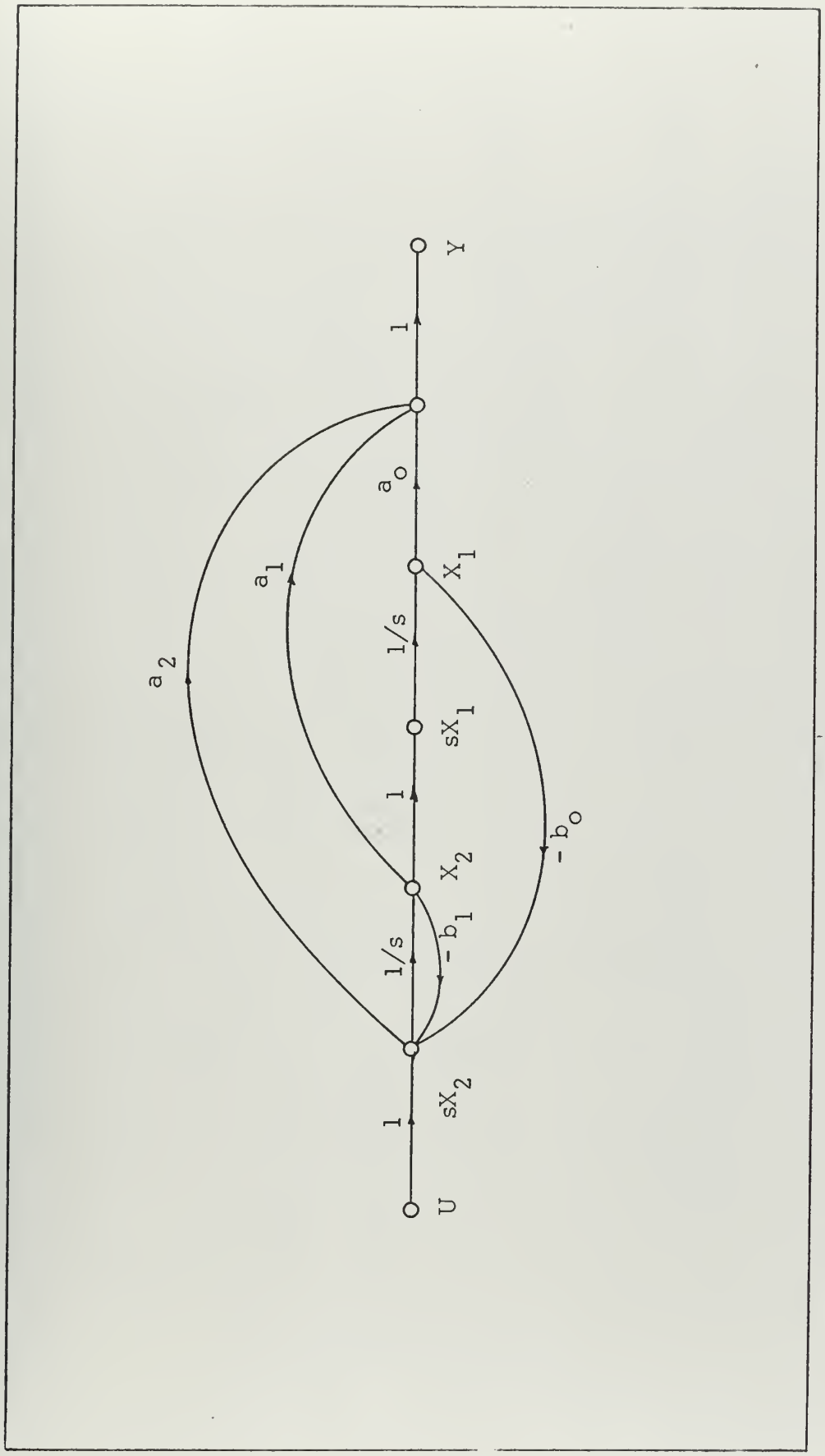

Figure 7-3. Signal flow graph of general second-order open-circuit voltage transfer function

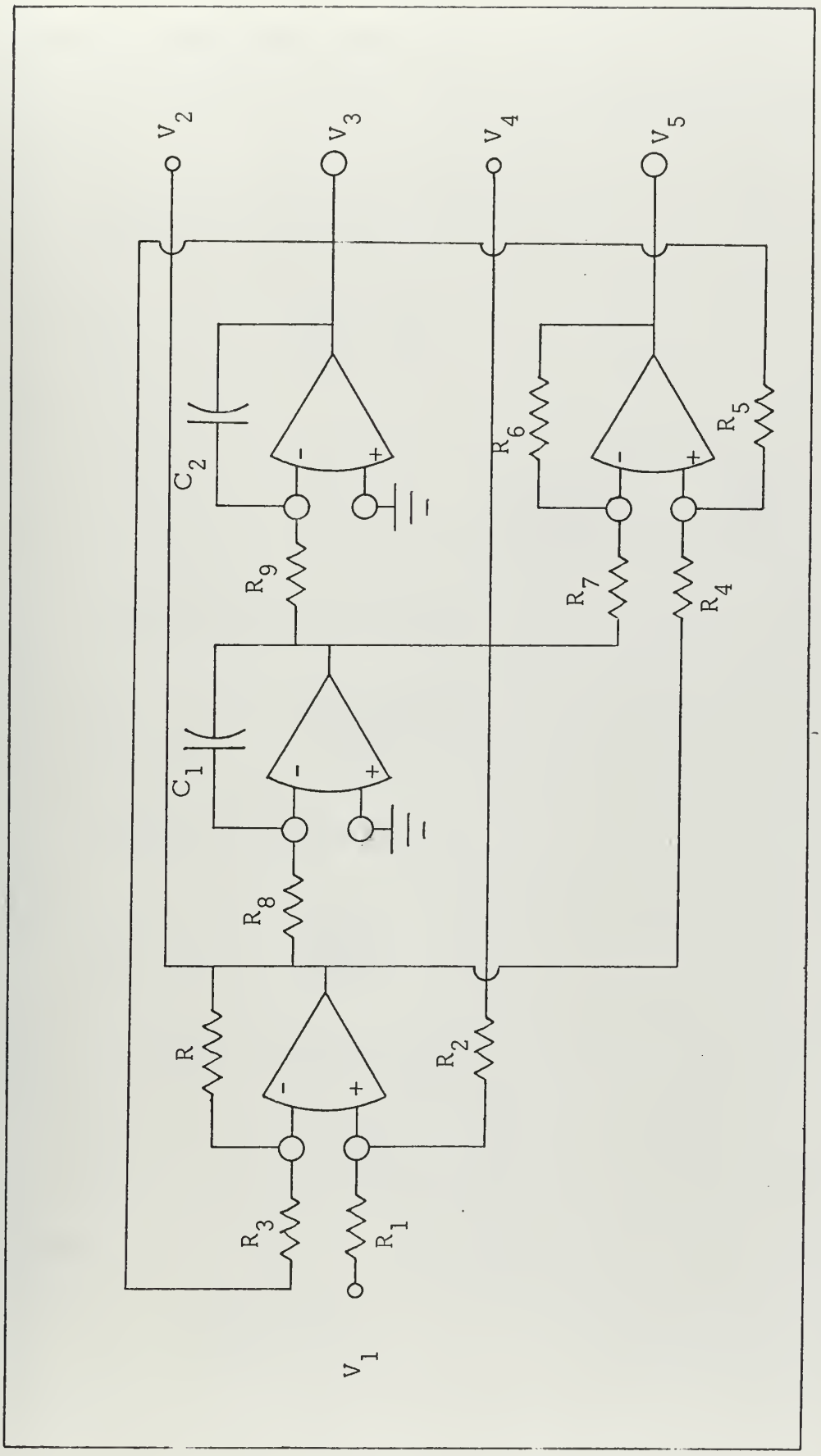

Figure 7-4. Second-order building-block network of Kerwin, Huelsman, and Newcomb

negative voltage inputs respectively, the different transfer functions for Figure 7-4 may be written in terms of the component elements as follows:

General Second-Order Transfer Function

$$\frac{V_5}{V_1} = K \cdot \frac{R_5(R_6 + R_7)}{R_7(R_4 + R_5)}$$

$$\cdot \frac{R_8C_1R_9C_2s^2 + \frac{R_6(R_4+R_5)}{R_5(R_6+R_7)}R_9C_2s + \frac{R_4}{R_5}}{D(s)} \qquad (7\text{-}12a)$$

High-Pass Transfer Function

$$\frac{V_2}{V_1} = K \cdot \frac{R_8C_1R_9C_2s^2}{D(s)} \qquad (7\text{-}12b)$$

Bandpass Transfer Function

$$\frac{V_3}{V_1} = -K \cdot \frac{R_9C_2s}{D(s)} \qquad (7\text{-}12c)$$

Low-pass Transfer Function

$$\frac{V_4}{V_1} = K \cdot \frac{1}{D(s)} \quad , \qquad (7\text{-}12d)$$

where

$$K = \frac{R_2\,(R + R_3)}{R_3\,(R_1 + R_2)} \quad , \qquad (7\text{-}13)$$

and

$$D(s) = R_8C_1R_9C_2s^2 + \frac{R_1(R + R_3)}{R_3(R_1 + R_2)} R_9C_2s + \frac{R}{R_3} \quad . \tag{7-14}$$

At the resonant frequency, ω_o,

$$\omega_o = \frac{R}{R_8C_1R_9C_2s} \tag{7-15}$$

for which $R_8C_1R_9C_2s^2 + R/R_3 = 0$,

$$\frac{V_3}{V_1}(j\omega_o) = -\frac{R_2}{R_1} \quad . \tag{7-16}$$

Use of Figure 7-4 and equation (7-12) is simplified if

$$R_1 = R_3 = R_5 = R_6 = R_8C_1 = R_9C_2 = 1 \quad , \tag{7-17}$$

such that the transfer functions in equation (7-12) become

$$\frac{V_5}{V_1} = K_1 \cdot \frac{1 + R_7}{R_7(1 + R_4)} \cdot \left[\frac{s^2 + \frac{1 + R_4}{1 + R_7} s + R_4}{s^2 + \frac{1 + R}{1 + R_2} s + R} \right] \tag{7-18a}$$

$$\frac{V_2}{V_1} = \frac{K_1 s^2}{s^2 + \frac{1 + R}{1 + R_2} s + R} \tag{7-18b}$$

$$\frac{V_3}{V_1} = \frac{-K_1 s}{s^2 + \frac{1+R}{1+R_2} s + R} \qquad (7\text{-}18c)$$

$$\frac{V_4}{V_1} = \frac{K_1}{s^2 + \frac{1+R}{1+R_2} s + R} , \qquad (7\text{-}18d)$$

where

$$K_1 = \frac{R_2 (1+R)}{(1+R_2)} . \qquad (7\text{-}19)$$

In this normalized case, $\omega_o = \sqrt{R}$ and

$$\frac{V_3}{V_1} (j\omega_o) = -R_2 . \qquad (7\text{-}20)$$

At this point, an example illustrating the realization of a desired transfer function using the second-order building-block network in Figure 7-4 is appropriate.

Example 7-1. Realize the bandpass filter transfer function of Example 2-4:

$$H(s) = \frac{-62.83 s}{s^2 + 1.257 s + 3947.84} . \qquad (7\text{-}21)$$

Since equation (7-21) was derived directly from the second-order bandpass transfer function form

$$H(s) = \frac{-K \omega_o s}{s^2 + (\omega_o/Q) s + \omega_o^2} , \qquad (7\text{-}22)$$

the two variable element values can be determined from equations (7-17) and (7-20) as

$$R = 3947.84 \text{ ohms} \tag{7-23a}$$

$$R_2 = \frac{62.83}{1.257} = 50 \text{ ohms} \quad . \tag{7-23b}$$

In the case where the realization of an odd-order transfer function is involved, the necessity for a first-order network becomes apparent. Such first-order sections can be realized to within a gain constant by lag-lead networks.

The lag network shown in Figure 7-5a is described by the transfer function

$$\frac{V_o}{V_1} = \frac{R_2 Cs + 1}{(R_1 + R_2)Cs + 1} \quad , \tag{7-24}$$

while the transfer function of the lead network shown in Figure 7-5b is

$$\frac{V_o}{V_1} = \frac{R_1 R_2 Cs + R_2}{R_1 R_2 Cs + R_1 + R_2} \quad . \tag{7-25}$$

C. HOLLENBECK [1969]

It is interesting to note that a simplified version of what is essentially the building-block network of Kerwin, Huelsman and Newcomb has already been put into production. Such a circuit, shown in Figure 7-6, was discussed by Hollenbeck [Ref. 36].

The different transfer functions can be derived in a manner analogous to those in equations (7-12). They are as follows:

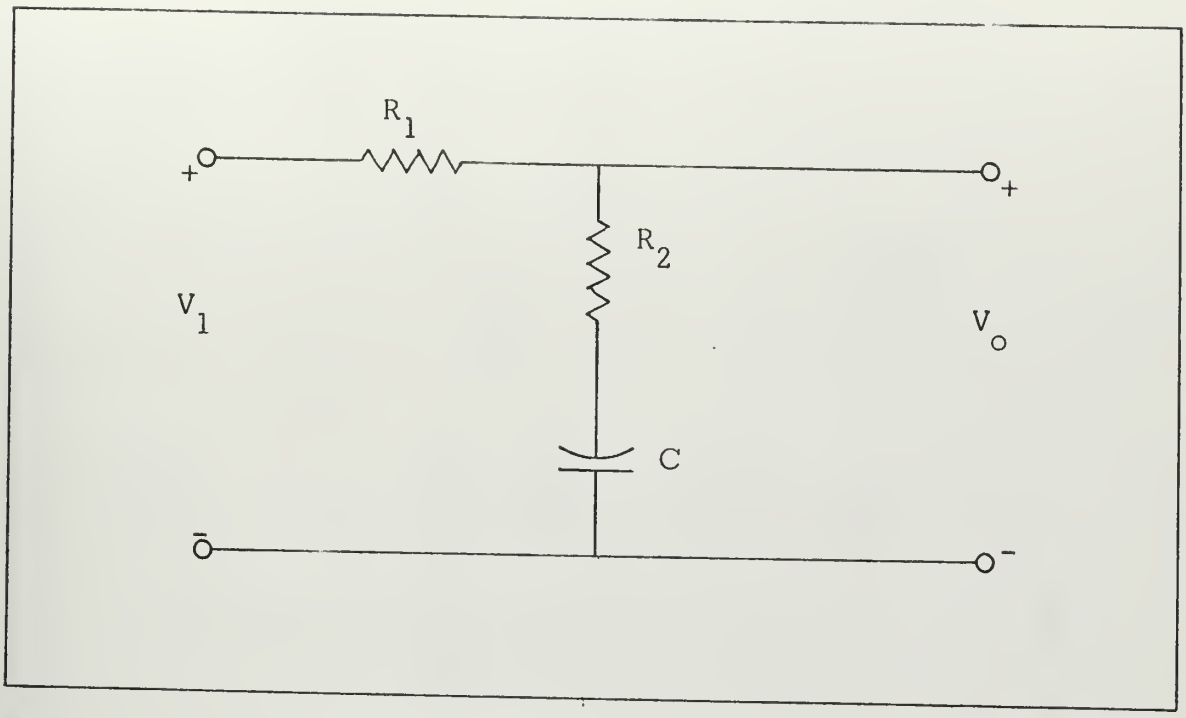

Figure 7-5a. First-order lag network

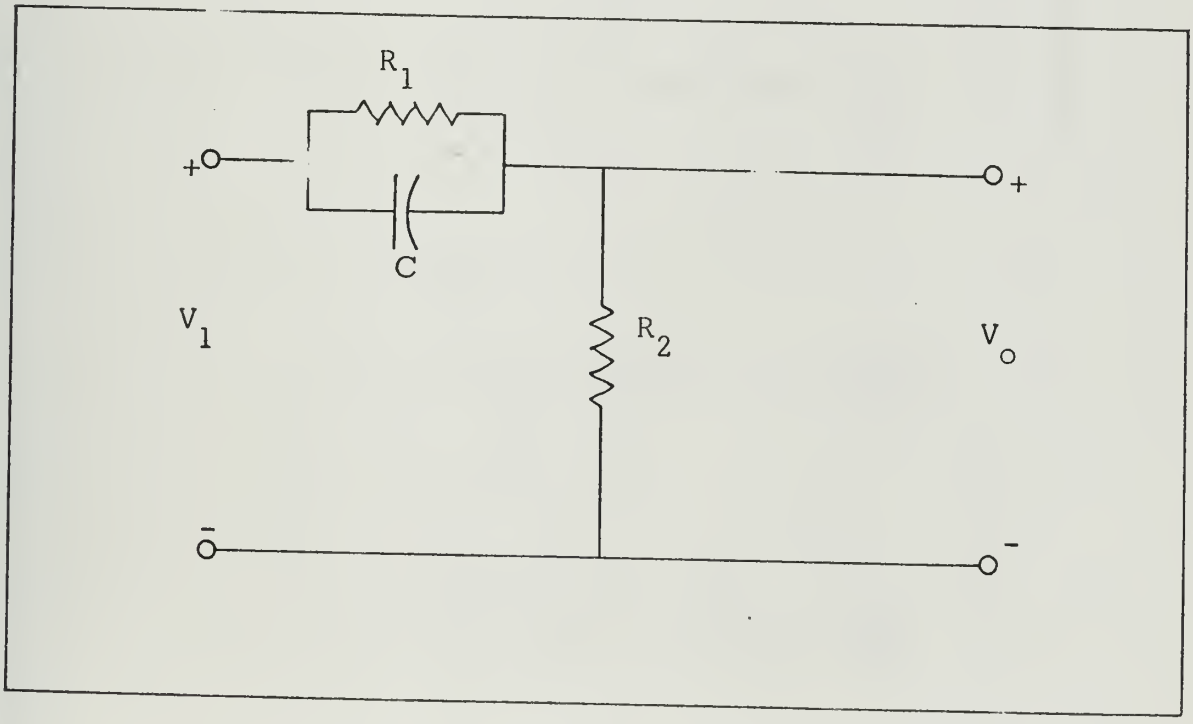

Figure 7-5b. First-order lead network

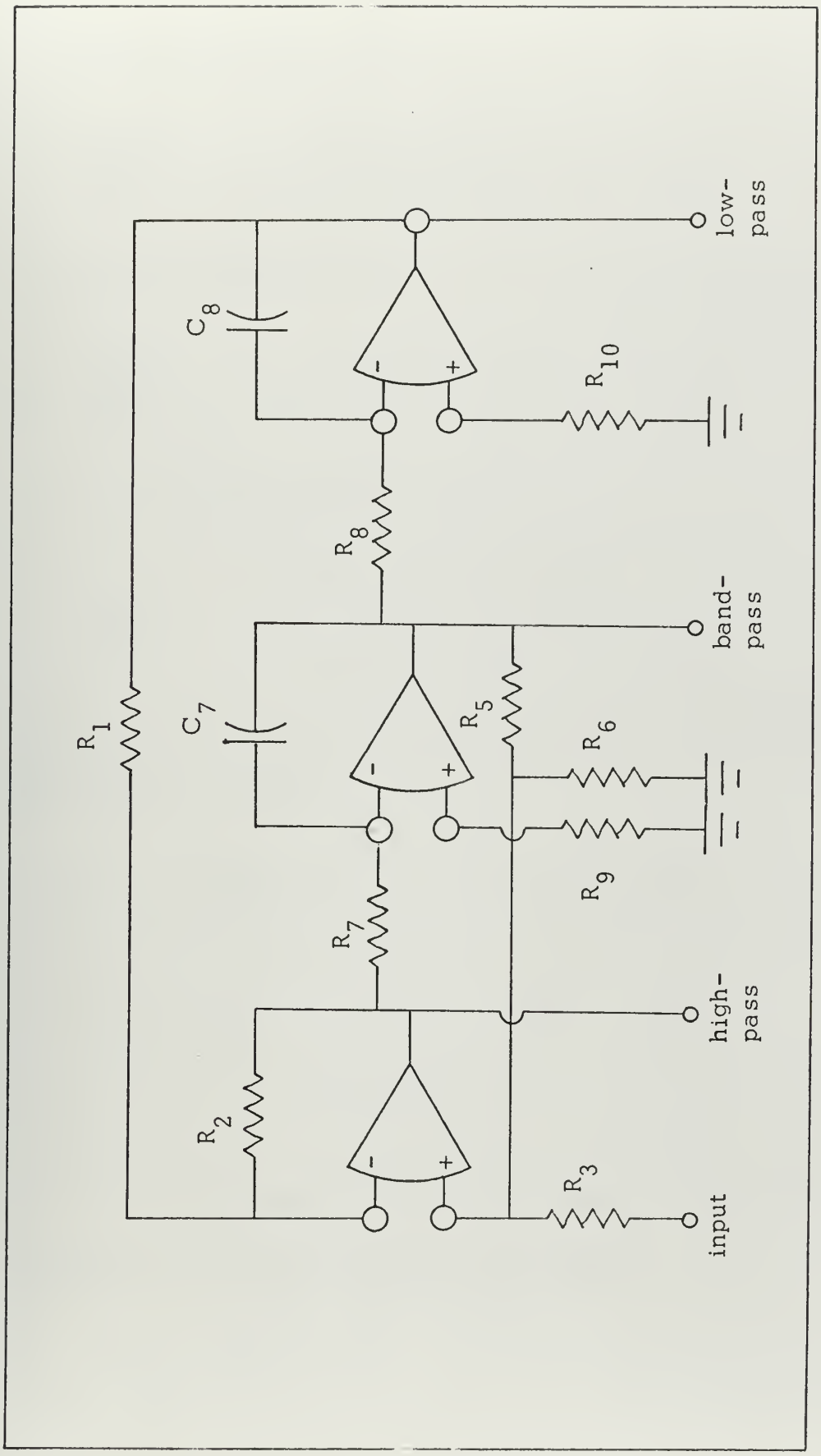

Figure 7-6. A universal hybrid active filter

For the high-pass output:

$$\frac{V_{HP}(s)}{V_1(s)} = \frac{F_1 (1 + F_2)\, s^2}{s^2 + \omega_1 F_1 (1 + F_2)\, s + \omega_1\, \omega_2 F_2} \qquad (7\text{-}26a)$$

For the bandpass output:

$$\frac{V_{BP}(s)}{V_1(s)} = \frac{F_1\, \omega_1 (1 + F_2)\, s}{s^2 + \omega_1 F_1 (1 + F_2)\, s + \omega_1\, \omega_2 F_2} \qquad (7\text{-}26b)$$

For the low-pass output:

$$\frac{V_{LP}(s)}{V_1(s)} = \frac{F_1\, \omega_1\, \omega_2 (1 + F_2)}{s^2 + \omega_1 F_1 (1 + F_2)\, s + \omega_1\, \omega_2 F_2} \qquad (7\text{-}26c)$$

The parameters in equations (7-26) are defined in relation to circuit components as follows:

$$F_1 = \frac{R_6}{2R_6 + R} \qquad \omega_1 = \frac{1}{R_7 C_7}$$

$$F_2 = \frac{R_2}{R_1} \qquad \omega_2 = \frac{1}{R_8 C_8}$$

$$R = R_3 = R_5$$

If the denominator coefficients of equations (7-22) and (7-26b) are compared, the following relations can be made:

$$\omega_o = \sqrt{\omega_1\, \omega_2 F_2} \qquad (7\text{-}28)$$

$$R_8 = \frac{10^6}{10.81} = 92.5\ K\Omega$$

$$R_6 = \frac{10^4}{8} = 1.125\ K\Omega \quad . \tag{7-33}$$

D. SALERNO [1969]

Using a slightly different approach, Salerno [Ref. 37] expanded the general voltage transfer function

$$\frac{V_o}{V_1} = \frac{a_n s^n + a_{n-1} s^{n-1} + \ldots + a_o}{s^n + b_{n-1} s^{n-1} + \ldots + b_o} \tag{7-34}$$

as follows:

$$V_o(s^n + b_{n-1} s^{n-1} + \ldots + b_o) = V_1(a_n s^n + a_{n-1} s^{n-1} + \ldots + a_o) \quad . \tag{7-35}$$

By rearranging the terms of equation (7-35), the following general relation is arrived at:

$$V_o = V_1\left(a_n + \frac{a_{n-1}}{s} + \ldots + \frac{a_o}{s^n}\right) - V_o\left(\frac{b_{n-1}}{s} + \ldots + \frac{b_o}{s^n}\right) \tag{7-36}$$

The general second-order transfer function

$$\frac{V_o}{V_1} = -\frac{a_2 s^2 + a_1 s + a_o}{s^2 + b_1 s + b_o} \tag{7-37}$$

can be similarly expressed as

$$V_o = -V_1\left(a_2 + \frac{a_1}{s} + \frac{a_o}{s^2}\right) - V_o\left(\frac{b_1}{s} + \frac{b_o}{s^2}\right) . \qquad (7\text{-}38)$$

Again using inverters whose gain is - 1 and integrators whose gain is - 1/s, a schematic representation of equation (7-38) can be made, as shown in Figure 7-7. The circuit corresponding to this schematic is shown in Figure 7-8. The coefficients of the desired transfer function can be related directly to the components of the circuit by the following equations:

$$a_o = \frac{1}{R_1C_1} \qquad b_o = \frac{1}{R_3C_1}$$

$$a_1 = \frac{R_4}{R_5} \qquad b_1 = \frac{R_4}{R_6} \qquad (7\text{-}39)$$

$$a_2 = \frac{R_7}{R_8}$$

The other components are governed by the following relations:

$$R_2 = 1/C_2$$

$$R_7 = R_9$$

$$R_{10} = 1/C_2 \quad . \qquad (7\text{-}40)$$

A similar procedure would realize a first-order transfer function if cascaded realizations of first- and second-order product terms are desired. An example of Salerno's procedure will clarify this point.

Example 7-3. Realize the fifth-order Butterworth low-pass transfer

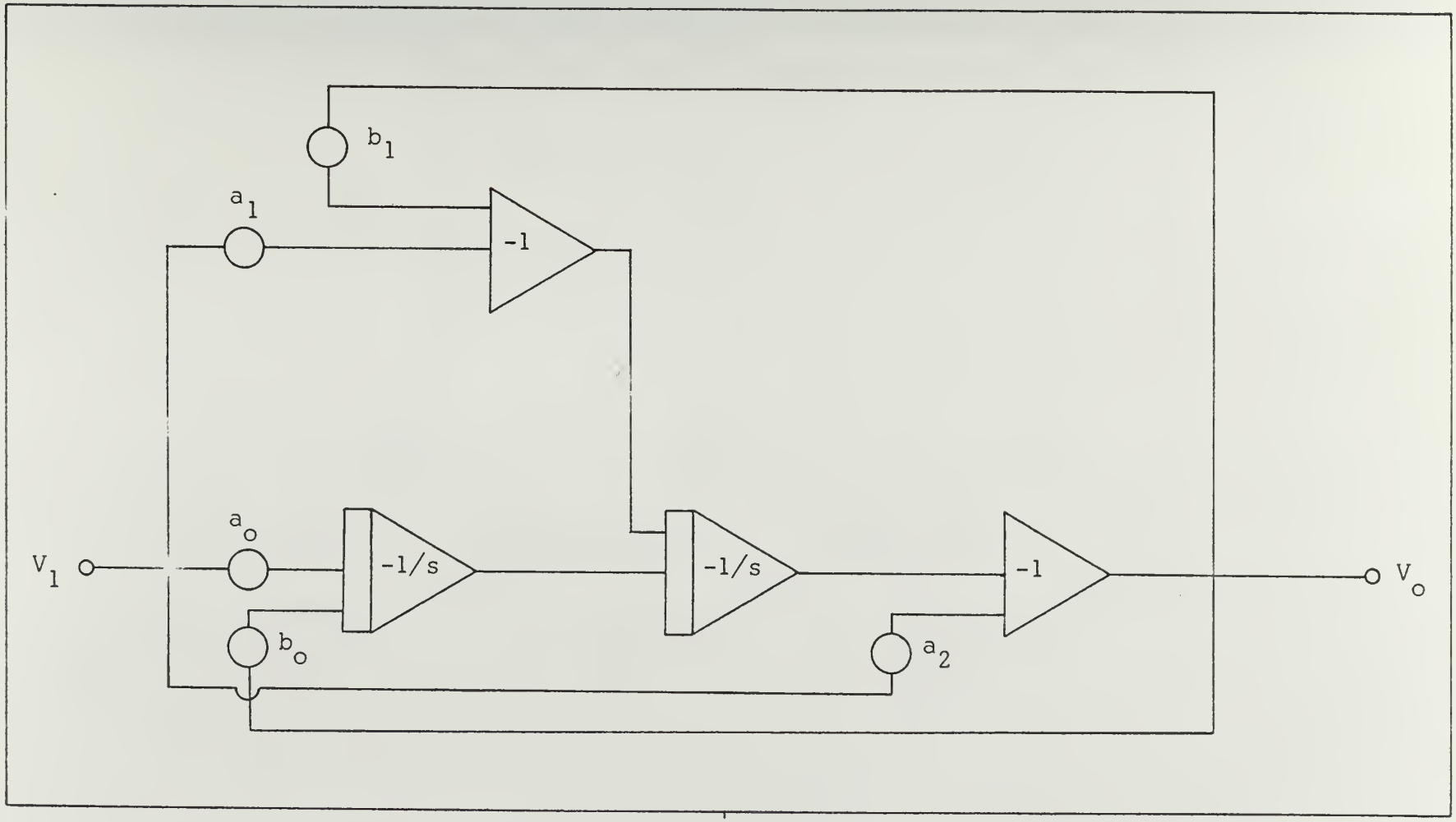

Figure 7-7. Schematic representation of Salerno's realization of the general second-order transfer function

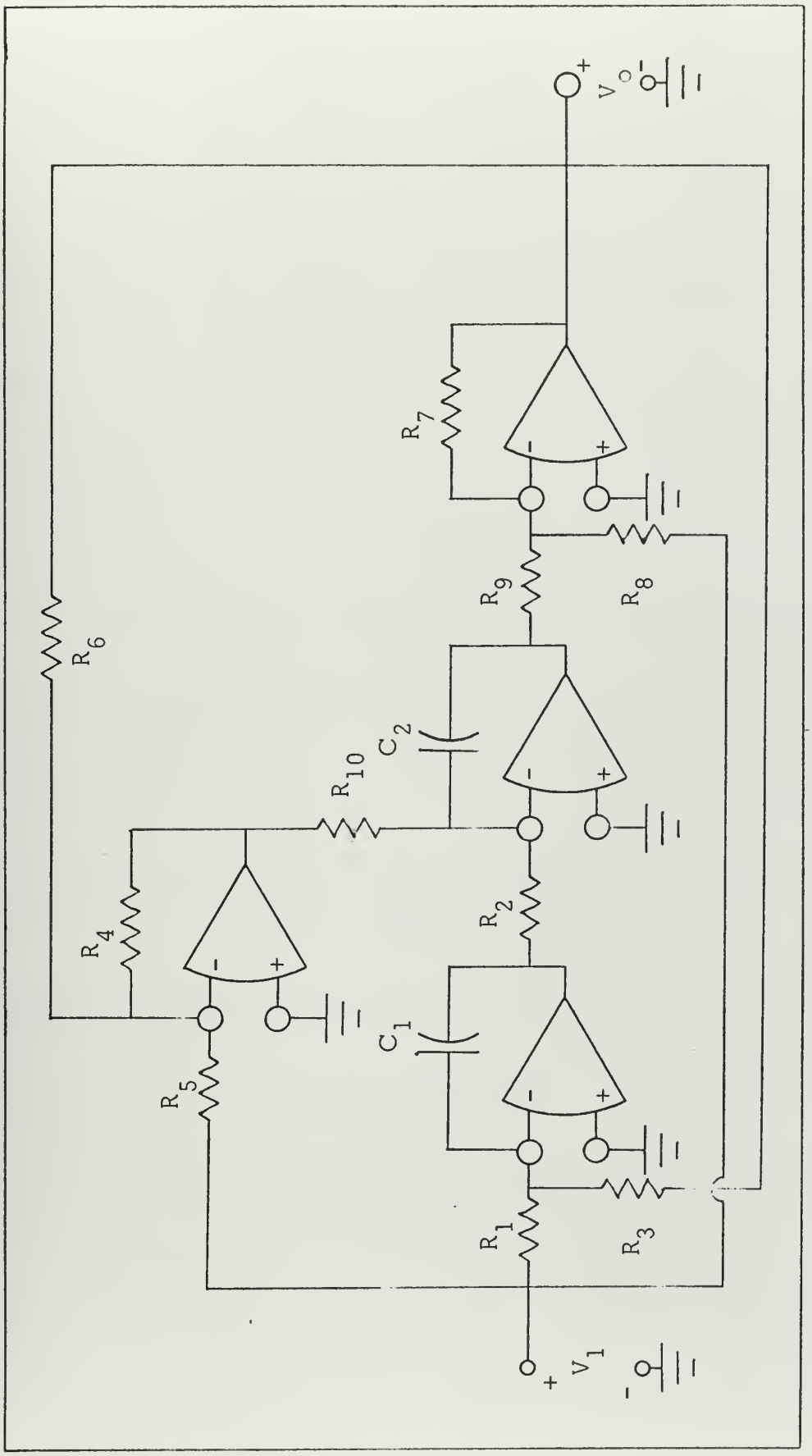

Figure 7-8. Salerno's circuit realization of the general second-order transfer function

function of Example 2-2:

$$\frac{V_o}{V_1} = - \frac{1}{\left(1+\frac{s}{\omega_o}\right)\left(1+\frac{0.618s}{\omega_o}+\frac{s^2}{\omega_o^2}\right)\left(1+\frac{1.618s}{\omega_o}+\frac{s^2}{\omega_o^2}\right)} , \quad (7\text{-}41)$$

where $\omega_o = 2\pi(10)$.

Equation (7-41) can be expressed as three cascaded transfer functions:

$$\frac{V_2}{V_1} = \frac{-1}{1+\frac{s}{\omega_o}} \quad (7\text{-}42a)$$

$$\frac{V_3}{V_2} = \frac{1}{1+\frac{0.618s}{\omega_o}+\frac{s^2}{\omega_o^2}} \quad (7\text{-}42b)$$

$$\frac{V_o}{V_3} = \frac{1}{1+\frac{1.618s}{\omega_o}+\frac{s^2}{\omega_o^2}} . \quad (7\text{-}42c)$$

Expanding equation (7-42a) gives

$$V_2 = -\frac{\omega_o}{s} V_1 - \frac{\omega_o}{s} V_2 , \quad (7\text{-}43)$$

the schematic and circuit realization of which are shown in Figure 7-9.

$$V_3 = \frac{\omega_o^2}{s^2} V_2 - V_3\left(\frac{\omega_o^2}{s} + \frac{0.618\,\omega_o}{s}\right) \quad (7\text{-}44)$$

$$V_o = \frac{\omega_o^2}{s^2} V_3 - V_o\left(\frac{\omega_o^2}{s^2} + \frac{1.618\,\omega_o}{s}\right) . \quad (7\text{-}45)$$

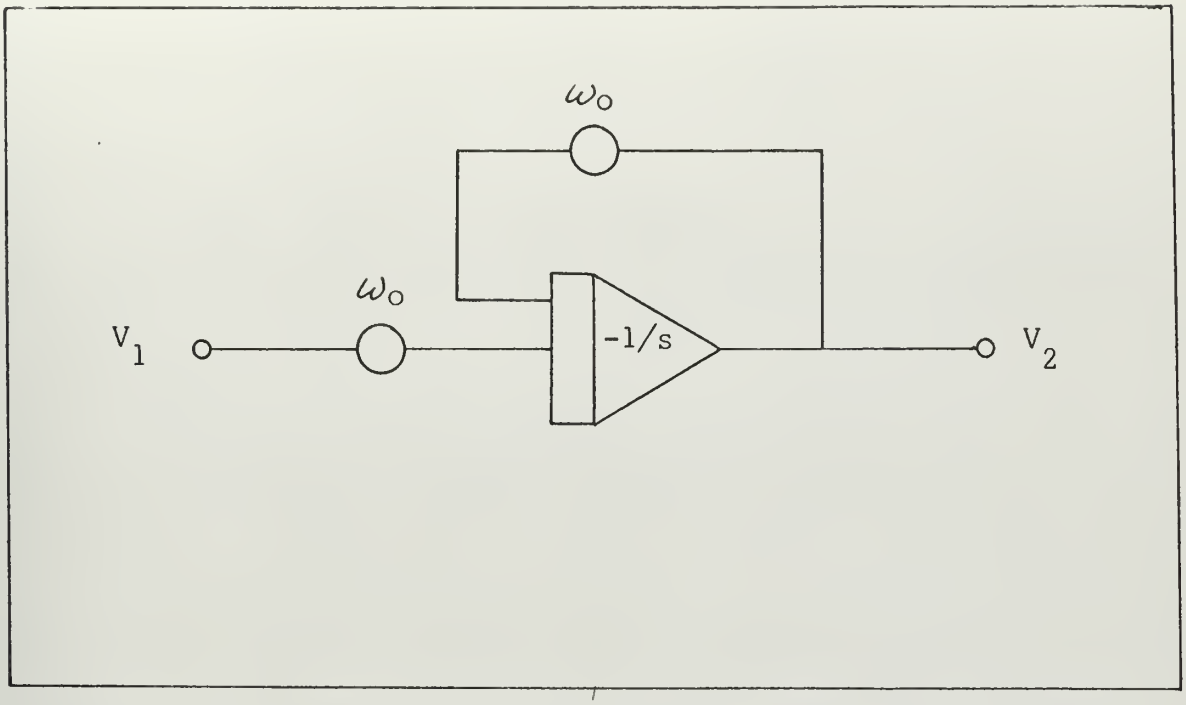

Figure 7-9a. Schematic representation of a first-order transfer function

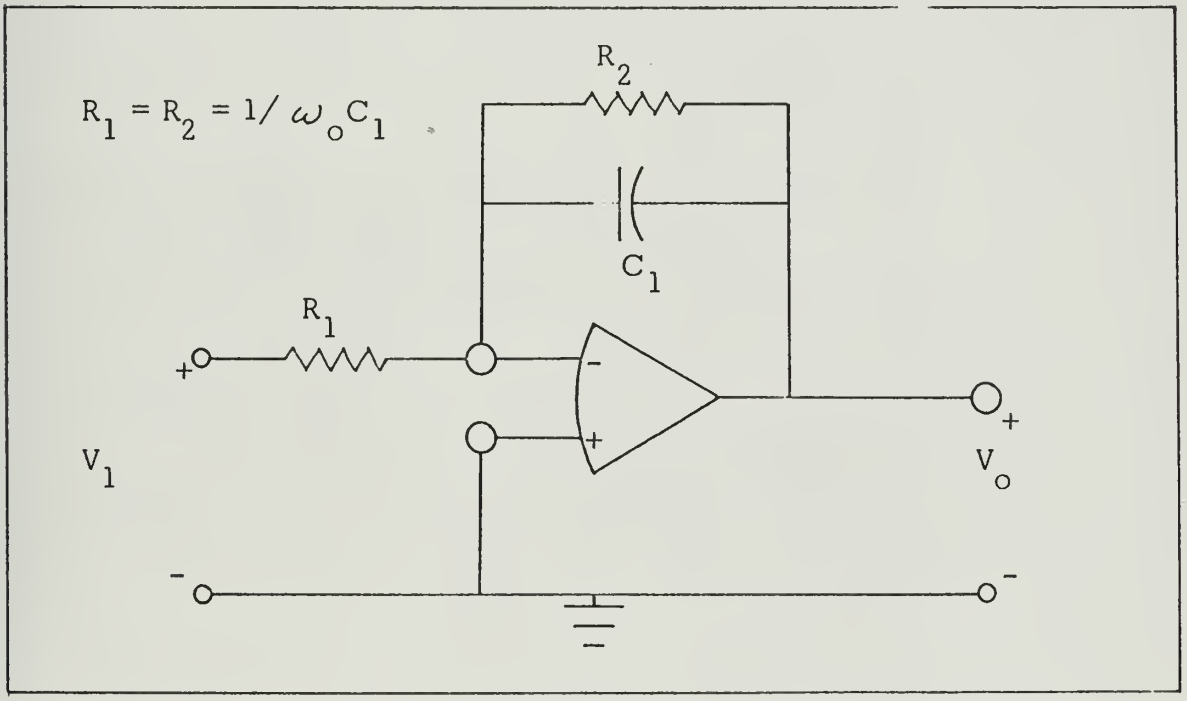

Figure 7-9b. Circuit realization of a first-order transfer function

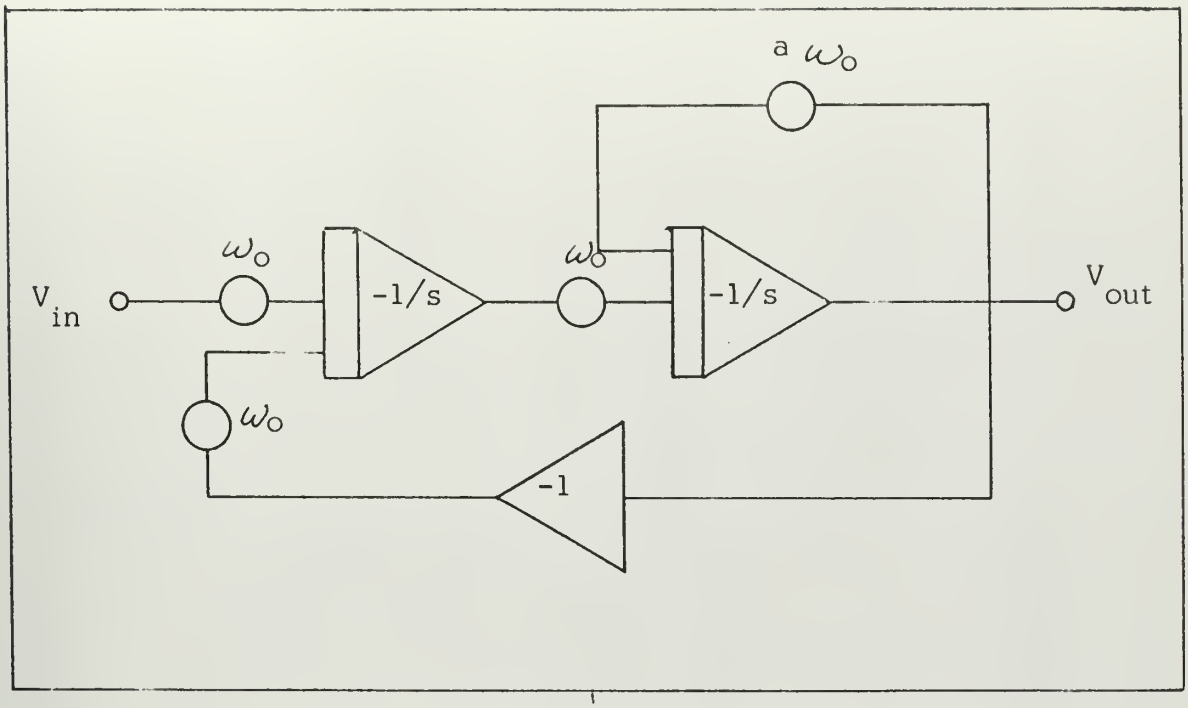

Figure 7-10. Schematic representation of a second-order low-pass transfer function

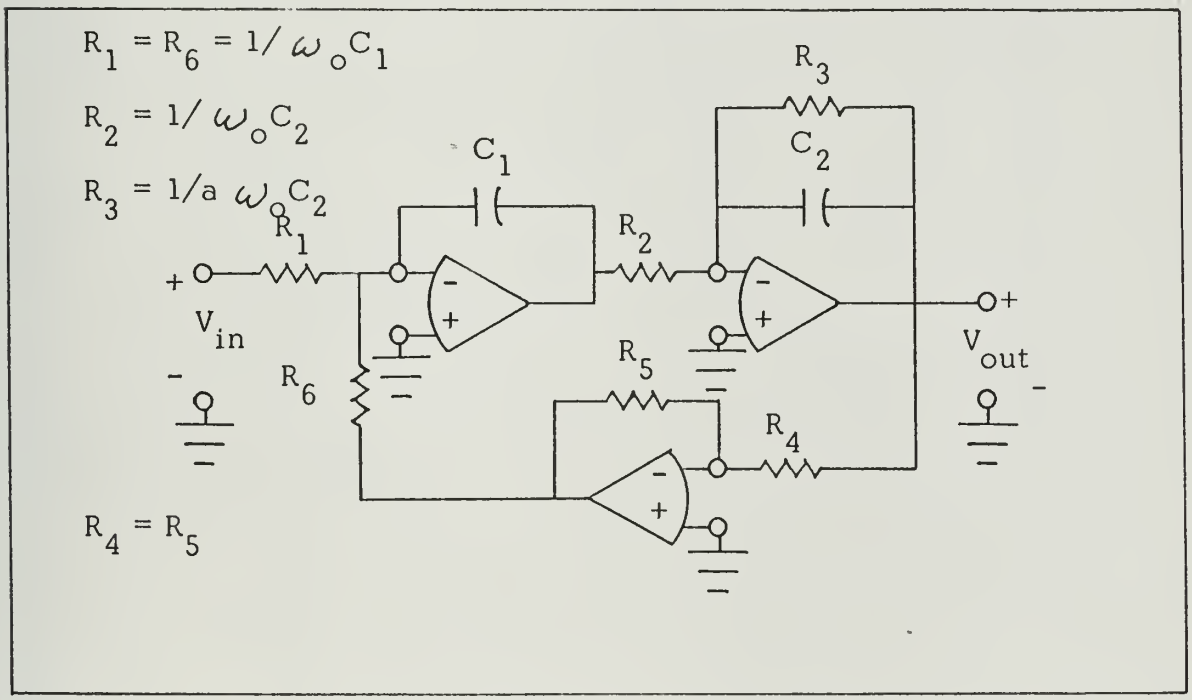

Figure 7-11. Circuit realization of a second-order low-pass transfer function

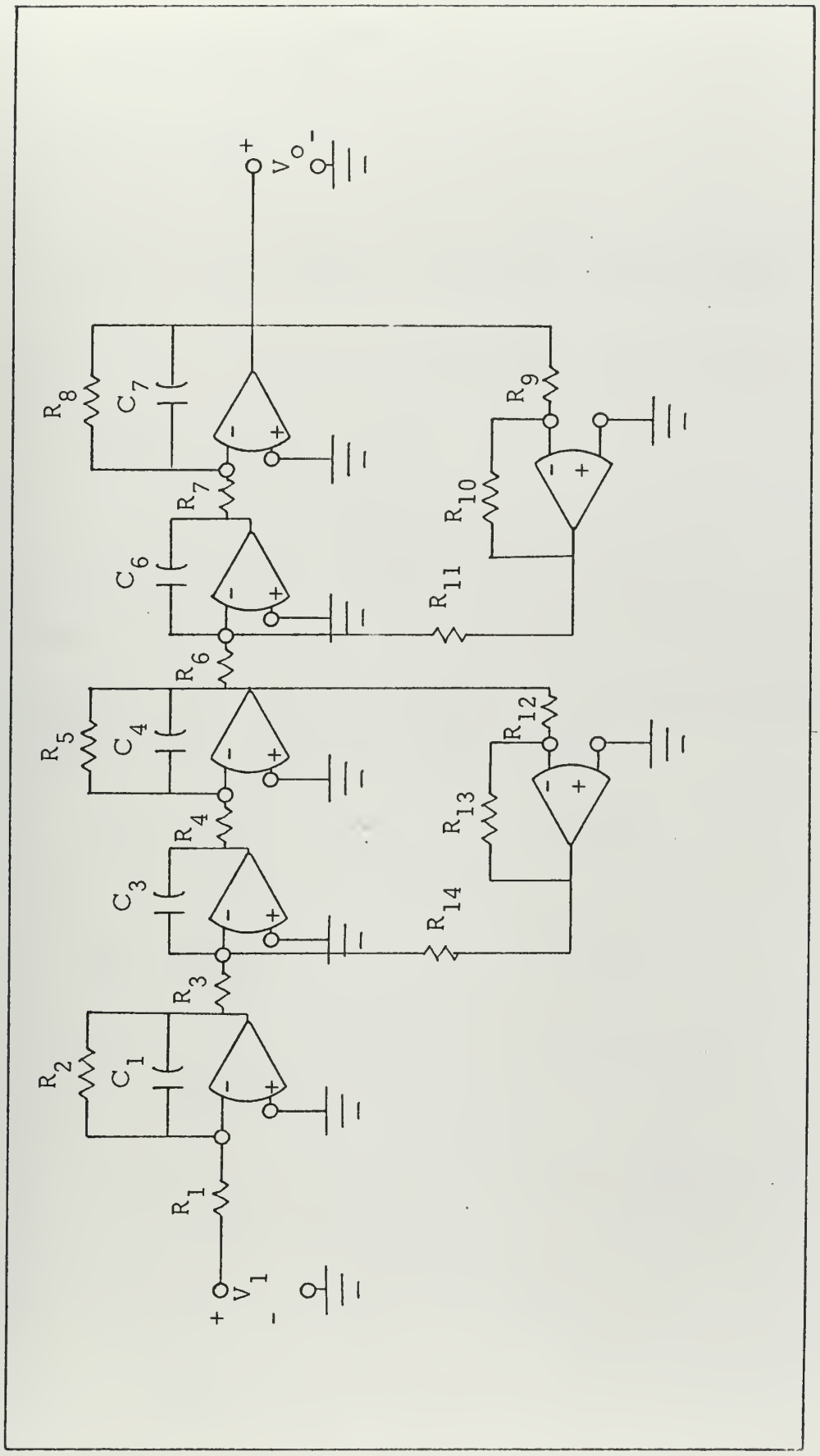

Figure 7-12. Circuit realization of Example 7-3

$$\dot{x}_1 = -ax_1 - k_1\sqrt{b}\,x_2 - k_2\,|ma - c|\,v_1 \qquad (7\text{-}48a)$$

$$\dot{x}_2 = \frac{\sqrt{b}}{k_1}\,x_1 \qquad (7\text{-}48b)$$

$$V_o = \frac{1}{k_2}\,\text{sgn}\,(ma - c)\,x_1 + \frac{k_1}{k_2}\,\frac{mb - d}{|ma - c|\sqrt{b}}\,x_2 + mv_1, \qquad (7\text{-}48c)$$

where k_1 and k_2 are arbitrary positive real numbers and where

$$\text{sgn}\,(K) = +\ \text{if } K \text{ is positive}$$
$$= -\ \text{if } K \text{ is negative} \quad . \qquad (7\text{-}49)$$

In relation to the notation in Ref. 34, $x_1 = \dot{w}$ and $x_2 = w$. The circuit configuration realizing equation (7-47) and the set of state equations in equation (7-48) is shown in Figure 7-13. The element-coefficient relations for this configuration are as follows:

$$R_1 = \frac{1}{aC_1} \qquad R_5 = R_3$$

$$R_2 = \frac{|k_1|}{\sqrt{b}\,C_2} \qquad R_6 = R_3$$

$$R_3 = \frac{1}{|k_1|\sqrt{b}\,C_1} \qquad R_7 = |k_2|\,R_{10}$$

$$R_4 = \frac{1}{|k_2|\,|ma - c|\,C_1} \qquad R_8 = \left|\frac{k_2}{k_1}\right| \frac{|ma - c|\sqrt{b}}{|mb - d|}\,R_{10}$$

$$R_9 = \frac{1}{m}\,R_{10} \quad \text{for Cases A, B, C}$$
$$= \frac{b}{d}\,R_{10} \quad \text{for Case D} \quad , \qquad (7\text{-}50$$

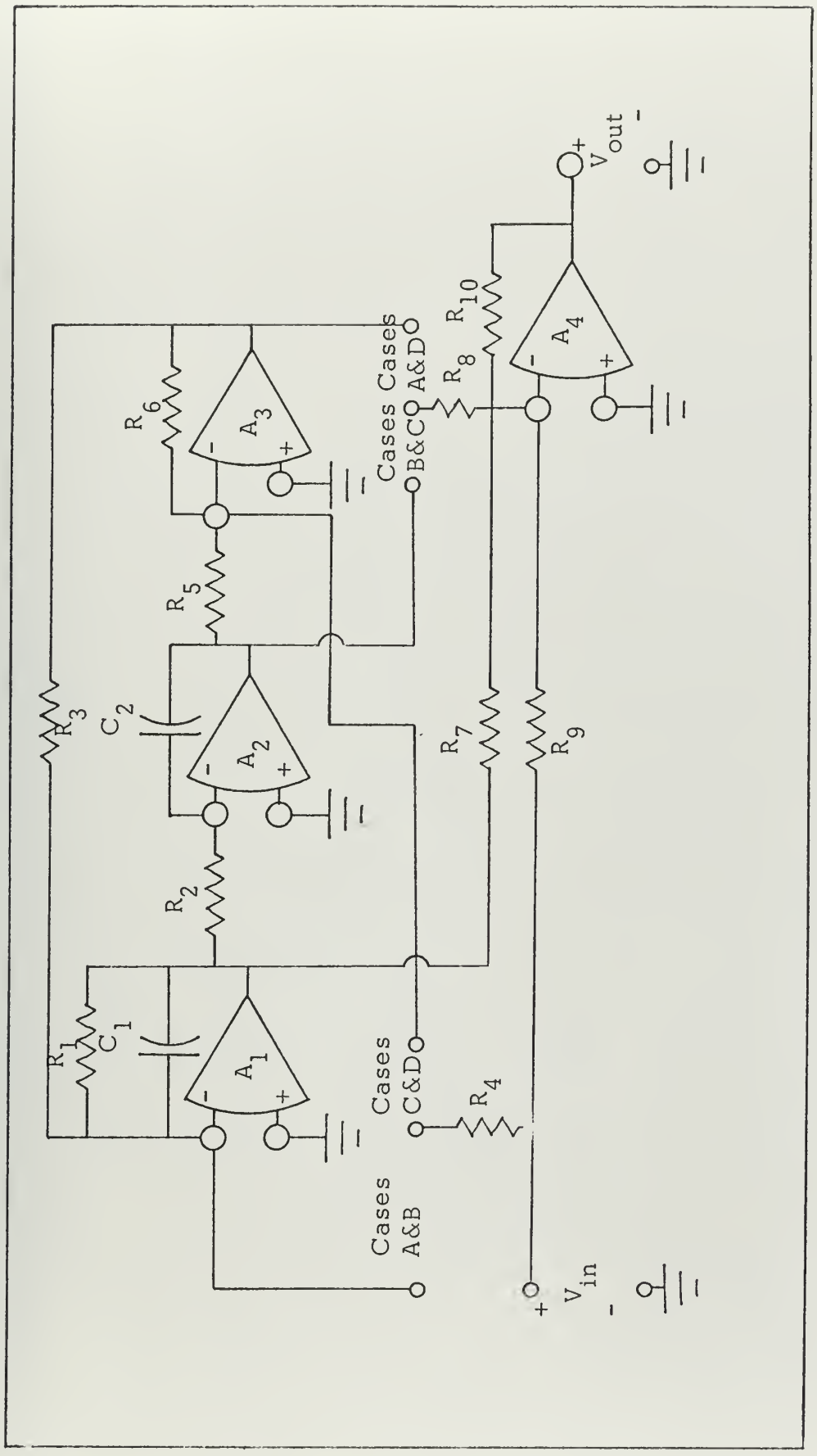

Figure 7-13. Tow's second-order building-block network

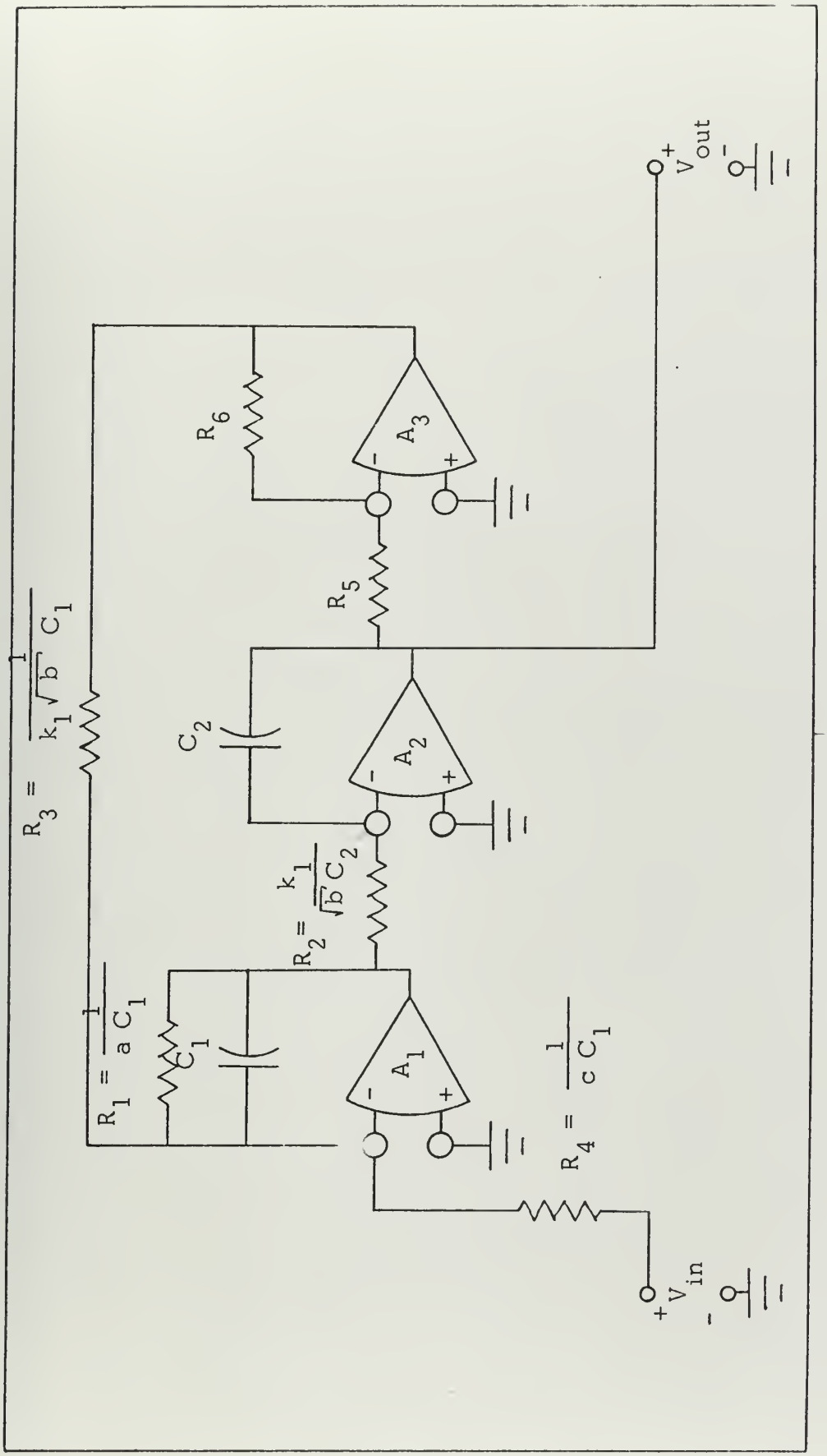

Figure 7-14. Tow's active bandpass network

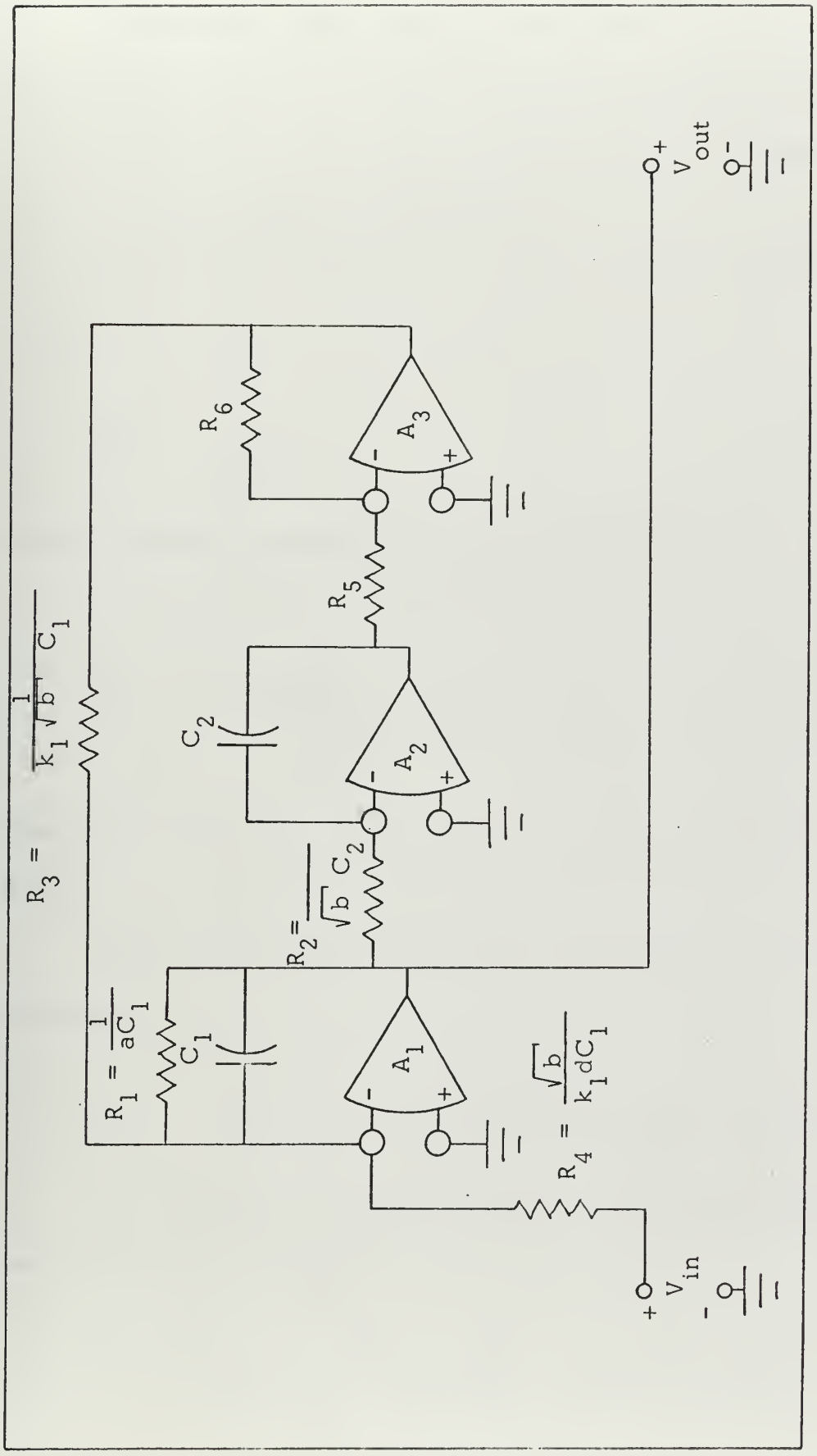

Figure 7-15. Tow's active low-pass network

To minimize change in pole locations due to finite gain of the operational amplifiers, k_1 and k_2 are generally chosen to be unity but in cases where it is desired to minimize the spread in element values, other convenient values may be chosen.

For cascaded realizations, Tow also specified a method for realizing the first-order product term of the form

$$\frac{V_o}{V_1} = \frac{K}{s + a} \quad . \tag{7-54}$$

Direct coefficient-matching of equation (7-54) with

$$\frac{V_o}{V_1} = \frac{\frac{1}{RC}}{s + \frac{R + R_{in}}{RR_{in}} \cdot \frac{1}{C}} \tag{7-55}$$

gives the values of R and C, where R, C, and R_{in} are as indicated in Figure 7-16.

Example 7-4. Realize the fourth-order bandpass transfer function of Example 2-4:

$$H(s) = \frac{1.18\, s^2}{(s^2 + 0.94\, s + 3913.80)\,(s^2 + 0.95s + 3982.18)} \tag{7-56}$$

For a cascaded realization, equation (7-56) can be factored into two product terms as follows:

$$H(s) = \left(- \frac{1.18s}{s^2 + 0.94s + 3913.80}\right)\left(- \frac{s}{s^2 + 0.95s + 3982.18}\right) . \tag{7-57}$$

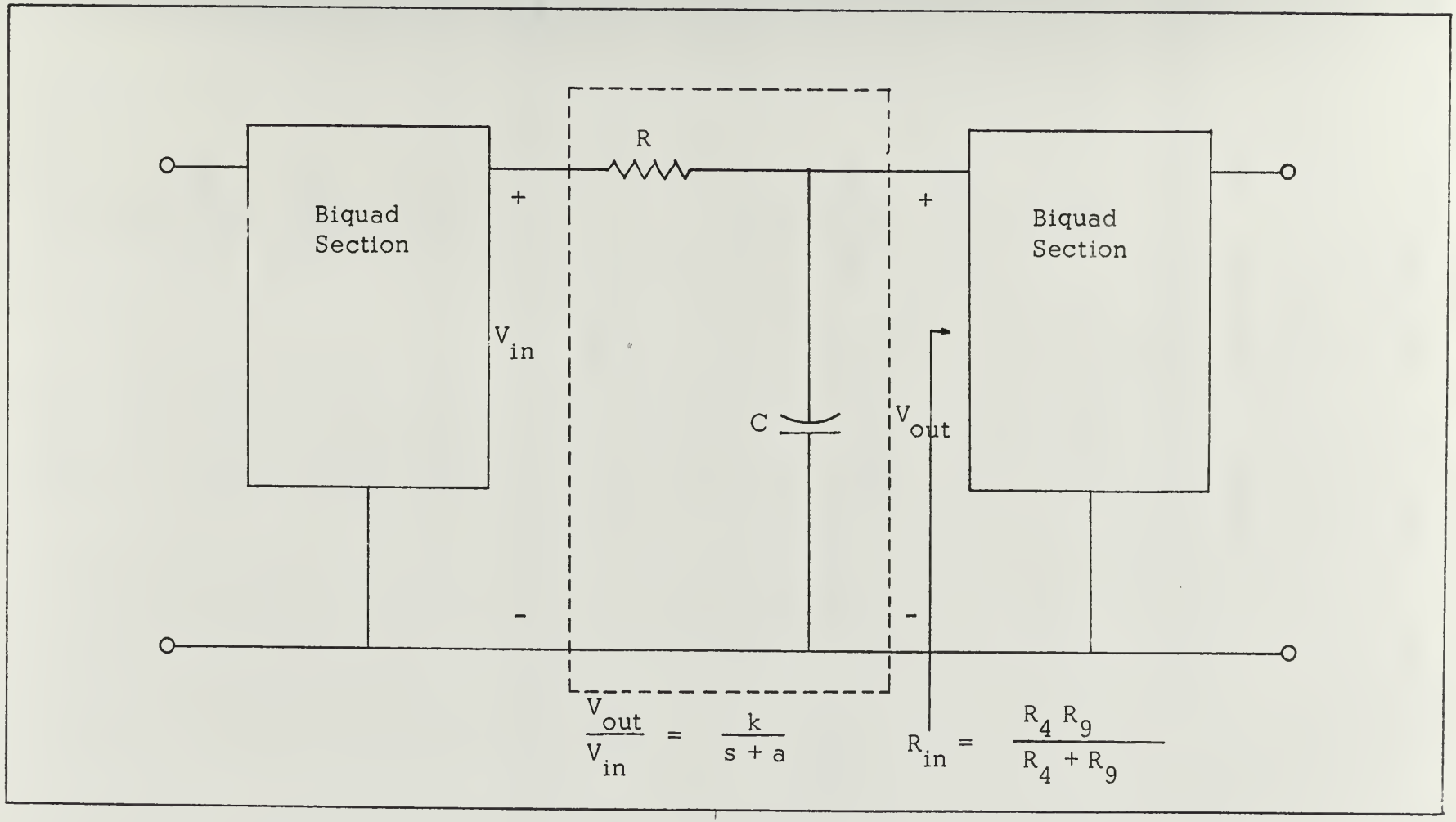

Figure 7-16. Cascaded first- and second-order sections where dotted block indicates realization of first-order pole

The first product term is first realized using the coefficient-element relations in equation (7-50) and noting that the required second-order section is bandpass and hence, does not require the summing amplifier, A_4, as in Figure 7-14. Arbitrarily choosing $C_1 = C_2 = 1\ \mu F$ and $k_1 = k_2 = 1$, the other element values are found to be:

$$R_1 = \frac{10^6}{0.94} = 1.063\ M\Omega$$

$$R_2 = \frac{10^6}{\sqrt{3913.80}} = 15.99\ K\Omega$$

$$R_3 = \frac{10^6}{\sqrt{3913.80}} = 15.99\ K\Omega$$

$$R_4 = \frac{10^6}{1.18} = 847.0\ K\Omega$$

$$R_5 = R_6 = R_3 = 15.99\ K\Omega \quad . \qquad (7\text{-}58)$$

Cimilarly, for the same choice of C_1, C_2, k_1, and k_2, the element values of the second-product term section are calculated to be:

$$R_1 = \frac{10^6}{0.95} = 1.052\ M\Omega$$

$$R_2 = \frac{10^6}{\sqrt{3982.18}} = 15.86\ K\Omega$$

$$R_3 = \frac{10^6}{\sqrt{3982.18}} = 15.86\ K\Omega$$

$$R_4 = 10^6 = 1\ M\Omega$$

$$R_5 = R_6 = R_3 = 15.86\ K\Omega \quad . \qquad (7\text{-}59)$$

F. ADVANTAGES AND DISADVANTAGES

The state-space approach used in the filter transfer function realizations in this chapter has the distinct advantage of using well-developed theories from system and control applications. It takes advantage of direct analog computer simulation. In addition, the concept of using first- and second-order building-block networks significantly increases the stability and insensitivity of such realizations to fluctuations in the values of the passive RC components and in the gains of the operational amplifiers used. These sensitivity considerations are well discussed in Refs. 35 and 40. The building-block networks themselves are versatile (low-pass, bandpass and high-pass outputs) and readily adaptable to cascade realization because of their low-output impedance. And most important from economic considerations, such building-block networks are compatible to the microminiaturization and mass production concepts of present-day technology.

VIII. CONCLUSION

The synthesis techniques presented in the last four chapters are by no means the only ones that are possible with the use of operational amplifiers. It has been shown [Ref. 41] that the operational amplifier can be used to realize the three other classes of active devices - controlled sources, the negative-immittance converter and the gyrator - and consequently all the realization procedures which are applicable using these active devices are possible using operational amplifiers. Reference 42 gives an excellent treatment of such realization procedures. Operational amplifiers may even be used to take advantage of highly-developed passive filter synthesis procedures by direct inductance simulation [Refs. 43 - 45].

The use of operational amplifiers, therefore, offers a filter designer many advantages, among which is a wide choice of realization techniques. The particular method chosen is, of course, still highly dependent on the specifications of the particular filter desired. It has been pointed out, however, that the realization techniques using the state-space approach in Chapter VII of this paper offer much in the way of doing away with the expensive process of custom-building filters.

One limitation of all realization techniques using operational amplifiers should be stressed at this time. Operational amplifiers typically have gain-bandwidth products of the order 1 MHz. Consequently, at frequencies much above a few kilohertz, the infinite-gain approximations,

on which feedback synthesis is based, break down. It should be emphasized, then, that realization techniques using operational amplifiers are limited to frequencies within and below the audio range. However, the fact that inductors become unwieldy at these very same frequencies brought the development of active RC filters in the first place.

In conclusion, it is hoped that this paper has served to provide an orderly transition from the concepts of modern filter theory to a better understanding of the synthesis techniques involved in the realization of active RC filters using operational amplifiers.

APPENDIX A

TOW'S FREQUENCY TRANSFORMATION PROCEDURE

Reference 9 contains the normalized low-pass poles and zeros up to n = 9 of four different characteristic types - Butterworth, Chebyshev, Inverted Chebyshev and Cauer Parameter. Tow's transformation procedure converts these poles and zeros into the poles and zeros of a desired bandpass or band-reject transfer function.

Let the normalized low-pass complex pole or zero from Ref. 9 be

$$S_{no} = -\sigma_n + j\,\omega_n \quad . \tag{A-1}$$

For a desired bandpass or band-reject filter, either the resonant or center frequency, f_o, or the lower and upper frequency limits, f_l and f_u, are normally specified. The following relations can consequently be determined:

$$\omega_o = 2\pi f_o \text{ or } \omega_o = 2\pi(\sqrt{f_l f_u}) \tag{A-2}$$

$$BW = f_u - f_l \tag{A-3}$$

$$x = BW/f_o = 1/Q \quad . \tag{A-4}$$

Equations (A-1) to (A-4) may now be used in the following low-pass-to-bandpass root transformation:

$$(S_n + \sigma_n - j\,\omega_n)(S_n + \sigma_n + j\,\omega_n) \longrightarrow \frac{(s - s_1)(s - s_1^*)(s - s_2)(s - s_2^*)}{K^2 s^2} \tag{A-5}$$

where s is the complex frequency variable of the frequency-transformed transfer function and where

$$s_1 = -1/2\,(\sigma + v)\,\omega_o + j\,1/2\,(\omega + u)\,\omega_o \qquad \text{(A-6)}$$

$$s_2 = -1/2\,(\sigma - v)\,\omega_o + j\,1/2\,(\omega - u)\,\omega_o \qquad \text{(A-7)}$$

$$K^2 = 4\,\pi^2\,(f_u - f_l)^2 \qquad \text{(A-8)}$$

and

$$\sigma = \sigma_n x \qquad \text{(A-9)}$$

$$\omega = \omega_n x \qquad \text{(A-10)}$$

$$u = \left[1/2\,(4 - \sigma^2 + \omega^2) + \left(\frac{4 - \sigma^2 + \omega^2}{2}\right)^2 + \sigma^2\,\omega^2\right]^{1/2} \qquad \text{(A-11)}$$

$$v = \sigma\omega/u \qquad \text{(A-12)}$$

s_1^* and s_2^* are the complex conjugates of s_1 and s_2 respectively. The normalized-low-pass-to-band-reject root transformation is:

$$(S_n + \sigma_n - j\,\omega_n)\,(S_n + \sigma_n + j\,\omega_n) \longrightarrow \frac{(s - s_1)(s - s_1^*)(s - s_2)(s - s_2^*)}{(s^2 + \omega_o^2)^2} \qquad \text{(A-13)}$$

where s_1, s_2, u, and v are as given by equations (A-6), (A-7), (A-11) and (A-12) respectively and

$$\sigma = \frac{\sigma_n{}^x}{(\sigma_n{}^2 + \omega_n{}^2)^2} \qquad \text{(A-14)}$$

$$\omega = \frac{\omega_n{}^x}{(\sigma_n{}^2 + \omega_n{}^2)^2} \qquad \text{(A-15)}$$

APPENDIX B

COMPUTER PROGRAM 1

```
SUBROUTINE FREQR(NCN,NCD,A,B,FMIN,FMAX,X,Y)

PURPOSE - TO PLOT THE FREQUENCY RESPONSE OF ANY GIVEN
  TRANSFER FUNCTION WITHOUT POLES ON THE JW-AXIS.

NCN - THE NUMBER OF NUMERATOR COEFFICIENTS.
NCD - THE NUMBER OF DENOMINATOR COEFFICIENTS.
A - THE ARRAY OF NUMERATOR COEFFICIENTS STARTING FROM THE
  THE LOWEST-DEGREE TERM.
B - THE ARRAY OF DENOMINATOR COEFFICIENTS STARTING FROM THE
  THE LOWEST-DEGREE TERM.
FMIN - THE LOWER FREQUENCY LIMIT IN HERTZ TO BE PLOTTED.
FMAX - THE UPPER FREQUENCY LIMIT IN HERTZ TO BE PLOTTED.
X - THE ARRAY OF FREQUENCY POINTS IN HERTZ TO BE PLOTTED.
Y - THE ARRAY OF MAGNITUDE POINTS TO BE PLOTTED.

ADDITIONAL SUBROUTINE REQUIRED

  SUBROUTINE DRAW FROM THE NPS W.R. CHURCH COMPUTER
  CENTER LIBRARY
```

```
      SUBROUTINE FREQR(NCN,NCD,A,B,FMIN,FMAX,X,Y)
      DIMENSION A(30),B(30),X(201),Y(201)
      COMPLEX H,S,D,BI
      REAL*8 ITITLE(12)/'  FIRST LINE OF DESIRED TITLE.
     .  SECOND LINE OF DESIRED TITLE FOR PLOT.'/
      REAL LABEL/4H    /
      WRITE(6,105)
      WRITE(6,104) (A(J),J=1,NCN)
      WRITE(6,103)
      WRITE(6,104) (B(J),J=1,NCD)
      WMIN=FMIN*6.283184
      WMAX=FMAX*6.283184
      DELW=(WMAX-WMIN)/200.
      DO 1000 M=1,201
      W=WMIN+DELW*(M-1)
      S=CMPLX(0.0,W)
      H=(0.0,0.0)
      D=(0.0,0.0)
      DO 1 I=1,NCN
      AI=A(NCN+1-I)
      BI=CMPLX(AI,0.0)
      H=H*S+BI
1     CONTINUE
      DO 2 I=1,NCD
      AI=B(NCD+1-I)
      BI=CMPLX(AI,0.0)
      D=D*S+BI
2     CONTINUE
      H=H/D
      X(M)=AIMAG(S)/6.283184
      X(M)=X(M)-WMIN/6.283184
      Y(M)=CABS(H)
1000  CONTINUE
      CALL DRAW(200,X,Y,0,0,LABEL,ITITLE,0,0,0,0,0,0,5,8,1,
     *LAST)
105   FORMAT(1H1,10X,'THE COEFFICIENTS OF THE NUMERATOR ARE'
     *,///)
103   FORMAT(///,10X,'THE COEFFICIENTS OF THE DENOMINATOR
```

```
     *ARE',///)
104   FORMAT(10X,F20.5,5X,F20.5,/)
      RETURN
      END
```

APPENDIX C

NATHAN'S METHOD OF MATRIX ANALYSIS

Consider the n-terminal network with an operational amplifier connected between its i th and j th terminals as shown below:

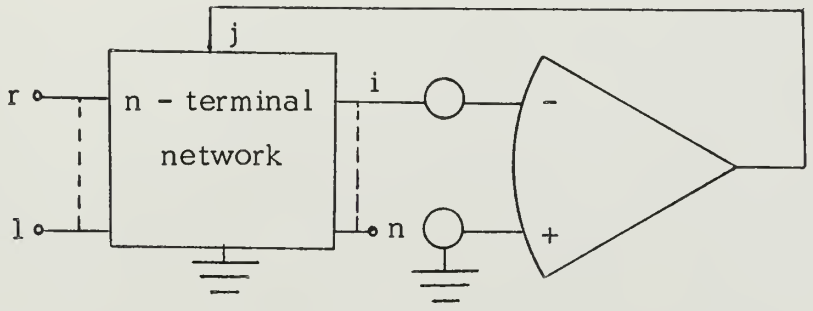

If the network is considered by itself, without the operational amplifier, it can be described by the following matrix equation:

$$[I] = [Y][E] \quad , \qquad (C-1)$$

where [I] is the column matrix of terminal currents, [E] is the column matrix of terminal voltages, and [Y] is the admittance matrix for the n-terminal network.

If the network is now considered taking the presence of the operational amplifier into consideration, several simplifying operations can be performed.

Since $E_i = 0$ by the concept of virtual earth, E_i may be removed from [E], cancelling effectively the i th column of [Y].

Also, since I_j will always be of such value to satisfy the constraint that $E_i = 0$, I_j may be eliminated, again effectively cancelling the j th row of [Y].

These operations yield a new matrix equation:

$$[I'] = [Y'] \; [E'] \quad , \tag{C-2}$$

where [I'] is [I] with I_j deleted, [E'] is [E] with E_i deleted, and [Y'] is [Y] with the j th row and the i th column deleted.

If the voltage transfer function between two terminals, p and q, of the n-terminal network is desired, matrix algebra yields:

$$[E'] = [Y']^{-1} [I'] \quad . \tag{C-3}$$

The voltage at terminal p can be written as

$$E_p = \frac{1}{|Y'|} \sum_{\substack{r=1 \\ r \neq j}}^{n} Y^{pr} I_r \quad , \tag{C-4}$$

where the Y^{pr} terms are cofactors associated with corresponding terms in [Y'].

If all terminals except p, i, and j are left open-circuited and if terminal p is excited by a voltage source, the only non-zero terminal currents will be I_p and I_j. $I_i = 0$ because of the operational amplifier's infinite input impedance. Application of these conditions into equation (C-4) gives

$$E_p = \frac{Y^{pp}}{|Y'|} I_p \quad . \tag{C-5}$$

Under these same conditions,

$$E_q = \frac{Y^{pq}}{|Y'|} I_p \quad . \tag{C-6}$$

Therefore, provided p is not driven and q is not driving,

$$\frac{E_q}{E_p} = \frac{Y^{pq}}{Y^{pp}} \quad . \qquad \text{(C-7)}$$

BIBLIOGRAPHY

1. Bode, H.W., Network Analysis and Feedback Amplifier Design, p. 226 - 248, D. Van Nostrand Co., Inc., New York, N.Y., 1945.

2. Guillemin, E.A., "Synthesis of RC-Networks," Journal of Math. and Physics, v. 28, p. 22, April 1949.

3. Dietzold, R.L., Frequency Discriminative Electric Transducer, U.S. Patent No. 2,549,065, 17 April 1951.

4. Linvill, J.G., "RC Active Filters," Proc. IRE, v. 42, p. 555-564, March 1954.

5. Handbook and Catalog of Operational Amplifiers, Burr-Brown Research Corp., Tucson, Ariz., p. 3-20, 1969.

6. Ghausi, M.S., Principles and Design of Linear Active Circuits, p. 90-96, McGraw-Hill Book Co., 1965.

7. Weinberg, L., Network Analysis and Synthesis, p. 506-507, McGraw-Hill Book Co., 1962.

8. Kuo, F.F., Network Analysis and Synthesis, p. 379-383, John Wiley & Sons, Inc., 1962.

9. Christian, E. and Eisenmann, E., Filter Design Tables and Graphs, John Wiley & Sons, Inc., 1966.

10. Weinberg, L., "Network Design by Use of Modern Synthesis Techniques and Tables," Proc. NEC, v. 12, p. 794-817, 1956.

11. Tow, J., "A Step-by-Step Active-Filter Design," IEEE Spectrum, v. 6, p. 65, December 1969.

12. Nathan, A., "Matrix Analysis of Networks Having Infinite-gain Operational Amplifiers," Proc. IRE, v. 49, p. 1577-1578, October 1961.

13. Bradley, F.R. and McCoy, R., "Driftless D-C Amplifier," Electronics, v. 25, p. 144-148, April 1952.

14. Mathews, M.V. and Seifert, W.W., "Transfer-Function Synthesis with Computer Amplifiers and Passive Networks," Proc. Western Joint Computer Conf., p. 7-12, March 1955.

15. Van Valkenburg, M.E., Introduction to Modern Network Synthesis, p. 145-148, John Wiley & Sons, Inc., 1962.

16. Fialkow, A.D. and Gerst, I., "The Transfer Function of General Two-Terminal-Pair RC Networks," Quart. Appl. Math., v. 10, p. 113-127, April 1952.

17. Guillemin, E.A., "Synthesis of RC Networks," Journal of Math. And Physics, v. 28, p. 22-42, April 1949.

18. Dasher, J., "Synthesis of RC Transfer Functions as Unbalanced Two-Terminal Pair Networks," Trans. of the IRE, v. PGCT-1, p. 20-34, December 1952.

19. Ozaki, H., "Synthesis of Three-Terminal Networks with Two Kinds of Elements," Trans. of the IRE, v. CT-5, p. 267-275, December 1958.

20. Van Valkenburg, M.E., Introduction to Modern Network Synthesis, p. 322-329, John Wiley & Sons, Inc., 1962.

21. Paul, R.J.A., "Simulation of Rational Transfer Functions with Adjustable Coefficients," Proc. IEE, v. 110, p. 671-679, April 1963.

22. Hakim, S.S., "RC-Active Circuit Synthesis Using an Operational Amplifier," Intern. J. Control, v. 1, p. 433-446, May 1965.

23. Muir, J.L. and Robinson, A.E., "Design of Active RC Filters Using Operational Amplifiers," Systems Technology, No. 4, p. 18-30, 1968.

24. Rauch, L. and Nichols, M.H., Radio Telemetry, p. 396, John Wiley & Sons, Inc., 1956.

25. Bridgman, A. and Brennan, R., "Simulation of Transfer Functions Using Only One Operational Amplifier," IRE WESCON Conv. Record, v. 1, p. 273-278, 1957.

26. Wadhwa, L.K., "Simulation of Third-Order Systems with One Operational Amplifier," Proc, IRE, v. 50, p. 201-202, February 1962.

27. Wadhwa, L.K., "Simulation of Third-Order Systems with Simple-Lead Using One Operational Amplifier," Proc. IRE, v. 50, p. 465, April 1962.

41. Morse, A.S., The Use of Operational Amplifiers in Active Network Theory, M.S. Thesis, University of Arizona, 1963.

42. Huelsman, L.P., Theory and Design of Active RC Circuits, Chapts. 3-5, p. 63-182, McGraw-Hill Book Co., 1968.

43. Ford, R.L. and Girling, F.E.J., "Active Filters and Oscillators Using Simulated Inductance," Electronics Letters, v. 2, p. 52, February 1966.

44. Riordan, R.H.S., "Simulated Inductors Using Differential Amplifiers," Electronics Letters, v. 3, p. 50-51, February 1967.

45. Keen, A.W. and Peters, J.L., "Operational Differentiation Using Simulated Inductance with Single-Ended Amplifiers," Electronics Letters, v. 3, p. 61-62, February 1967.

Security Classification

DOCUMENT CONTROL DATA - R & D

(Security classification of title, body of abstract and indexing annotation must be entered when the overall report is classified)

1. ORIGINATING ACTIVITY *(Corporate author)*
Naval Postgraduate School
Monterey, California 93940

2a. REPORT SECURITY CLASSIFICATION
Unclassified

2b. GROUP

3. REPORT TITLE
Synthesis Techniques for Active RC Filters Using Operational Amplifiers

4. DESCRIPTIVE NOTES *(Type of report and, inclusive dates)*
Master's Thesis; June 1970

5. AUTHOR(S) *(First name, middle initial, last name)*
Hernani Mationg Jover

6. REPORT DATE	7a. TOTAL NO. OF PAGES	7b. NO. OF REFS
June 1970	198	45

8a. CONTRACT OR GRANT NO.	9a. ORIGINATOR'S REPORT NUMBER(S)
b. PROJECT NO.	
c.	9b. OTHER REPORT NO(S) *(Any other numbers that may be assigned this report)*
d.	

10. DISTRIBUTION STATEMENT
This document has been approved for public release and sale; its distribution is unlimited.

11. SUPPLEMENTARY NOTES	12. SPONSORING MILITARY ACTIVITY
	Naval Postgraduate School Monterey, California 93940

13. ABSTRACT

The stimulus provided by the trend towards microminiaturization has generated considerable interest in active RC filters utilizing operational amplifiers. A comprehensive and unified presentation of the many different techniques to synthesize such filters is made along the lines of modern filter theory in this thesis.

DD FORM 1 NOV 65 1473 (PAGE 1) 201

S/N 0101-807-6811

Security Classification

A-31

KEY WORDS	LINK A		LINK B		LINK C	
	ROLE	WT	ROLE	WT	ROLE	WT
Synthesis Techniques						
Active RC Filters						
Operational Amplifiers						